

STATE

# LIBRARY Michigan State University

This is to certify that the

dissertation entitled

ALKALI METAL ANION AND ELECTRIDE SALTS VIA CRYPTANDS AND CROWN-ETHERS; SOME OPTICAL AND ELECTRICAL PROPERTIES

presented by

Michael Robert Yemen

has been accepted towards fulfillment of the requirements for

Ph.D degree in Chemistry

Date 9/2/86

MSU is an Affirmative Action/Equal Opportunity Institution

0-12771



RETURNING MATERIALS:
Place in book drop to remove this checkout from your record. FINES will be charged if book is returned after the date stamped below.

# ALKALI METAL ANION AND ELECTRIDE SALTS VIA CRYPTANDS AND CROWN-ETHERS; SOME OPTICAL AND ELECTRICAL PROPERTIES

Ву

Michael Robert Yemen

### A DISSERTATION

Submitted to

Michigan State University
in partial fulfillment of the requirements

for the degree of

DOCTOR OF PHILOSOPHY

Department of Chemistry

1982

#### ABSTRACT

ALKALI METAL ANION AND ELECTRIDE

SALTS VIA CRYPTANDS AND CROWN-ETHERS;

SOME OPTICAL AND ELECTRICAL PROPERTIES

Ву

#### Michael Robert Yemen

Evaporation of ethylamine or methylamine solutions which contain an alkali metal and a cation-complexer results in the formation of blue or gold-colored solids. Some of these solids have been studied by optical transmission spectroscopy and D.C. electrical conductivity.

Evaporation of these solutions can also yield thin solvent-free films which were examined over the region  $4000-40000~\rm cm^{-1}$ . Ethylamine solutions of  $(Na^+C222)Na^-$  gave films which were blue by transmitted light, but bright gold-colored by reflected light. Methylamine-potassium-C222 solutions with a metal to complex mole ratio, R, of 2 gave film spectra with a peak assigned to K<sup>-</sup>. Similar solutions of rubidium and cesium gave peaks, assigned to Rb<sup>-</sup> and Cs<sup>-</sup> respectively. The band positions for M<sup>-</sup> in the solvent-free solid films agreed well with M<sup>-</sup> band positions in ethylenediamine

solution. Spectra of films formed from R=1 methylamine solutions of potassium and C222 showed a single band assigned to the trapped electron,  $e_{t}$ . Spectra of films from K-C222 or Rb-C222 methylamine solutions with R between 1 and 2 showed both K and  $e_{t}$  bands.

Evaporation of solutions of Na, K, Rb, or Cs and 18-C-6 in methylamine also yielded thin films for optical study. When sodium solutions with R=2 were evaporated, the films were gold colored by reflectance as long as some methylamine was present. When the methylamine was completely removed the color changed from gold to purple. This color change was accompanied by pronounced spectral changes. A number of films were also prepared from K, Rb, and Cs solutions with 18C6 present. Potassium films with R=2 have absorptions at 12200 cm<sup>-1</sup> (assigned to K<sup>-</sup>) and a shoulder at 9000 cm<sup>-1</sup> (assigned to e<sub>+</sub>).

The physical appearance of crystalline (Na<sup>+</sup>C222)Na<sup>-</sup> stimulated interest in measuring the D.C. electrical conductivity of the crystals. Initial pressed powder studies of (Na<sup>+</sup>C222)Na<sup>-</sup> indicated it was a semiconductor with an energy gap of 2.6-3.0 eV. Other sodide salts, (KC222)Na<sup>-</sup>, "(Ba<sup>++</sup>C222)"Na<sup>-</sup>, (RbC222)Na<sup>-</sup>, (K<sup>+</sup>18C6)Na<sup>-</sup>, and (Cs<sup>+</sup>18C6)Na<sup>-</sup> were prepared for measurement in the pressed powder apparatus. Two other salts, (K<sup>+</sup>C222)K<sup>-</sup> and (Li<sup>+</sup>C222)e<sup>-</sup>, were measured by the pressed powder method. These salts had complex plots of log R vs 1/T and are not fully understood.

To My Parents

#### ACKNOWLEDGMENTS

I am grateful to Professor James Dye for his enthusiasm and thoughtful guidance during this work. To all other members of Dr. Dye's research group, past and present, I would like to give thanks for their many helpful suggestions and discussions. In particular, thanks go to Michael DaGue, Steve Landers, and Patrick Smith. Also the M.S.U. glassblowers, Keki Mistry, Andrew Seer, and Jerry DeGroot, have given excellent service and technical advice.

I appreciate having received teaching and research assistantships financed by the State of Michigan and the U.S. Government, respectively. A portion of this work was supported by NSF Grant DMR-79-21979.

Finally, a special thanks to my parents and Champoonute Kamthong, a special friend, for their encouragement during this work.

# TABLE OF CONTENTS

Chapter	Page
LIST OF TABLES	vii
LIST OF FIGURES	viii
SELECTED SYMBOLS AND ACRONYMS	хx
I. INTRODUCTION	1
A. Metal-Ammonia Solutions	2
B. Metal Solutions in Amines and Ethers	6
C. Alkali-Metal Cation Complexing Agents	15
D. Use of Complexing Agents in Metal Solutions	19
E. D.C. Electrical Conductivity	22
II. EXPERIMENTAL	28
A. Reagents	28
1. Solvents	28
2. Metals	30
3. Complexing Agents	34
4. Miscellaneous Reagents	35
B. Glass Apparatus Cleaning	36
C. Greaseless High Vacuum System	37
D. Inert Atmosphere Box and Glove Bags	38
E. Sample Preparation and Instrumental Techniques	39
1. (Na <sup>+</sup> C222)Na <sup>-</sup> Preparation	39

Chapter			Page
	2.	Optical Spectra	 44
	3.	Film Conductivity	 47
	4.	Pressed Powder Conductivity	 52
III. O	ptic	al Spectra	 60
A.	M/C	2222 Films	 61
	1.	Na/C222 Films from Ethylamine Solutions	 61
	2.	M/C222 Films from Methylamine Solutions	 66
	3.	Discussion	 70
В.		8C6 Spectra from Methylamine utions	 75
	1.	Na/18C6 Films from Methyl- amine Solutions	 76
	2.	<pre>K, Rb, and Cs/18C6 Films from Methylamine Solutions</pre>	 79
c.	Sum	mary of Optical Spectra	 81
		Electrical Conductivity	 85
A.	Pre	essed Powder	 85
	1.	Pressed Powder Conductivity Cell (A)	 86
		a. Pressed Powder Conductivity of (Na <sup>+</sup> C222)Na <sup>-</sup>	 87
		b. Pressed Powder Conductivity of Other Sodide Salts	 90
	2.	Cold Jacket Pressed Powder Cell (B)	 93
		a. Trial Test of the Cold Jacket Pressed Powder Cell with TiO <sub>2</sub> and HgS	 96
		b. D.C. Conductivity Measure- ment of Different Salts	, ,
		Containing C222 and the Sodium Anion, Na	 99

Chapter	Page
<pre>c. D.C. Conductivity Measure- ments of Salts Containing 18C6 and the Sodium Anion, Na</pre>	108
<pre>d. D.C. Conductivity Measure- ments of (K+C222)K- and (Li+C211)e</pre>	114
B. D.C. Conductivity and Photocon- ductivity of Thin Films of (Na+C222)Na	119
V. Conclusions and Suggestions for	117
Future Work	133
A. Conclusions	133
B. Suggestions for Future Work	134
APPENDIX A: Thermodynamic Stability of (Na <sup>+</sup> C222)Na <sup>-</sup> at 273°K	136
APPENDIX B: Effect of Optical Film Non- Uniformity	139
REFERENCES	153

# LIST OF TABLES

Table		Page
1	Peak Positions in Metal-Ethylene-	
	diamine Solutions	. 9
2	Comparison of Alkali Metal Anion	
	Peak Positions in Solid Films from	
	Methylamine and in Metal-EDA Solu-	
	tions	. 64
3	Summary of Peak Positions in Optical	
	Spectra of Films	. 83
4	Current Flow in a Film of (Na <sup>+</sup> C222)Na <sup>-</sup>	. 128
5	Current Characteristics of the Silver	
	Lines	. 130
B-1	Film Shape Effects: A for	
	b = -a/2	. 144
B-2	Film Shape Effect: A <sub>max</sub> for	
	b = a/2	. 145
B-3	Film Shape Effect: A <sub>max</sub> for	
	a = 0, b 0	. 145
B-4	Film Shape Effect: A <sub>max</sub> for	
	b = -a	. 146
B-5	Film Shape Effect: A <sub>max</sub> for	
	b = 0; uniform thickness	. 146

# LIST OF FIGURES

Figure		Page
1	Optical spectra of alkali metal-EDA	
	solutions	8
2	Models for species of stoichiometry M <sup>-</sup> .	
	A fourth structure is the spherically	
	symmetric alkali metal anion M with an	
	s <sup>2</sup> configuration	12
3	Molecular structure of 18-Crown-6 and	
	cryptand (2,2,2)	16
4	Selectivity and stability of cryptand	
	(2,2,2) complexes with alkali metal	
	cations in 95% methanol	18
5	Structure of (Na <sup>+</sup> C222)Na <sup>-</sup> based on x-	
	ray study	23
6	Band scheme for intrinsic conductivity	
	in a semiconductor. At 0°K the conduc-	
	tivity is zero because all states in the	
	valence band are filled and all states in	
	the conduction band are vacant. As tem-	
	perature is increased electrons are ther-	
	mally excited from the valence band to	
	the conduction band	25

Figure Page

7 In (a) the lowest point of the conduction band occurs at the same value of k as the highest point of the valence band. A direct optical transition is drawn vertically with no significant change of k, because the absorbed photon has a very small wavevector. The threshold frequency  $\omega_{\sigma}$  for absorption by the direct transition determines the energy gap  $E_{\sigma}^{-}$ The indirect transition in (b) involves both a photon and a phonon because the band edges of the conduction and valence bands are widely separated in k space. threshold energy for the indirect process in (b) is greater than the true band gap. The absorption threshold for the indirect transition between the band edges is at  $h\omega = E_{\alpha} + h\Omega$ , where  $\Omega$  is the frequency of an emitted phonon of wavevector  $K = -k_c$ . At higher temperatures phonons are already present; if a phonon is absorbed along with a photon, the threshold energy is  $h\omega = E_{\alpha} - h\Omega$  . Note: the figure shows only the threshold Transitions occur generally transitions. between almost all points of the two bands

Figure		Page
	for which the wavevectors and energy can	
	be conserved	27
8	Vacuum bottle with sidearm for alkali	
	metal distillation	29
9	Apparatus for the preparation of storage	
	tubes for sodium or potassium metal	32
10	Apparatus for distribution of alkali metal	
	under vacuum	33
11	Apparatus for preparation of (Na <sup>+</sup> C222)Na <sup>-</sup>	
	crystals	40
12	Vacuum tee used	42
13	Apparatus used to obtain spectra of	
	(M <sup>+</sup> C222)N <sup>-</sup> films	45
14	An apparatus with four parallel silver	
	lines on the glass to act as electrical	
	contacts for film conductivity	48
15	The male and female parts of the vacuum	
	electrical connector. (a) Teflon plug	
	connector which connects the silver	
	lines to the tungsten wire. (b) 9 mm	
	Fisher-Porter cap with four tungsten	
	wires sealed in its glass which plugs	
	into the teflon plug	50

16	(a) Arrangement for resistance measure-	
	ment by potential-probe method. (b) Ar-	
	rangement for resistance measurement by	
	V-I method	51
17	The pressed powder cell or cell A. (a)	
•	Open cell. From left to right the parts	
	are: Cap: used to apply pressure to elec-	
	trodes by screwing it tightly on the body.	
	First electrode: with cylindrical post and	
	its teflon and "o"-ring seals. Second	
	Electrode: with cup for powder sample.	
	Brass body: into which all the rest fit.	
	(b) Closed cell	53
18	(a) Open cold jacket cell or cell B showing	
	the stainless steel plunger in the top	
	assembly and the quartz capillary in the	
	bottom assembly. Above these is the	
	cylindrical outer body and brass stand.	
	(b) Closed cell B with brass stand above	
	it	55
19	Cooling jacket for Cell B. (a) Picture	
	looking down the inside of the cooling	
	jacket and top. (b) Drawing of how the	
	cold inert gas flows through the jacket	57

Page

Figure

Figure		Page
20	(a) The base on which the cooling jacket	
	sets. (b) Insert which fits in the center	
	hole in the base. Through this insert the	
	cooling gas passes by a platinum tempera-	
	ture sensor and a small heater	58
21	Baseline-corrected normalized spectra of	
	the sodium anion under various conditions:	
	solid line, (Na <sup>+</sup> C222)Na <sup>-</sup> film from ethyl-	
	amine; dashed line, (K <sup>+</sup> C222)Na <sup>-</sup> film from	
	methylamine; dotted line, Na in ethylene-	
	diamine	62
22	Spectra of films prepared by evaporation	
	of methylamine solutions which contain	
	$M^{+}C222$ and $M^{-}$ ; from left to right (peak	
	positions) M = Cs, Rb, K, Na, respectively.	
	The arrows indicate the position of the	
	absorption maxima for the corresponding	
	anions in ethylenediamine	63
23	Spectra of films produced by evaporation	
	of methylamine from solutions containing	
	cryptand (2,2,2) and various relative	
	amounts of potassium: spectra of films	
	produced from solutions containing pro-	
	gressively lower concentrations of solvated	
	electrons and higher concentrations of K	
	are in the order A, B, C	67

24	spectra of films produced by evaporation	
	of methylamine solutions containing cryp-	
	tand (2,2,2) and various relative amounts	
	of rubidium anions and solvated electrons	
	(solid and dashed lines). The dotted line	
	spectrum is from a film prepared from a	
	sodium borosilicate glass apparatus; the	
	solution presumably contained some Na	68
25	Spectra of metal-18-crown-6 films from	
	methylamine. A (····) sodium film, R=2,	
	with methylamine vapor present; B ()	
	dry sodium film, R=2; C () dry film	
	from Na-K-18C6 solution	77
26	Spectra of potassium/18-crown-6 films	
	with different ratios of K/18-C-6. Curve	
	A is the spectrum of potassium film with	
	R=2, and the curve B is the spectrum of	
	potassium film with R=1	80
27	Dry film spectra of metal-18-crown-6 films	
	from methylamine with R=2. A (····) po-	
	tassium; B () rubidium; C ()	
	cesium. With R=1, 0.5 and 0.1 spectra of	
	dry cesium films are essentially identical	
	with curve C	82

:	28	Ohm's law plot, voltage vs. current, for	
		a powdered sample of (Na <sup>+</sup> C222)Na <sup>-</sup>	88
:	29	Semi-log plot of the resistance of powdered	
		samples of (Na <sup>+</sup> C222)Na <sup>-</sup> versus the recip-	
		rocal of the temperature. Sample A was	
		relatively loosely-packed. The data shown	
		for the tightly-packed sample B were measured	
		at both increasing and decreasing tempera-	
		tures. Final dimensions of the sample	
		were 4.7 mm dia. and 0.25 mm thick	89
	30	Curve A is (K <sup>+</sup> C222)Na <sup>-</sup> exposed to high	
		temperature for approximately one-half	
		hour. Curve B is (K+C222)Na exposed to	
		high temperature longer than A (1 to 3	
		days). Curve C is (K+C222)Na exposed to	
		high temperature for over thirty days	91
	31	TCl is the thermocouple imbedded in the	
		stainless steel base of the quartz sample	
		chamber. It is used to measure the tem-	
		perature of the powder in the experiments.	
		TC2 is a thermocouple imbedded in the	
		powdered TiO <sub>2</sub> which is not present in the	
		conductivity experiments	95
;	32	Schematic diagram of the cold jacket	
		pressed nowder cell V regulated voltage	

Page

Figure

	supply. I, Keithly electrometer. C.J.C.
	cold jacket cell and T.C. is a thermocouple
	readout
33	Ohm's law plot for a sample of powdered
	TiO2 in the cold jacket pressed powder
	cell
34	Log R vs 1/T for a sample of powdered
	TiO2 in the cold jacket pressed powder
	cell
35	Log R vs 1/T for (Na <sup>+</sup> C222)Na <sup>-</sup> from
	measurements made with the cold jacket
	pressed powder cell 102
36	Ohm's law plot for the second sample of
	(K <sup>+</sup> C222)Na <sup>-</sup> powder measured in the cold
	jacket pressed powder cell. The first
	sample's Ohm's law plot is very similar 104
37	Log R vs 1/T for (K+C222)Na samples.
	The lower set of points are for the first
	sample and the upper set of points are
	for the second sample 105
38	Log R vs 1/T for (Rb <sup>+</sup> C222)Na <sup>-</sup> . The
	band gap energies for the square data
	points and the round data points outside
	of the circled area are 2.05 eV and 1.20
	eV. The circled area between -39.9°C

	and -41.0°C was an area where the cur-
	rent wandered
39	A plot of current versus voltage for a
	sample of (Cs <sup>+</sup> 18C6)Na <sup>-</sup> in cold jacket
	powder cell
40	Log R versus 1/T for second sample of
	(Cs <sup>+</sup> 18C6)Na <sup>-</sup> . The round solid dots are
	data points taken under low pressure,
	25.5 bar and decreasing temperature. The
	square dots were taken under low pressure
	and increasing temperature. The tri-
	angular dots were taken under high pres-
	sure, 59.3 bar and decreasing tempera-
	ture. The hollow circular dots were taken
	under high pressure and increasing tempera-
	ture. The curvature of this line was not
	due to any possible temperature lag. If
	it was due to the sample temperature lag-
	ging behind the temperature of the ther-
	mocouple, the curvature would be in the
	opposite direction 111
41	A plot of current versus voltage for a
	sample of (K <sup>+</sup> 18C6)Na <sup>-</sup> in powder cell B 112
42	Log R versus 1/T for a sample of (K+18C6)Na
	in pressed powder cell B. The round dots

	were taken under decreasing temperature
	and low pressure, 25.5 bar; band gap energy
	1.10 eV. The squares were taken under
	increasing temperature and low pressure;
	band gap energy 0.88 eV. The triangles
	were taken under decreasing temperature
	and high pressure, 59.3 bar; band gap
	0.94 eV. The hollow dots were taken under
	increasing temperature and high pressure
	band gap energy 0.98 eV 113
43	A plot of current versus voltage for a
	sample of (K <sup>+</sup> C222)K <sup>-</sup> . Note the curve is
	not a straight line and therefore not
	Ohmic
44	Log R versus 1/T for a sample of (K+C222)K
	Curve A's band gap energy equals 3.05 eV,
	curve B's band gap energy is 0.28 eV,
	curve C's band gap energy is 0.22 eV, and
	curve D shows metallic character 116
45	Log R versus 1/T for a sample of (Li <sup>+</sup> C211)e <sup>-</sup>
	as obtained from readings made with powder
	cell B
46	A plot of current versus voltage for two
	different pairs of probes for a film of
	(Na <sup>+</sup> C222)Na <sup>-</sup> . The straight line was for

	probes 1 and 3 and was later in time than	
	the two curved lines, which were for probes	
	1 and 2	121
47	Log R versus 1/T for a film of (Na <sup>+</sup> C222)Na <sup>-</sup>	
	exposed to fluorescent room light	123
48	Plots of current versus voltage for a film	
	of (Na <sup>+</sup> C222)Na <sup>-</sup> . The squares are for a	
	film of (Na <sup>+</sup> C222)Na <sup>-</sup> in the dark between	
	probes 1 and 4, whereas the round points are	
	for the same film exposed to fluorescent	
	room lights. The current scale is y x	
	$10^{-10}$ amps for the square points and y x	
	$10^{-9}$ amps for the round	124
49	Log R versus 1/T for a film of (Na <sup>+</sup> C222)Na <sup>-</sup>	
	in the absence of light	126
50	A plot of current versus wavelength at	
	a constant voltage, 5 V. The light source	
	was a 50 watt xenon lamp shown through a	
	Bausch and Lomb grating monochrometer,	
	350 to 800 nm	127
51	A plot of current versus wavelength for a	
	film made from the same solution as made	
	the film in Figure 51, but a week later.	
	Curve A was a freshly made film. Curve B	
	was for the film ∿30 min later	129

Figure		Page
B-1	Effect on the peak amplitude of an	
	optical film which is of non-uniform	
	thickness (shape as indicated) and	
	which fills various amounts of the	
	optical beam	147
B-2	Effects on the peak amplitude of an	
	optical film which is of non-uniform	
	thickness (shape as indicated) and	
	which fills various amounts of the	
	optical beam	148
B-3	Effect on a Lorentzian absorption	
	peak with a nominal 1.50 absorbance	
	when the optical film is of non-	
	uniform thickness (shape as indicated)	
	and when it fills various amounts of	
	optical beam	150
B-4	Effect on a Lorentzian absorption	
	peak with a nominal 2.00 absorbance	
	is of non-uniform thickness (shape	
	as indicated) and when it fills	
	various amounts of the optical	
	beam	151

#### SELECTED SYMBOLS AND ACRONYMS

```
cation-anion distance (in A)
a
        Angstroms, 10^{-10} m
Α
C222
         cryptand (2,2,2)
18C6
         18-crown-6
Cell A pressed powder cell
c.j.c. Cold jacket pressed powder cell
Cell B c.j.c.
        charge transfer to solvent
ctts
CTTS
         ctts
EDA
         ethylenediamine
         solvated electron
e_
         trapped electron
k
         Boltzmann constant
M
         alkali metal monomer
м+
         alkali metal cation
м-
         alkali metal anion
(M<sup>+</sup>C222) a cation, M<sup>+</sup>, complexed by C222
M<sup>+</sup>C
        M<sup>+</sup> and complexant
        number of electrons per unit volume
n/V
        mole ratio of metal to complexing agent
R
THF
         tetrahydrofuran
λ
         wavelength
        wavenumber (cm<sup>-1</sup>
\overline{\mathsf{v}}
```

#### INTRODUCTION

A new field of alkali metal chemistry was made possible by the synthesis of efficient alkali metal cation complexing agents. The study of alkali metal solutions in ammonia and in some amines and ethers dates back to research done on metal ammonia solutions in 1863 (1) and is still very active. Five international conferences have been held on the subject, all with published proceedings (2-6). A branch of this research was begun in the early 1970's by Dye and coworkers who demonstrated the tremendous solubility enhancement that the cyclic polyethers provide for alkali metals in amine and ether solvents (7-9). This work led to the isolation of solvent-free compounds of alkali metals and cyclic polyethers, including the single crystal x-ray structure of one such compound (10).

A review of metal-ammonia solutions (MAS), metal-amine and -ether solutions, alkali-metal cation complexing agents and their use in metal solutions provides some background for the current work. Species in ammonia solutions serve as models for species in amine and ether metal solutions. Evidence for one of these species, the alkali metal anion (M<sup>-</sup>), will be summarized. The essential role that the synthetic alkali metal cation complexing agents

pl

₫e 0:

er

I.

ti Ce

<u>h:</u> 20

K, рe

àl Di

s:

аb te

IJе gį

si

đc

Се

āņ.

played in opening a new field of alkali metal chemistry is described. These agents permitted synthesis of a new class of compounds, salts of the alkali metal anions. The properties of the first member of this class are also discussed.

## I.A. Metal-Ammonia Solutions

Alkali metals dissolve in ammonia to form blue solutions when dilute, and metallic bronze solutions when concentrated. The alkali metals dissolve in ammonia to high concentrations, the saturation concentration (11) is 20 mole per cent metal for Li and 16 mole per cent for Na, K, and Rb. The saturation concentrations show little temperature dependence. Cesium is miscible with ammonia in all proportions at the melting point of cesium (27.7°C). Dilute metal-ammonia solutions (₹1 mole per cent ≈ 0.5 M) show electrolytic behavior. At concentrations greater than about 8 mole per cent the solutions exhibit metallic characteristics. The mid-range concentration represents the metal-to-nonmetal transition region. The concentrations given above for the three regions are somewhat arbitrary since the properties which change during this transition do so gradually.

In metal ammonia solutions which are <2.10 $^{-4}$  mole per cent (<10 $^{-3}$  M), the major species are the solvated cation and the solvated electron ( $e_{\rm solv}^-$ ) which form as

The

How the

of of

(1.

en.

is by

an:

то

50

ti Wa

to

20

$$M_{(s)} \rightarrow M^{+} + e_{solv}^{-}$$
 (1)

The solvated electron is thermodynamically unstable and can react with the solvent:

$$e_{solv}^{-} + NH_3 \stackrel{?}{\neq} H_2 + NH_2^{-}$$
 (2)

However, if the solvent is free of catalysts such as iron, then the solutions are kinetically stable. The blue color of the dilute solutions is caused by the high energy tail of an absorption peak in the near infrared at 6900 cm<sup>-1</sup> (1450 nm). The absorption is asymmetric and the high energy tail extends into the red portion of the spectral region.

The most widely accepted model for the solvated electron is the cavity model first proposed by Ogg (12) and refined by Jortner (13). The electron is trapped in a cavity in the ammonia with a radius of 3.2-3.4 Å in the simple Jortner model. The electron is stabilized by orientation of the molecules in the first solvation sphere and by long range polarization effects from molecules outside the first solvation sphere. Jortner used hydrogenic ls and 2p variational wavefunctions to account for the optical spectrum as a ls to 2p transition. Several other experimental values were correctly derived. The potential function used was

i С i S ť Ī. В 1 ť II. Ą i W g: 20 **e**] H: Ъе þе

ŗę

oversimplified and others have tried more complex computations (14).

The properties of dilute metal ammonia solutions are independent of the cation. As the concentration increases, such properties as optical spectrum, magnetic susceptibility, conductivity, activity coefficient and density remain nearly independent of the cation. This suggests that any new species formed must retain the essential characteristics of the solvated cation and probably the solvated electron. This is the basis of the ionic aggregation model (15,16). Between M<sup>+</sup> and e<sup>-</sup> a nonconducting ion-pair forms which leads to a weak magnetic interaction of the electron with the metal nucleus. This interaction is observed in the paramagnetic shifts in the alkali metal NMR spectra (17,18). As the concentration is increased, the model predicts that ion triples will form. Ion triples such as e · M · e would have electron-electron interactions strong enough to give a singlet ground state. Static susceptiblities (19, 20) and ESR spin susceptibilities (21-23) show that the electron spins pair and form a diamagnetic ground state. Higher aggregates with stoichiometries such as  $M_2$  and  $M_2$  could also form.

As the metal concentration is increased from 3 mole per cent metal to 8 mole per cent metal, the electrical behavior of the solution changes from electrolytic or non-metallic to metallic. This nonmetal-to-metal transition is of great interest to physicists. Six theories and

their hybrids which "explain" the transition have been reviewed by Thompson (24).

Metal-ammonia solutions at concentrations higher than 8 mole per cent metal qualitatively behave as liquid metals. The conductivity of the most concentrated metal ammonia solutions is greater than that of liquid mercury. Optical studies of these solutions have been almost exclusively reflectance spectra which show the solvated electron band disappearing between 5.3 and 6.2 mole per cent metal, while an absorption edge (plasma edge) due to conduction electrons grows with increasing concentration (25). This plasma edge is at about 10,000 cm<sup>-1</sup> (1000 nm) when first formed but shifts to the blue at higher concentrations. Other properties of concentrated metal ammonia solutions have been reviewed by Thompson (24).

Gold-colored compounds are formed upon freezing concentrated metal ammonia solutions of the six metals Li, Ca, Sr, Ba, Eu and Yb. The compounds have the stoichiometry  $M(NH_3)_6$  except Li, which is  $Li(NH_3)_4$ . These compounds are metallic with the metal's valence electrons contributing to formation of a conduction band. The conductivity of  $Li(NH_3)_4$ , for example, is about equal to that of platinum.

Lithium tetrammine is the most studied of these solids. Single crystals have not been obtained and the stoichiometry is slightly variable. The structure was first thought to be hexagonal below 82 K and face centered cubic between 82 K

and 88 K (24), although the low temperature data have recently been re-evaluated and assigned to a face-centered cubic structure (80). The distance between Li(NH<sub>3</sub>)<sup>+</sup> ions in the face centered cubic form is 7 A. By comparison, the Li-Li distance in lithium metal is 3.5 A. The large effective ionic radius makes these compounds low-density metals or expanded metals. Expanded metals are on the edge of the metal-nonmetal transition. They also provide experimental tests for metal-nonmetal transition theories.

Except for the very dilute solutions, the nature of the species present in metal-ammonia solutions up to the concentrations at which the nonmetal-to-metal transition begins is still controversial. In contrast, metal solutions in amines and ethers give specific evidence for three reducing species: the solvated electron  $(e_{solv}^-)$ , a species of stoichiometry M, and the alkali metal anion  $(M^-)$ .

# I.B. Metal Solutions in Amines and Ethers

The alkali metals dissolve in certain amines and ethers to form blue solutions. The amine and ether metal solutions have saturation concentrations much lower for the most part than metal ammonia solutions. The exception is lithium in methylamine. The solubility of sodium in ethylenediamine, EDA, at 25 C is only 2.4 x  $10^{-3}$  M (26). Sodium and lithium will not produce blue solutions in the ethers, indicating that their solubility is lower than

10 am

op gi

ba (2

so en

En Ed

> tr si

> ā.

be

so se

M.

de to

so Na

th,

ומת

Another distinguishing characteristic is that amine and ether metal solutions may display both the esolv optical absorption band and a second band at higher energies than the M band. The position of this higher-energy band depends on which alkali metal is dissolved in the EDA (27) as shown in Figure 1. The spectrum produced by dissolving Li is only that of  $e_{solv}^-$ . The asymmetry and high energy tail mentioned early for e<sub>solv</sub> can be clearly seen. The  $e_{\text{solv}}^{-}$  band appears as a shoulder on the spectra from EDA solutions of K, Rb, and Cs. The sodium solution spectrum does not contain appreciable amounts of esolv. single peak in the visible region for sodium solutions has been called a v-band, as have the main peaks in K, Rb, and Cs spectra. The  $e_{\text{solv}}^{-}$  band in the near-infrared is sometimes referred to as the R-band. The V-bands have been assigned to spherically symmetric alkali metal anions, м-.

The ratio of the absorbances of the  $e_{\rm solv}^-$  and M bands depends on the solvent and the metal. The ratio decreases, together with metal solubility, along the solvent series: NH<sub>3</sub>, HMPA, EDA, MeNH<sub>2</sub>, EtNH<sub>2</sub>, PrNH<sub>2</sub>, ethers. For a given solvent this ratio and the solubility decrease from Cs to Na.

Two papers which appeared in 1968 and 1969 accelerated the identification of the V-bands as M<sup>-</sup>. In 1968, Hurley, Tuttle, and Golden (28) clarified the confusion about the

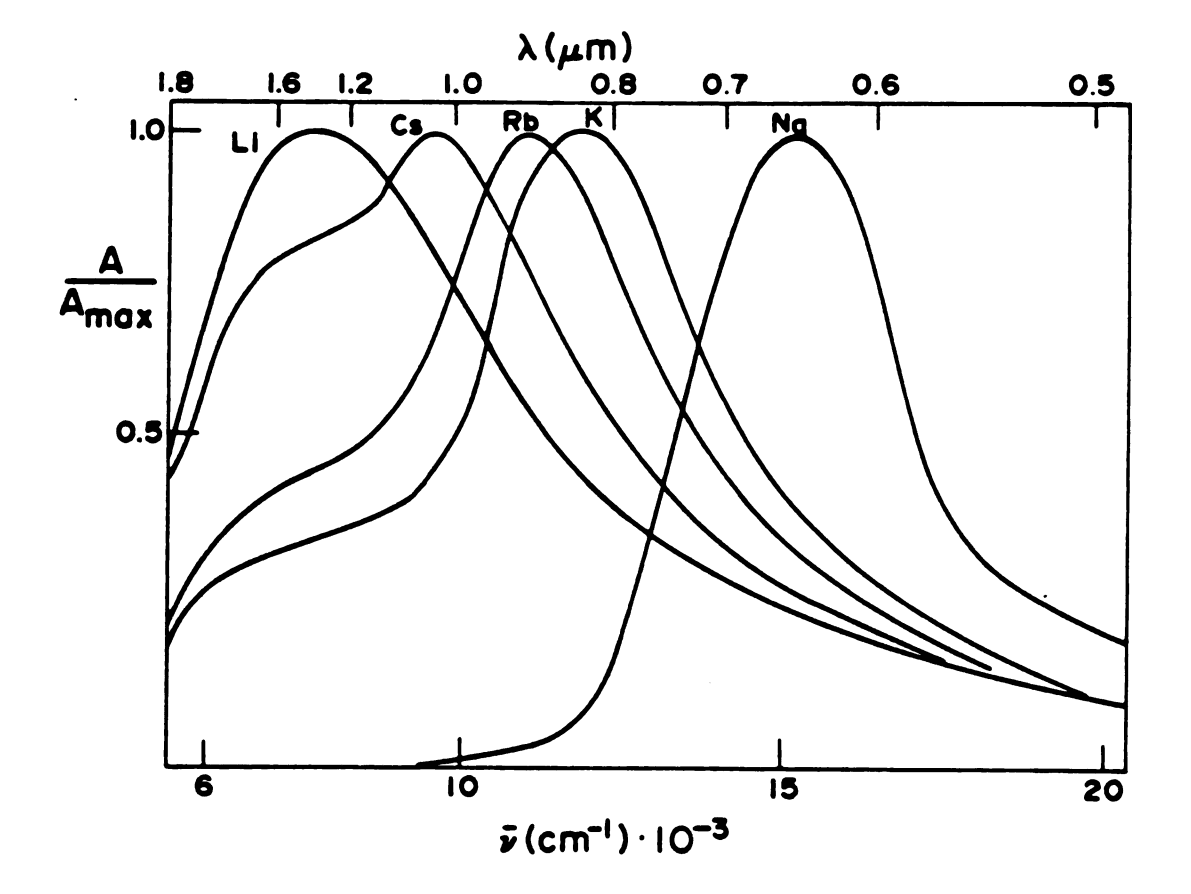


Figure 1. Optical spectra of alkali metal-EDA solutions.

Tab

ŊŢ

re

S

}

+

•

.

}

Table 1. Peak Positions in Metal-Ethylenediamine Solutions.

Species Na	Peak Position (27)		
	15,400 cm <sup>-1</sup>	650 nm	
<b>K</b> -	12,000	833	
Rb <sup>-</sup>	11,200	893	
Cs <sup>-</sup>	9,800	1020	
e_ solv	7,810	1280	

number and types of optical bands in metal amine and ether solutions. For K, Rb, and Cs solutions, some workers had reported an R-band, a metal-dependent V-band, and a metal-independent V-band, while other workers observed only the first two of the three bands. The metal-independent V-band was also seen with lithium solutions. Hurley, et al. realized that the metal-independent V-band arose from contamination of the solution with sodium by exchange of Li<sup>+</sup>, K<sup>+</sup>, Rb<sup>+</sup>, or Cs<sup>+</sup> with Na<sup>+</sup> from the sodium borosilicate glass of the apparatus. Thus, it is now known that a given metal in solution gives rise to no more than two absorption bands.

In 1969, Matalon, Golden, and Ottolenghi (29) suggested that the metal-dependent V-bands were due to a species having the stoichiometry M<sup>-</sup>. This suggestion was based on their comparison of the solvent, temperature and metal

de<sup>.</sup>

te

ti

mu A

a: t:

a

t

IJ

}

]

dependence of the V-bands with predictions of charge transfer to solvent (CTTS) theory. Several relationships characteristic of a CTTS transition were observed. The absorption maximum shows a marked solvent dependence and the maximum shifts to lower energies with an increase in temperature. A correlation exists between the peak position in a solvent and the temperature coefficient of the peak. The absorption maximum shifts to lower energies for larger sized anions. Also the CTTS theory predicts that the transition energy minus the atomic electron affinity is a linear function of the inverse of the anion radius. The agreement of experiment with the predictions of CTTS theory alone does not show that species has stoichiometry M, because, for example, the spectrum of  $e_{solv}$  also shows most of the above behavior. However, this assignment of the V-bands to a singlet ground state species M is consistent with earlier ESR studies (30-32) on solutions which showed only Vbands. The ESR studies indicate a diamagnetic species in solution.

De Backer and Dye (33) determined the extinction coefficient of the V-band in EDA/sodium solutions. They calculated an oscillator strength of 1.9±0.2 assuming one sodium in each absorbing unit. This result requires that two equivalent electrons be involved in the species undergoing transition. This requirement is met by the stoichiometry Na. Other studies indicating M as the correct

ass

(34

Far

pos

à

assignment were pulse radiolysis of EDA/sodium solutions (34), M photolysis (34-40), conductivity (26,41) and the Faraday effect (42).

The structure of M was still unknown; however, four possibilities existed:

- (1) an ion triple between two solvated electrons and the cation;
- (2) an ion pair between the cation and the dielectron  $e_2^{-2}$  (two spin-paired electrons residing in one cavity),
- (3) an expanded orbital species in which the two electrons were located on the solvation shell molecules for the cation; and
- (4) a genuine anion, M, where the two electrons were located in a cation s orbital.

The first three of these models are shown in Figure 2. Discriminating among these models depends on the use of alkali metal NMR along with the synthetic cation-complexes and will be briefly described in section I.D.

The solvated cation, anion, and electron are the three major species in metal amine and ether solutions. A fourth species whose relative concentration is too low in static solutions to be observed optically is called the monomer and has stoichiometry M. The first clear indication that the monomer exists was the observation of ESR hyperfine

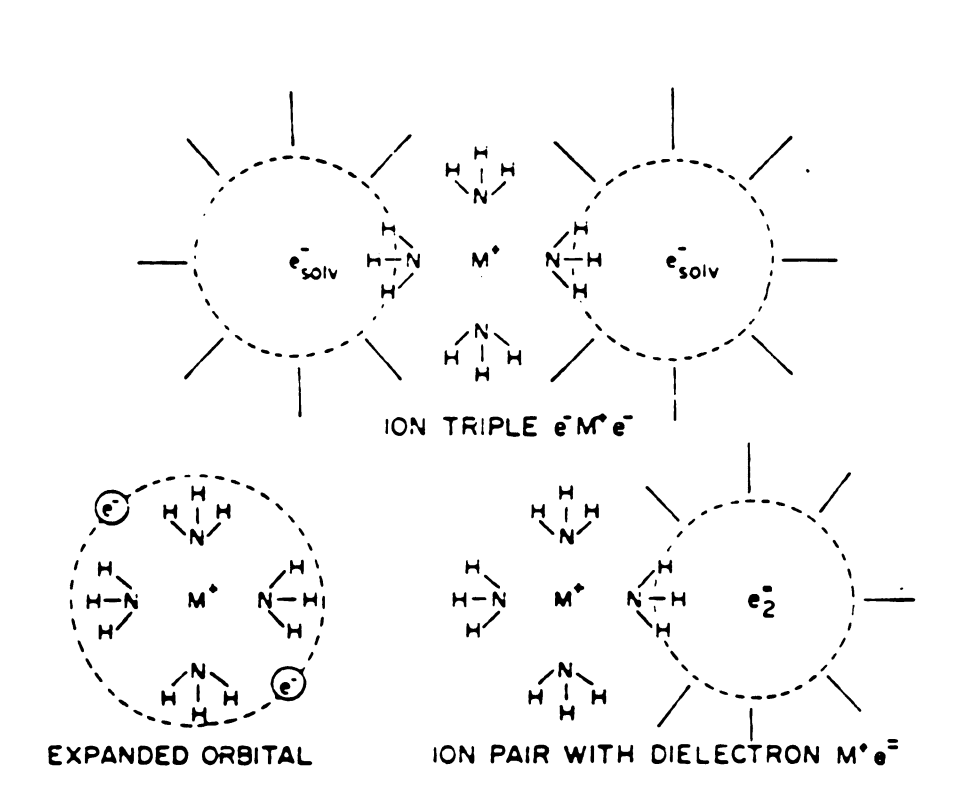


Figure 2. Models for species of stoichiometry M<sup>-</sup>. A fourth structure is the spherically symmetric alkali metal anion M<sup>-</sup> with an s<sup>2</sup> configuration.

splitting (43-45) in metal-amine solutions. When the monomer has a long lifetime and the electron exchange is slow, the ESR signal shows 2I + 1 hyperfine lines where I is the alkali metal nuclear spin. The hyperfine splitting is proportional to the average contact density of the electron at the nucleus. The percent atomic character can reach nearly 30% for Cs in i-PrNH<sub>2</sub> (46). The hyperfine splitting is greatly influenced by solvent and temperature.

Optical spectra of the monomer as a transient have been obtained by photolysis of  $M^-$  (35,36,38) and by pulsed radiolysis of solutions which contain  $M^+$  (47,48). The monomer band occurs between that of  $M^-$  and  $e^-_{solv}$ . The shift of the M band from the  $e^-_{solv}$  band is solvent dependent and can be as large as 3600 cm<sup>-1</sup> for the potassium monomer in THF (42).

Two models have been proposed for the monomer. In the static or continuum model, there is a single species whose structure depends on temperature. In the dynamic or multistate model, there is a temperature-dependent equilibrium between two (or more) species, each of whose structure is relatively independent of temperature. Pulsed radiolysis techniques have been used to show that the optical spectrum arises from the same monomer species as observed by ESR (49). The optical shift between the monomer and esolv was correlated with the hyperfine splitting observed (50). Pulsed radiolysis (50) also showed two optical bands for the

monomer species in THF, dimethoxyethane, diglyme, and triglyme where the latter three are glymes with the general formula  $\text{CH}_3\text{O}(\text{CH}_2\text{CH}_2\text{O})_n\text{CH}_3$  with n=1,2, and 3, respectively. The two bands were assigned to two monomer species; one a contact ion pair between  $\text{M}^+$  and  $\text{e}^-_{\text{solv}}$  and the other a solvent-shared ion pair. This observation supports the dynamic model with an equilibrium between two species. In better solvents such as the amines, only one optical band is observed and the monomer structure must lie between the extremes of contact and solvent shared ion pairs. Here the static model is appropriate. Both models are needed to explain all of the observed behavior.

The following equilibrium scheme was proposed by Dye (51):

$$2M_{(s)} \stackrel{?}{\leftarrow} M^+ + M^- \tag{3}$$

$$M^{-} \stackrel{\rightarrow}{\leftarrow} M + e_{solv}^{-}$$
 (4)

$$M \stackrel{\rightarrow}{\leftarrow} M^{+} + e_{solv}^{-}$$
 (5)

The three species M, M, and esolv may be detected in solutions of MeNH<sub>2</sub>, EDA, and HMPA depending on the metal.

M predominates in EtNH<sub>2</sub>, THF, and the glymes. An additional equilibrium is added when an alkali metal cation complexant is also in solution.

I.

We

Pe wh

(F

Wa

po

( <u>:</u>

W:

s:

Πę

e (

ĝ:

Ę.

Ţ

t:

t

f

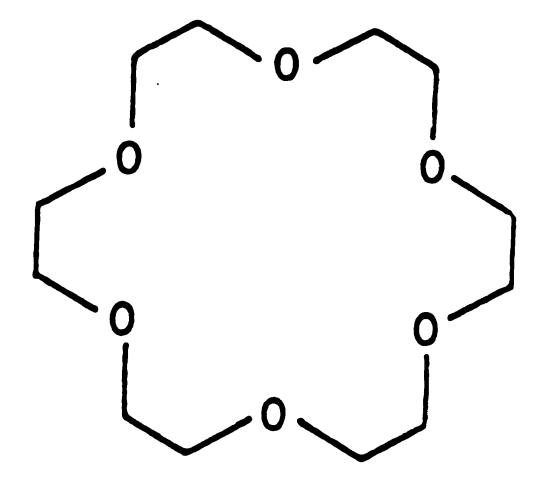
A.

# I.C. Alkali-Metal Cation Complexing Agents

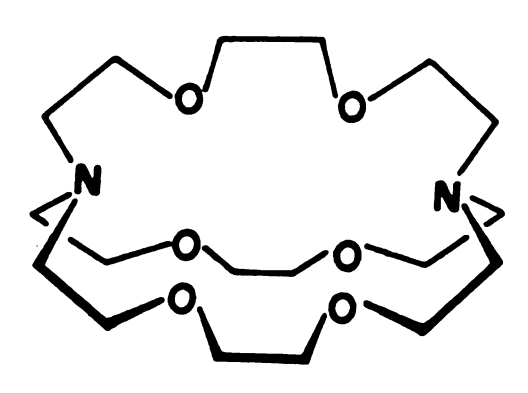
A few complexing agents for the alkali metal cations were known prior to 1967 (53) but it was at that time that Pedersen (52,53) synthesized the first of fifty complexes which he called crowns. The compound, 18-crown-6, or 18C6 (Figure 3), with 18 atoms in the ring and six ether oxygens, was used in this work. (The IUPAC names (81) of these compounds are cumbersome and the trivial nomenclature of Pedersen (53) is now widely used.) Pedersen also demonstrated (53) selectivity among cations in complex formation for a given crown and the solubilization of salts in solvents in which they would otherwise be insoluble. The crown 18C6 surrounds the cation and usually takes on a planar arrangement resulting in two dimensional complexation.

Lehn and co-workers (54) synthesized a series of cation complexing agents which enclose the cation inside a molecular cavity to give three dimensional complexes. These are the well-known cation complexants called cryptands. The cryptand (2,2,2), or C222, appears in Figure 3. (The IUPAC names for cryptands (81) are even more cumbersome than for crowns.) The numbers in the trivial name refer to the number of oxygens in each strand.

The cryptands exhibit very high complexation constants for the alkali metal cations  $-10^8$  or higher in some cases. Additionally, the cryptands are selective with respect to which cations they complex. The selectivity depends largely



18-Crown-6



Cryptand(2,2,2)

Figure 3. Molecular structure of 18-Crown-6 and cryptand (2,2,2).

on the cation size compared to the cryptand cavity size and also on the cation charge. Complexation constants and cation selectivity are shown in Figure 4 for C222, C221, and C211 with alkali metal cations in 95% methanol (55). The complexation properties of the cryptands are characterized by high stability, high selectivity, and shielding of the complexed cation from the environment. Kauffmann, Lehn, and Sauvage (56) have found that these properties are due to enthalpic effects and not entropy effects.

The general impact of macrocyclic ligands is too great to be reviewed in detail here. Broad areas of application will be described and detailed references can be found in reviews (57-62). The cryptands have been used:

- (1) to solubilize salts;
- (2) to break up ion pairs, increasing the anion reactivity or elucidating the cation's role in reaction mechanism;
- (3) to study cation transport in membranes;
- (4) to cause anionic polymerization or phase transfer catalysis,
- (5) to effect separations of isotopes and racemic mixtures; and
- (6) to study possible medical and toxicological applications.

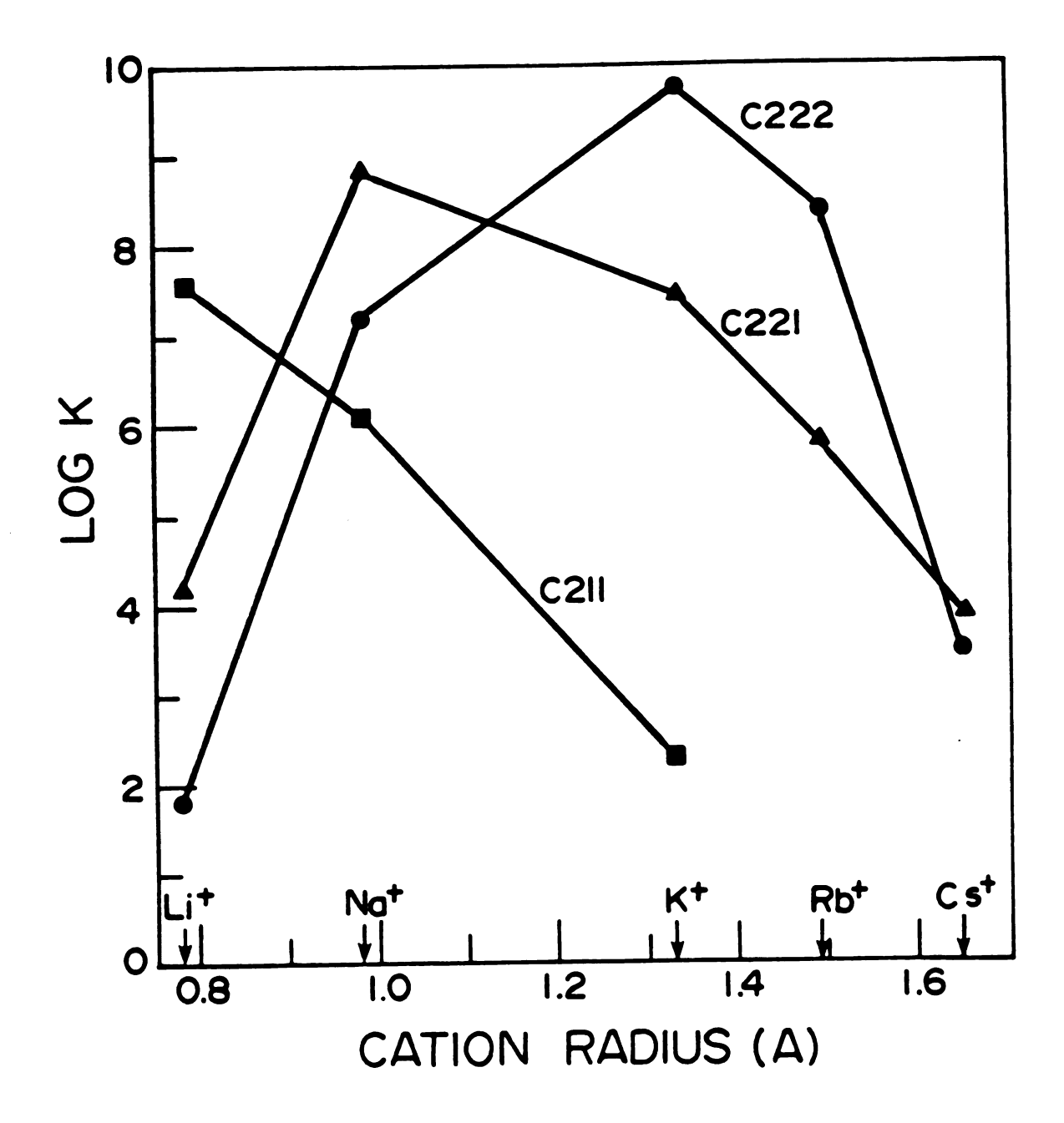


Figure 4. Selectivity and stability of cryptand (2,2,2) complexes with alkali metal cations in 95% methanol.

## I.D. Use of Complexing Agents in Metal Solutions

Use of cryptands in metal solution research began when Dye et al. reported in 1970 (63) and 1971 (64) the use of complexing agents to solubilize alkali metals in solvents which do not otherwise dissolve metal. Potassium, for example, was dissolved in several ethers using dicyclohexano-18-crown-6 (52) and C222.

Metal solutions in amines and ethers which contain a complexant, C, can be described by the equilibria given in Equations (3-5) and the equilibrium

$$M^{+} + C \stackrel{?}{/} M^{+}C$$
 (6)

and (5) to the right by dissolving more metal and converting monomer M to M<sup>+</sup> and e<sub>solv</sub>. If the amount of metal is limited with respect to complexant, then it is possible in good solvents such as MeNH<sub>2</sub> to prepare solutions consisting mainly of M<sup>+</sup>C and e<sub>solv</sub>. In the poorer solvents such as the ethers, solutions containing only M<sup>+</sup>C and M<sup>-</sup> can be prepared (65) by limiting the complexes relative to the metal. As a result, metal solutions which were impossible to prepare may be prepared and some control over solution species is possible. The cryptands' resistance to reduction is another important property.

Cryptands made possible experimental differentiation

بر بر

p.

t: an

s: b:

Ti

S

a]

0:

s:

I)

ch e1

ch ch

ca ve

£į

s::

between models (see Figure 2) for the solution structure of M in amines and ethers. This differentiation was accomplished by Dye, Ceraso, and Andrews (66,67) using alkali metal NMR. In order to measure the alkali metal NMR spectrum, the solutions had to be concentrated. Also, the amount of  $e_{solv}$  had to be limited since the presence of significant amounts of  $e_{solv}$  could broaden the M peaks by exchange to the point that the signal would disappear. The use of cryptand solved both of these problems through solubilization to give concentrated solutions and through stoichiometry control to give primarily M C222 and M.

Sodium exchange was slow enough to permit observation of a <sup>23</sup>Na NMR signal from both Na<sup>+</sup> C222 and Na<sup>-</sup>. Dye et al. found that the 2p electrons in Na are well shielded from interaction with the solvent and that Na is highly symmetric as indicated by the narrowness of its NMR signal. The former observation follows since the chemical shift for sodium depends on solvent interaction with the sodium 2p electrons. Popov et al. (68-71) had shown that sodium chemical shifts correlate well with solvent donicity as The Na measured by the Guttman solvent donor number. chemical shift shows no solvent dependence among the solvents methylamine, ethylamine and THF and is equal to that calculated for Na (q). These observations eliminate the first three models for M, leaving only the spherically symmetric anion with two electrons in an s orbital.

Resonances were also observed by Dye et al. for  $^{87}\text{Rb}^-$  and  $^{133}\text{Cs}^-$  with the counterion being the corresponding cryptated cation.

Solids have been obtained from concentrated amine and ether metal solutions which contained complexants. This has been done in two ways. Crystals form when the solutions are cooled below the saturation temperatures. The second technique is solvent evaporation to dryness.

Crystals of (Na<sup>+</sup>C222)Na<sup>-</sup> were grown (72) from an ethylamine solution and are the most fully characterized (73, 74) of the solids. The shiny gold-colored crystals which grow as thin hexagonal plates were prepared as described in detail in the Experimental section (75).

The crystals are stable for long periods under vacuum at -10°C. Some have been kept in a freezer at this temperature for five years. The crystals are air, water, and temperature sensitive but they may be handled in an inert atmosphere box at room temperature for a quarter of an hour or longer. This compound is the most stable of the solids studied to date, especially with respect to temperature sensitivity.

An x-ray structure determination of (Na<sup>+</sup>C222)Na<sup>-</sup> was made by Tehan, Barnett and Dye in 1974 (74). The sodium anions form parallel planes which are separated by cryptated sodium cations. The cryptand has three-fold symmetry and an antiprismatic oxygen atom arrangement about Na<sup>+</sup>

(see Figure 5). The structure is similar to that of  $(Na^{+}C222)I^{-}$  but  $Na^{-}$  seems to be slightly larger than  $I^{-}$ . The closest distance between sodium anions in the same plane is 8.83 A, while the closest distance between anions in different planes is 11.0 A.

A number of kinds of solids have been produced by solvent evaporation from solutions containing  $M^+C$  and  $M^-$ ,  $M^+C$  and  $N^-$  and  $M^+C$  and  $e^-$  Many solvent, complexant, and metal combinations were tried and blue or gold solid films were observed by solvent evaporation (76).

The gold solids were of the type M<sup>+</sup>CM<sup>-</sup> or M<sup>+</sup>CN<sup>-</sup>. The blue solids may be solids of a new class of compounds in which the counterion for M<sup>+</sup>C is an electron. These blue solids were characterized as having "paramagnetic character" (77) or as "strongly paramagnetic solids" (74,78). The blue solids are called electrides (79). Some optical and electrical properties of these two types of solids are the subject of this dissertation.

# I.E. D.C. Electrical Conductivity

The "gold" color of (Na<sup>+</sup>C222)Na<sup>-</sup> that stirred interest in its optical spectrum also prompted interest in its electrical properties. M. T. Lok (77 Part IV) started the investigation of the D.C. electrical conductivity of (Na<sup>+</sup>C222)Na<sup>-</sup> powder. Although his methods did not meet with complete success, they showed that (Na<sup>+</sup>C222)Na<sup>-</sup>

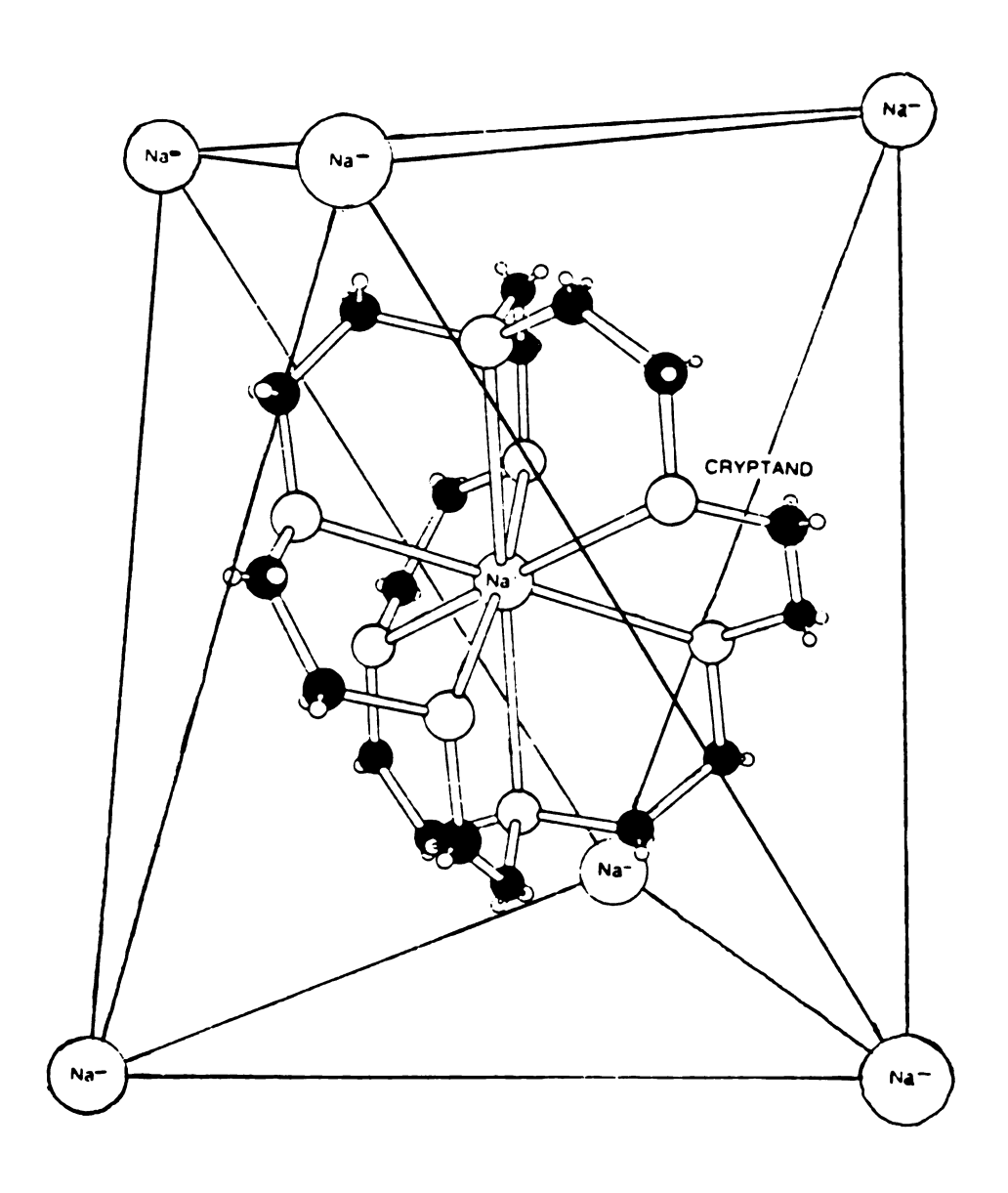


Figure 5. Structure of (Na<sup>+</sup>C222)Na<sup>-</sup> based on x-ray study.

powders had a band gap of about 2.5 eV. This investigation of  $(Na^+C222)Na^-$  was carried further in the present work and other investigations of similar powders,  $(M^+C)M^-$ ,  $(M^+C)N^-$ , and  $(M^+C)e^-$  were started. The electrical conductivity of these materials puts them in the class of conductors called semiconductors. Semiconductors are electronic conductors with electrical resistivity values generally in the range of  $10^{-2}$  to  $10^9$  ohm-cm at room temperature, intermediate between good conductors  $(10^{-6} \text{ ohm-cm})$  and insulators  $(10^{14} \text{ to } 10^{22} \text{ ohm-cm})$ .

The characteristic semiconducting properties are brought about by thermal excitation, impurities, lattice defects (in crystals), or departure from nominal chemical composition. A highly purified semiconductor exhibits intrinsic conductivity, as distinguished from the impurity conductivity of less pure specimens. In the intrinsic temperature range the electrical properties of a semiconductor are not essentially modified by impurities in the sample. An electronic band scheme leading to intrinsic conductivity is indicated in Figure 6. The conduction band is vacant at absolute zero and is separated by an energy gap Eg from the filled valence band. The band gap is the difference in energy between the lowest point of the conduction band and the highest point of the valence band. As the temperature is increased, electrons are thermally excited from the valence band to the conduction band. Both the

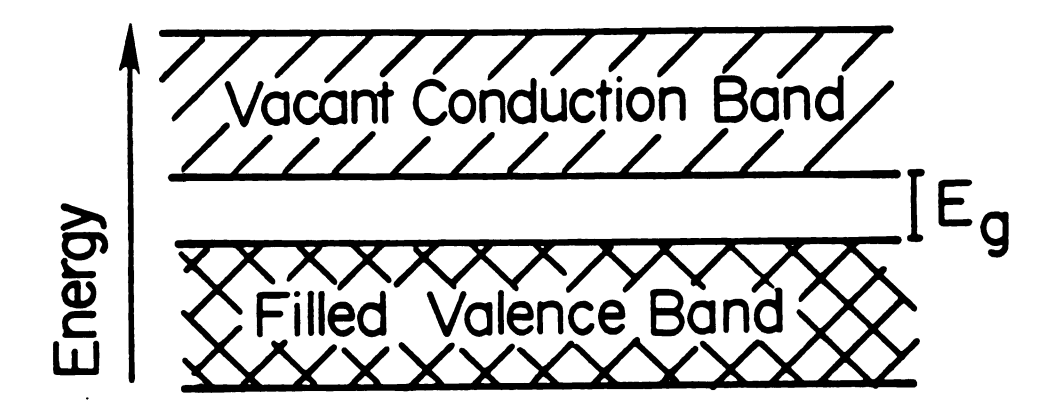


Figure 6. Band scheme for intrinsic conductivity in a semiconductor. At 0°K the conductivity is zero because all states in the valence band are filled and all states in the conduction band are vacant. As temperature is increased electrons are thermally excited from the valence band to the conduction band.

electrons in the conduction band and the vacant orbitals or holes left behind in the valence band can contribute to the electrical conductivity. The intrinsic conductivity is largely controlled by  $E_g/k_BT$ , the ratio of the band gap to the temperature via the Boltzman expression  $n_c = n_o e^{-Eg/2k_BT}$  in which  $n_c$  is the number of electrons in the conduction band and  $n_o$  is the number in the ground state.

Absorption of light can also excite an electron from the valence band to the conduction band. This process can be direct absorption of a photon or indirect absorption as shown in Figure 7 (117). Transitions occur generally between almost all points of the two bands so an absorption peak need not correspond to the band gap energy but must lie at an energy greater than or equal to the band gap. Furthermore, in the case of (Na<sup>+</sup>C222)Na<sup>-</sup> powders or films, thermal or optical excitation of an electron might occur to a trap or defect which is close to the conduction band followed by thermal or optical excitation from this trap or defect to the conduction band.

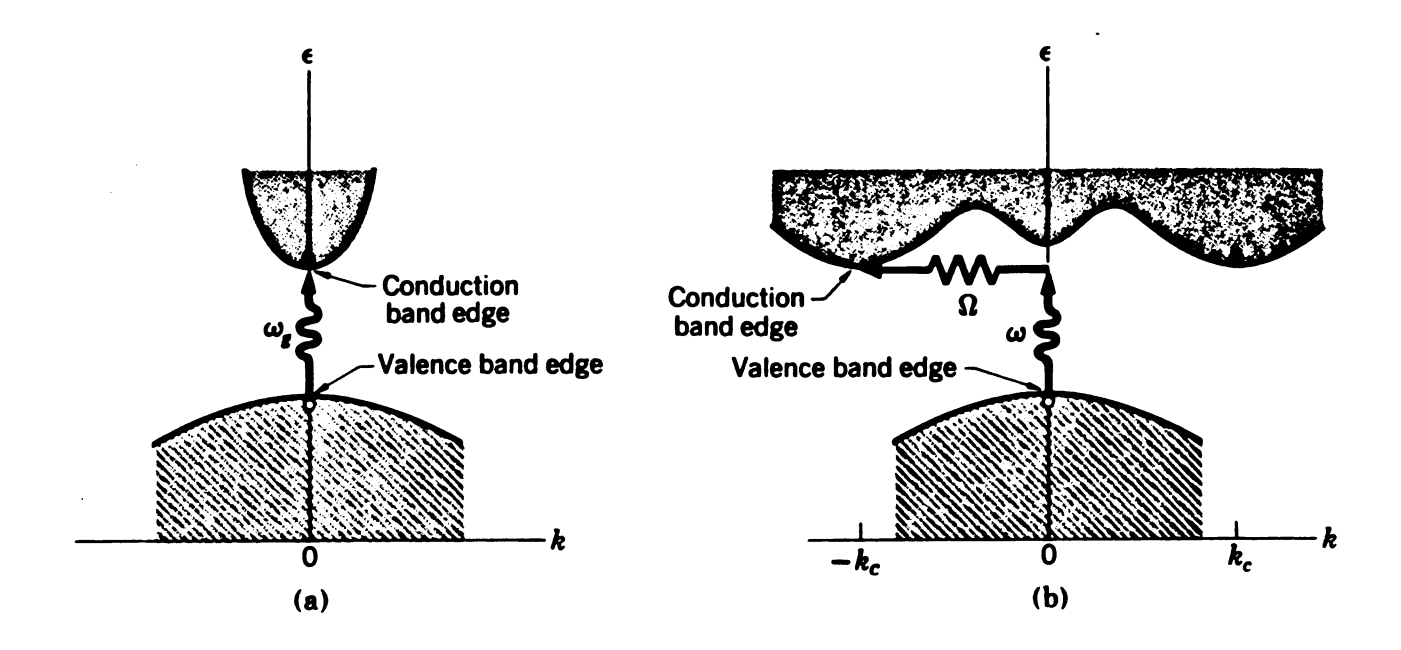


Figure 7. In (a) the lowest point of the conduction band occurs at the same value of k as the highest point of the valence band. A direct optical transition is drawn vertically with no significant change of k, because the absorbed photon has a very small wavevector. The threshold frequency  $\omega_{_{f C}}$  for absorption by the direct transition determines the energy gap  $E_{g} = h\omega_{g}$ . The indirect transition in (b) involves both a photon and a phonon because the band edges of the conduction and valence bands are widely separated in k space. The threshold energy for the indirect process in (b) is greater than the true band gap. The absorption threshold for the indirect transition between the band edges is at  $h\omega =$  $E_{G}+h\Omega$ , where  $\Omega$  is the frequency of an emitted phonon of wavevector  $K = -k_C$ . At higher temperatures phonons are already present; if a phonon is absorbed along with a photon, the threshold energy is  $h\omega=E_g-h\Omega$ . Note: The figure shows only the threshold transitions. Transitions occur generally between almost all points of the two bands for which the wavevectors and energy can be conserved.

#### EXPERIMENTAL

### II.A. Reagents

## II.A.1. Solvents

All solvents were stored in vacuum storage bottles
(Figure 8) after treatment with appropriate drying agents.
Before each use all solvents were degassed by freeze-pumpthaw cycles with liquid nitrogen.

Ammonia (NH<sub>3</sub>). Ammonia (anhydrous, 99.99%, Matheson) was treated twice with Na-K alloy (30% Na, 70% K), then transferred to a vacuum storage bottle.

Methylamine (MA). Methylamine (98%, J. T. Baker) was stirred over calcium hydride for 48-78 hours. It was then treated with Na-K alloy until the characteristic dark blue color remained for at least 72 hours at ambient temperature. If the color faded the Na-K alloy treatment was repeated after vacuum transfer of MA into a clean bottle. The dry MA was then vacuum-transferred into a vacuum storage bottle.

Ethylamine (EA). Ethylamine (anhydrous, Eastman Kodak) was treated in the same way as the methylamine.

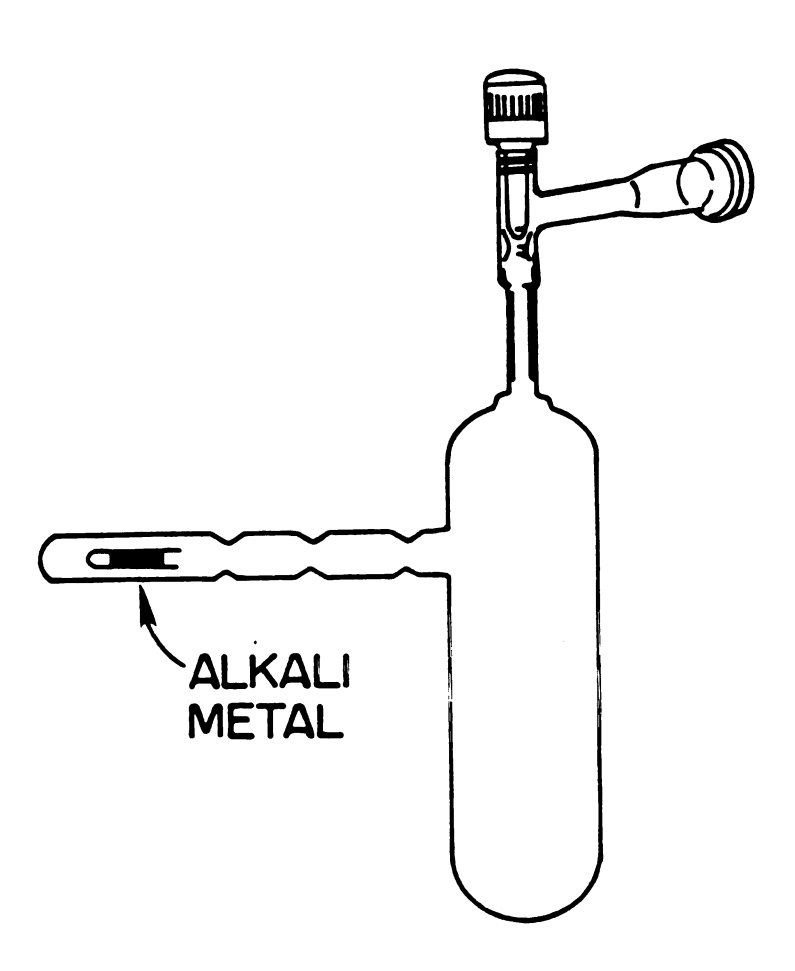


Figure 8. Vacuum bottle with sidearm for alkali metal distillation.

Isopropylamine (PA). Isopropylamine (Eastman Kodak)
was treated in the same manner as the other amines (EA
and MA).

n-Pentane. Pentane (98%, Matheson Coleman & Bell) was first dried over calcium hydride and then transferred into a vacuum bottle containing an excess of Na-K alloy over benzophenone. The blue or purple benzophenone ketyl served as a drying agent and a dryness indicator (82). If the color remained 72 hours at ambient temperature the n-pentane was vacuum transferred to a vacuum bottle with a potassium mirror. The potassium mirror was necessary to insure that no benzophenone had been transferred along with the n-pentane. If benzophenone had been transferred along with the n-pentane it would have formed the benzophenone ketyl with the potassium and turned the n-pentane blue. If no blue color occurred, the n-pentane was transferred to a vacuum storage bottle.

<u>Diethylether (DEE)</u>. Diethyl ether (anhydrous, Fisher) was treated in the same way as n-pentane.

#### II.A.2. Metals

Sodium-potassium Alloy (Na-K Alloy). Sodium and potassium metals used in the making of the Na-K alloy to dry solvents were purchased from J. T. Baker Co. Small pieces of the

metal were cut and most of the oxide was scraped off the surface. These pieces of metal were then placed into a 40 mm diameter tube containing 20 to 30 lengths of one (1) to four (4) mm diameter tubing which had been sealed at one end (Figure 9). The system was evacuated and then gradually heated under dynamic vacuum. After the metal had melted to form a pool at the bottom of the tube, helium gas was introduced (P = 0.5 to 1.5 atm) to force the molten metal up into the small glass tubes. These open-ended tubes were stored under mechanical pump vacuum to retard oxidation and subsequent deliquescent action of the oxide. To prepare the alloy, appropriate lengths of tubing, of known internal diameter, containing sodium and potassium were co-distilled under vacuum into the sidearm of the solvent bottle and finally into the bottle (Figure 8).

Sodium, Potassium, and Rubidium. These metals (Alfa-Ventron) were supplied under argon in sealed 5 gm. glass ampules with breakseals. Total purities were 99.95% for sodium, 99.95% for potassium, and 99.93% for rubidium according to the suppliers. Vacuum transfer of metal from the 5 gm. ampule to Pyrex tubes of 2-8 mm O.D. was accomplished as follows. The ampule was attached to the distribution apparatus as shown in Figure 10. The distribution apparatus was evacuated and the breakseal broken.

The metal was slowly heated under dynamic vacuum to pump

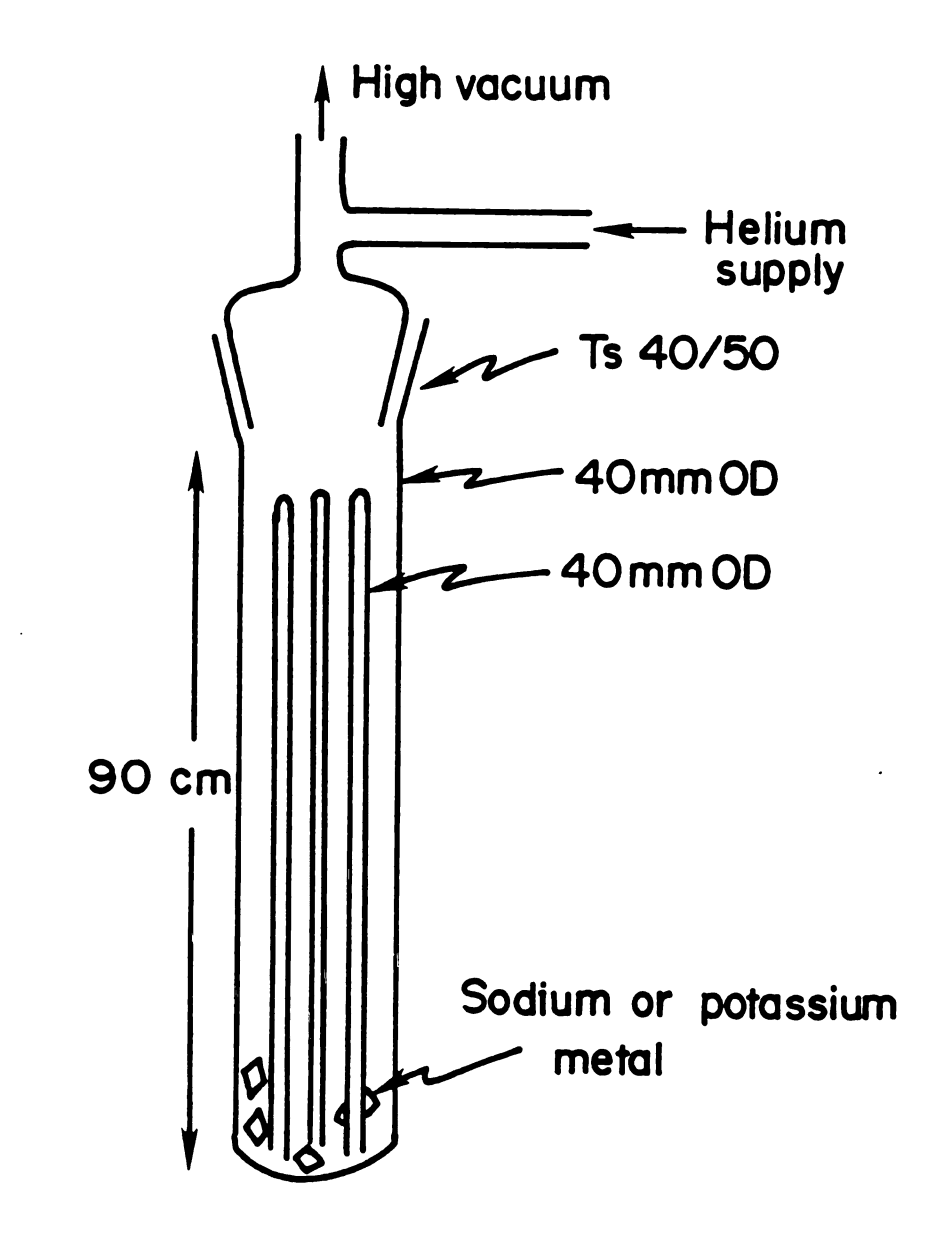


Figure 9. Apparatus for the preparation of storage tubes for sodium or potassium metal.

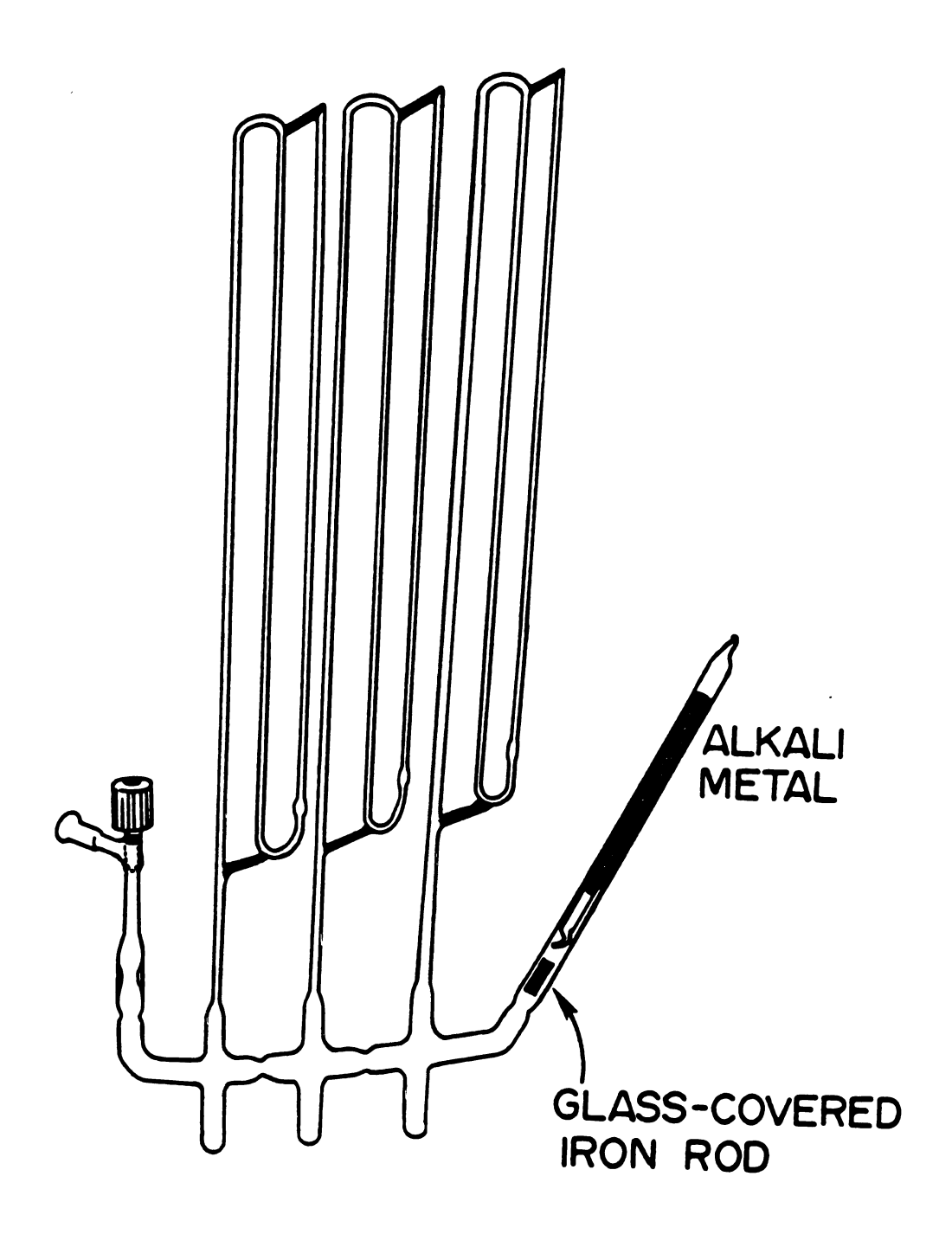


Figure 10. Apparatus for distribution of alkali metal under vacuum.

0. m ٧ T t Ε i

S

С

(

F

27 10 12

out the argon gas that had been released by the melting metal. The molten metal ran downhill to fill the reservoirs. Vacuum seal-offs were made at the constrictions. The metal was then heated and allowed to run into the small tubes attached to the reservoir. Vacuum seal-offs were made to separate the partly filled tubes of different known internal diameters.

Potassium, rubidium and cesium were always heated with a "cool" torch flame (no added tank oxygen) to avoid exchange of sodium from the glass at higher temperatures (33).

Cesium. This metal (donated by Dow Chemical Co.) was distributed from a large initial ampule (50 grams) into smaller ampules (approximately 10 grams) with breakseals. The distribution was made in an inert atmosphere box. These smaller ampules with breakseals were then distributed into tubes as described above.

### II.A.3. Complexing Agents

2,2,2-Cryptand (C222 or IUPAC: 4,7,13,16,21,24-hexa-oxa-1,10-diazabicyclo-(8,8,8)-hexacosane). 2,2,2-cryptand was manufactured by E. Merck, A. G., Germany, and purchased from PCR, Inc. It was further purified by recrystallization from hexane followed by a high-vacuum sublimation.

The sublimed product was stored in the dark under mechanical pump vacuum. The melting point was  $68-69^{\circ}$  (Lit. (124):  $68-69^{\circ}$ ).

18-Crown-6 (18C6 or IUPAC: 1,4,7,10,13,16-hexaoxy-acyclooctadecane). 18-Crown-6 (PCR, Inc.) was recrystallized from warm acetonitrile to give a crown acetonitrile complex (83). 18-Crown-6, obtained from vacuum decomposition of the acetonitrile complex, was sublimed under high-vacuum at ~100°C. The white product had a melting point of 39°C (lit. (84): 39-40°). The sublimed 18-Crown-6 was stored in the dark under mechanical pump vacuum.

# II.A.4. Miscellaneous Reagents

Aqua Regia,  $HC1/HNO_3$ . Aqua regia was prepared by mixing three parts hydrochloric acid (HCl) with one part nitric acid (HNO<sub>3</sub>). All acids were reagent grade.

 $\underline{\text{HF/HNO}_3/\text{Detergent Solution}}$ . The HF glass cleaner was 33%  $\underline{\text{HNO}_3}$  (16  $\underline{\text{M}}$ ), 5% HF (28  $\underline{\text{M}}$ ), 2% acid soluble detergent, and 60% distilled water, by volume (85). All acids were reagent grade.

Conductivity Water. House distilled water was deionized (Crystlab Deeminizer) and distilled in glass with a high reflux ratio through a 70 cm column packed with

i

þ

12

C

c:

13

щe

ri

ri

fi

re

7 cm lengths of glass tubing. Final storage was in a sealed polypropylene container.

1,4-Diazabicyclo[2.2.2]Octane (DABCO). This bicyclic compound (Aldrich, 97%) was recrystallized twice from warm acetone to give white crystals which were sublimed. The hygroscopic crystals were handled in an inert atmosphere before and after sublimation.

Mercuric Sulfide (HgS). Mercuric sulfide was purchased from J. T. Baker Chemical Co. as a Baker Analyzed Chemical reagent lot number 103045. It was used without further preparation.

Titanium Dioxide (TiO<sub>2</sub>). Titanium dioxide was purchased from J. T. Baker Chemical Co. as a Baker analyzed chemical reagent lot number 28365. It was used without further preparation.

# II.B. Glass Apparatus Cleaning

Apparatus which contacted solutions with dissolved metals was cleaned as follows. The apparatus was first rinsed with HF/HNO<sub>3</sub>/detergent solution, followed by six rinses with distilled water. The apparatus was then filled as full as possible with freshly-prepared aqua regia. This was allowed to stand overnight (12 to 24

a

hours). The vessel was then emptied, rinsed six times with distilled water and six times with conductivity water, and oven dried overnight at 120-135°C. For particularly unstable solutions or for final cleaning of apparatus which had silver electrodes (and hence could not be cleaned with aqua regia) an extra step was added. Conductivity water was heated to boiling in the partially filled apparatus prior to oven drying.

## II.C. Greaseless High Vacuum System

A greaseless, all Pyrex vacuum manifold was evacuated through a liquid nitrogen trap by using an oil diffusion pump (Varian M4, Dow-Corning 704 oil) backed by a two-stage mechanical pump (Cenco HV-7). Exclusive use of Teflon vacuum stopcocks (Kontes No. K-826610) and five or nine-millimeter Solv-Seal glass joints with Teflon seals (both joints and seals from Lab-Crest Division, Fischer and Porter Co. No. 571-190) permitted routine working pressures to 1 x 10<sup>-6</sup> torr possible on the manifold and on individual apparatuses. The manifold was continuously heated to about 70°C with heating tape. Pressure measurements were made with a Veeco RG 75p glass ionization tube and an RGLL6 control unit.

# II.D. <u>Inert Atmosphere Box and Glove Bags</u>

## II.D.l. Inert Atmosphere Box

An inert atmosphere box gas recirculation and purification system was constructed similar to that described by Ashly and Schwartz (86). Oxygen, H<sub>2</sub>O, and certain hydrocarbons were removed from the Argon atmosphere by the purification system.

Diffusion of air and water vapor through the gloves was a major source of contamination, even though special elastomers were used for the gloves (87). Since the box was evacuable this daily diffusion could be reduced by pushing the gloves into the box and sealing the glove ports. The gloves could then be flushed with box atmosphere, thus greatly reducing the surface area of elastomer exposed to air diffusion.

## II.D.2. Glove Bags

Plastic glove bags (purchased from I<sup>2</sup>R) with a dry nitrogen atmosphere were also used. The tank nitrogen was dried by passing it through Drierite and 5A molecular sieves (Alltech Associates).

These glove bags were used in place of the inert atmosphere box in two instances. First if the experiment required the use of liquid nitrogen, which would contaminate the argon atmosphere of the box, and second if the

experimental apparatus was so large that the air lock of the box could not accommodate it. Glove bags were used successfully if none of the compounds were nitrogen sensitive and if care was taken not to introduce water into the bag on cold items.

## II.E. Sample Preparation and Instrumental Techniques

# II.E.l. (Na<sup>+</sup>C222)Na<sup>-</sup> Preparation

The synthesis of crystals of (Na<sup>+</sup>C222)Na<sup>-</sup> involves many general techniques used in preparing other samples and will be described in detail (75). The apparatus in Figure 11, having been cleaned as described earlier, was ready for reagent loading. Sodium in the mg range was prepared and introduced as follows. The sodium stock, sealed under vacuum in tubes of known internal diameter (see Reagents), was heated until a length of metal occupied one end of the partially filled tube. A seal-off was then made, giving a known amount of clean metal. The amount of sodium was determined by volume and density. This ampule of sodium was scored with a glass-knife and placed in the apparatus sidearm. A piece of shrink tubing (Flo-Tite tubing, Pope Scientific Co.) was heat-sealed onto the end of the side-The other end of the shrink tubing was sealed onto a short piece of glass tubing which had been sealed at one end.

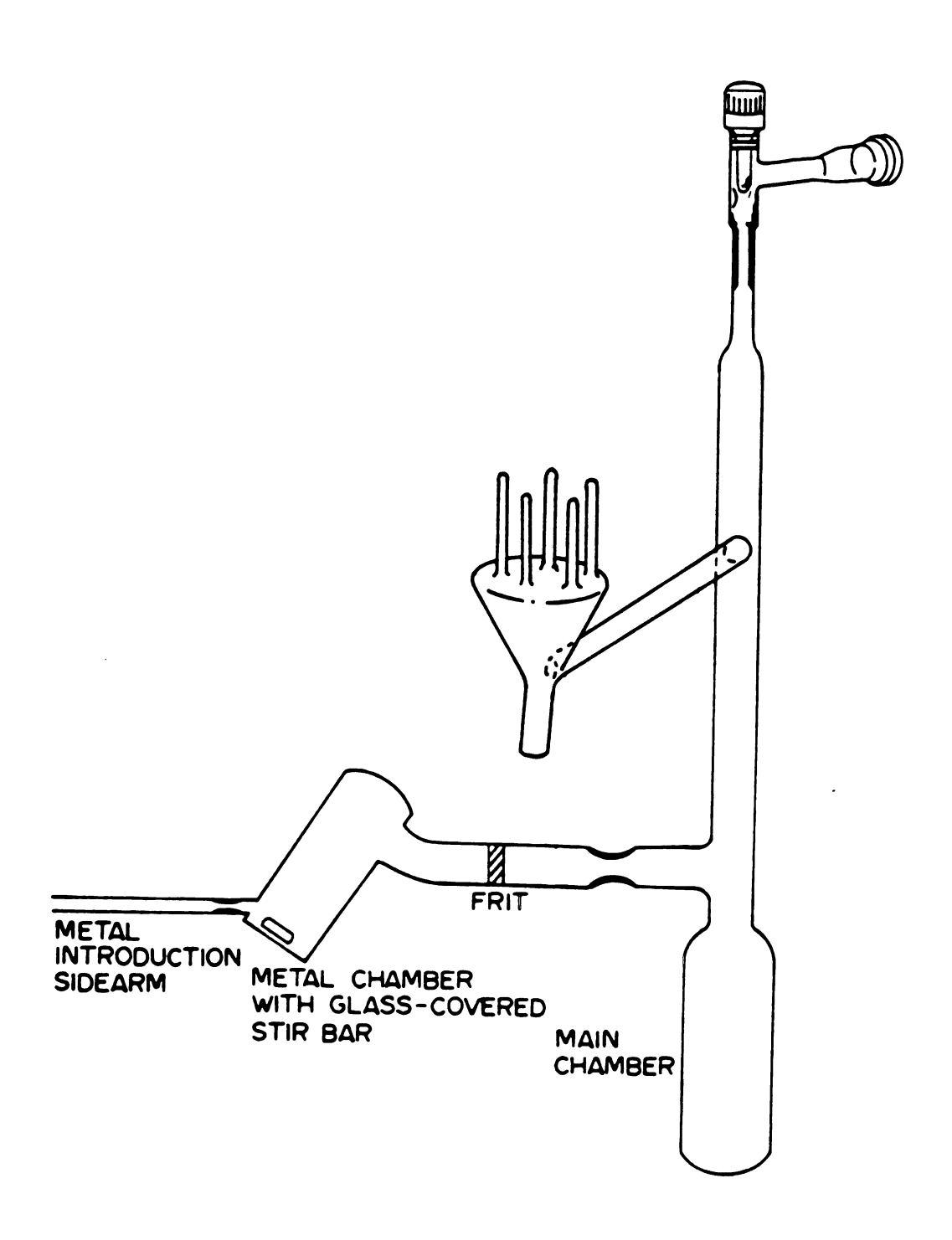


Figure 11. Apparatus for preparation of (Na<sup>+</sup>C222)Na<sup>-</sup> crystals.

A weighed amount of C222 was introduced through the valve and the valve stem was inserted. The apparatus was pumped down to  $\sim 10^{-5}$  torr and left overnight under a static vacuum. With the valve shut and the apparatus off the vacuum line, the sidearm was bent at the Teflon connection which contained the sodium ampule. This procedure broke the ampule as shown in Figure 13. The broken ampule was shaken down the sidearm until it was close to the constriction. The apparatus was then returned to the vacuum line and the shrink-tubing end of the sidearm was removed by a glass seal-off under a dynamic vacuum of  $\sim 10^{-5}$  torr. The apparatus and the solvent bottle were attached to a vacuum tee (Figure 12) which was connected to the vacuum manifold. With the apparatus and tee under dynamic vacuum, the sodium was distilled into the metal chamber (Figure 11) and a seal-off was made at the constriction. With the tee valve shut, ethylamine was condensed into the main chamber from the solvent bottle through the tee by chilling the main chamber with liquid nitrogen. Use of the vacuum tee for all solvent distillations is very important, since it prevents contamination of the high-vacuum manifold. With the apparatus valve shut, the apparatus was removed to a large ice-water bath. Using the ice-water bath and a cheesecloth "baster", the glass in contact with the reactive solution was kept cold and solution decomposition was minimized. The ethylamine cryptand solution was poured

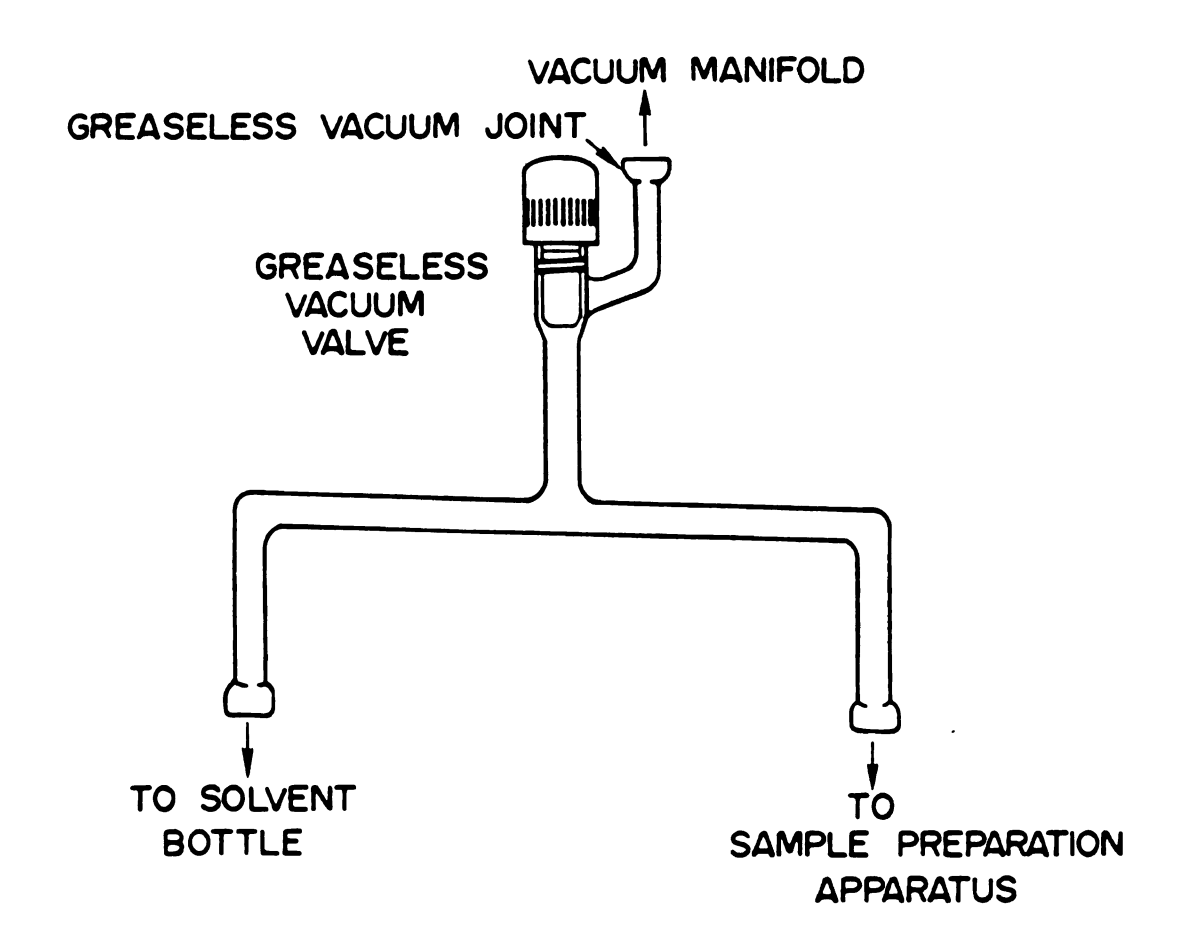


Figure 12. Vacuum tee used.

over the sodium mirror. A dark blue solution formed immediately. In order to collect any cryptand which remained on the walls of the main chamber, the blue solution was poured back and forth between the metal and main chambers.

The stoichiometric amount of sodium mirror was dissolved by agitating the solution over the mirror for a few hours at 0°C. The solution was then poured back into the main chamber for crystal growth at -78°C. The frit prevented sodium mirror flakes from entering the main chamber during the various pouring operations.

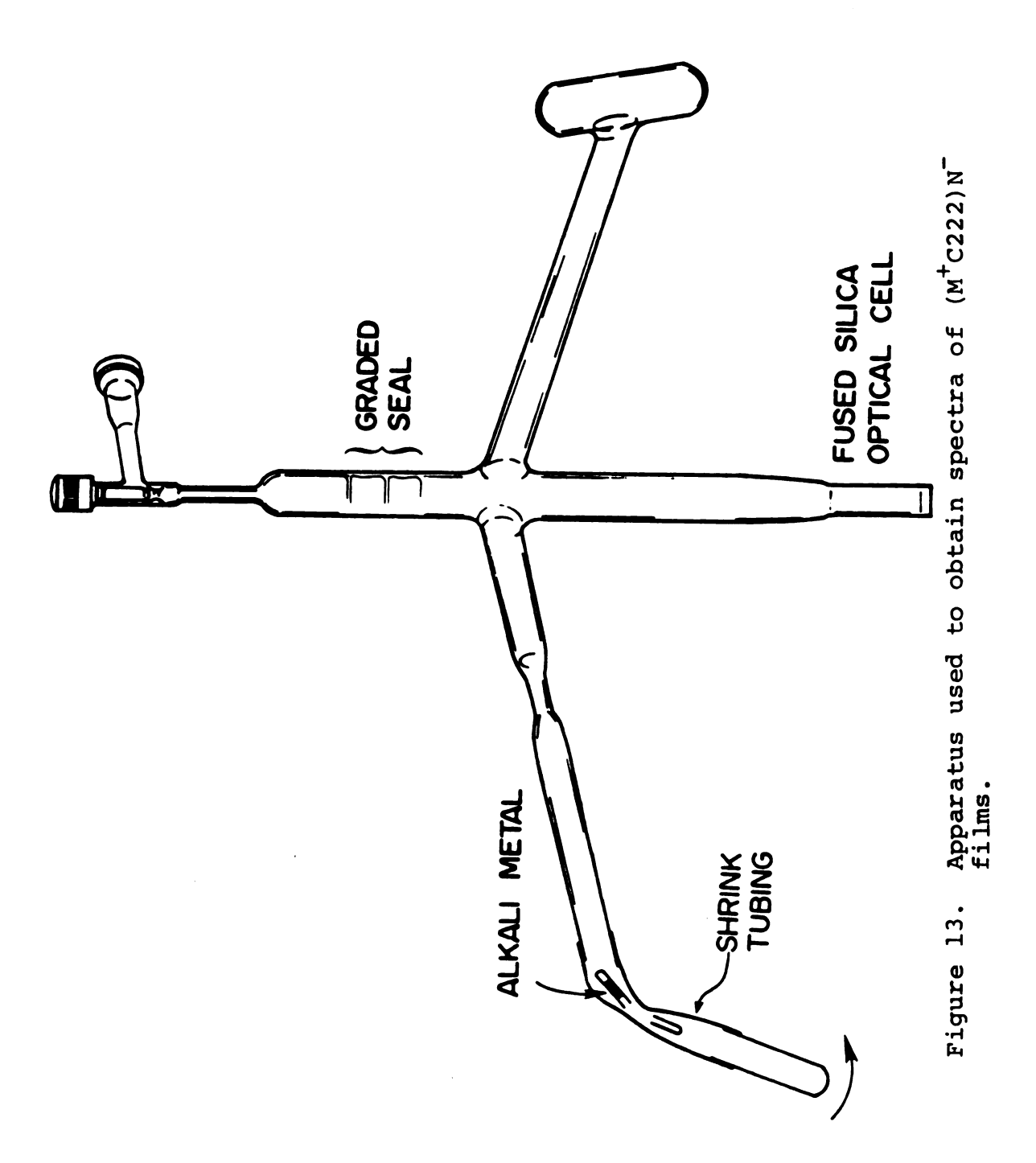
Crystals developed as the solution stood overnight at -78°C. The solution was decanted into the metal chamber and frozen with liquid nitrogen. The constriction next to the frit was then sealed off under dynamic vacuum with the crystals in the main chamber at -78°C. Diethylether was condensed onto the crystals and the slurry was transferred to the upper chamber. The ether was then used to wash the crystals five or six times. The ether was frozen in the main chamber and the crystals pumped while they were at 0°C. A seal-off was then used to separate the frozen ether from the apparatus. The upper chamber was then turned over and the dry crystals were distributed among the tubes. The tubes containing crystals were placed in liquid nitrogen and a glass seal-off separated each partially filled tube from the apparatus. The crystals were kept at -30°C until they were used.

## II.E.2. Optical Spectra

Solutions were prepared in the apparatus shown in Figure 13. Spectra of films made from these solutions were obtained through the optical cell on the apparatus. The apparatus was constructed of fused silica except for the sodium borosilicate valve and connecting graded seal. Fused silica was used to avoid the well-known sodium exchange contamination of alkali metal solutions in contact with sodium borosilicate glass (28,33).

Appropriate amounts of metal, solid complexing agent (complexer) and solvent were loaded into the apparatus by using the techniques described in the last section, except that to prevent breakage the solvent must not be frozen in the optical cell. Ethylamine or methylamine was used as the solvent for most samples. Solutions were made such that the complexer concentration was about 0.05 M. The solutions were handled at -25°C and below in a large isopropanol bath cooled with dry ice.

Films were formed in the optical cell by first pouring most of the solution into the reservoir. While freezing the bulk of solution with liquid nitrogen, the cell was kept in a cold isopropanol bath and shaken vigorously. The vigorous shaking was done to splash solution onto the optical cell window, which resulted in the flash evaporation of the solvent and the formation of a film on the window. This process was repeated until a film was formed



which had a maximum absorbance of 2 or below.

To check the quantity of solvent remaining in the films from methylamine solutions, an analysis was made on D<sub>2</sub>O solutions of powders prepared under conditions similar to those of film formation. Films of (Na<sup>+</sup>C222)Na<sup>-</sup>, (K<sup>+</sup>C222)K<sup>-</sup>, and two films of (Na 18C6) Na , prepared under different conditions, were tested. Patrick Smith determined the methylamine/cryptand mole ratio by using proton magnetic resonance (PMR) (Bruker Model WH-180). The detection limit is a ratio of 0.001. A mole ratio of <0.002 was found for the powder from a (Na<sup>+</sup>C222)Na<sup>-</sup> solution and <0.2 was found for powder from a (K+C222)e\_solv solution. One of the (Na+-18C6)Na powders was formed in the usual manner for a "dry" The other was made by cooling the bulk solution with a bath at about -40°C instead of liquid nitrogn to give a "wet" film. A mole ratio of <0.05 was found for the "dry" powder and ∿1.0 for the "wet" powder. No impurities or decomposition products were seen in the PMR spectra. Therefore, the "dry" films were essentially free of solvent and were stoichiometrically identical to the solute.

The spectra were obtained with a double beam recording spectrophotometer (Beckman DK-2A) capable of scanning from the infrared to the ultraviolet. With an arrangement similar to that used by Douthit (88), the optical cell and film could be maintained at a constant temperature ranging from 0°C to -70°C. A thermocouple placed near the cell provided the signal for temperature readout (Doric Model

DS-350).

The spectra were obtained with air in the reference beam and were baseline-corrected by subtracting either the spectrum of an empty quartz cell or that of a decomposed In either case the general spectral features were The observed baseline may shift due to light the same. scattering, so the lowest absorbance in each spectrum was arbitrarily set to zero. Each spectrum was then normalized to the highest absorbance, and appears as A/A max in the figures which show spectra. Because of these problems, the spectral shapes are only qualitative in nature. The true shapes are probably somewhat different, particularly because thickness variations in the films could not be avoided. When the thickness varies over the region sampled by the optical beam the shape can be distorted, especially at high absorbances. Accordingly, film thickness which gave maximum absorbances between 1.0-1.5 were preferred.

## II.E.3. Film Conductivity

The films used for D.C. conductivity measurements were prepared in the same manner as those used for optical spectra. The films were prepared in an apparatus which had four parallel silver lines on the glass to act as electrical contacts (Figure 14). The films were deposited in such a way that they formed across all four silver lines in an isolated area. The silver lines were 20 cm long,

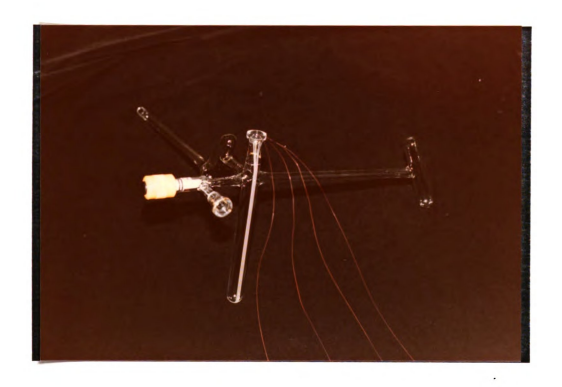
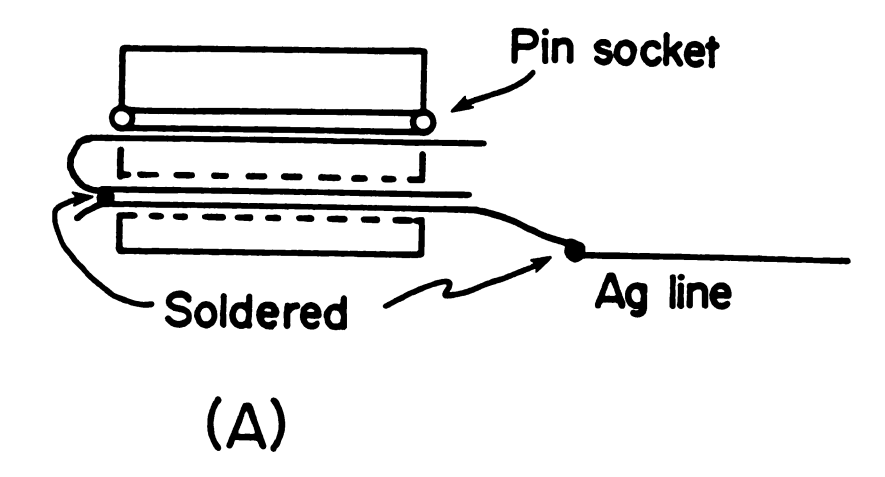


Figure 14. An apparatus with four parallel silver lines on the glass to act as electrical contacts for film conductivity.

0.05 cm wide, and spaced 0.01 cm apart. The silver lines were applied to the inside of the apparatus by decal (Decalcraft). The apparatus with the decal in place was then fired in an annealing oven, resulting in four metallic silver lines bonded to the glass. The fired decal leaves only silver and glass behind, which was found to be compatible with (Na<sup>†</sup>C222)Na<sup>†</sup>/ethylamine and Cs<sup>†</sup>C222Cs<sup>†</sup>/ethylamine solutions. Contacts to the four silver lines had to be made so that leads could be attached to instruments outside the apparatus, while still maintaining a vacuum of  $\sim 10^{-5}$  torr inside the apparatus. This was accomplished by tungsten wires sealed through a 9 mm solv-seal joint which fitted into four brass pin-sockets in a Teflon plug. Each socket was soldered to a short piece of copper wire (34 Ga) which in turn was soldered to a silver line (Figure 15). Finding the proper conditions for attaching the silver lines and the leads was a major bottleneck in this research and required a large number of attempts.

The D.C. electrical conductivity and band gap of films were determined by potential-probe measurements (4 probe) and/or voltmeter-anmeter (V-I) measurements (2 probe) (Figure 16) (89). The tungsten wires were attached to shielded leads which were then attached to a Keithley 610 BR electrometer and a Heathkit Regulated L.V. power supply in the appropriate circuit (Figure 14a and 14b). Data were then collected for an Ohm's law plot, voltage vs current, and a log R vs 1/T plot.



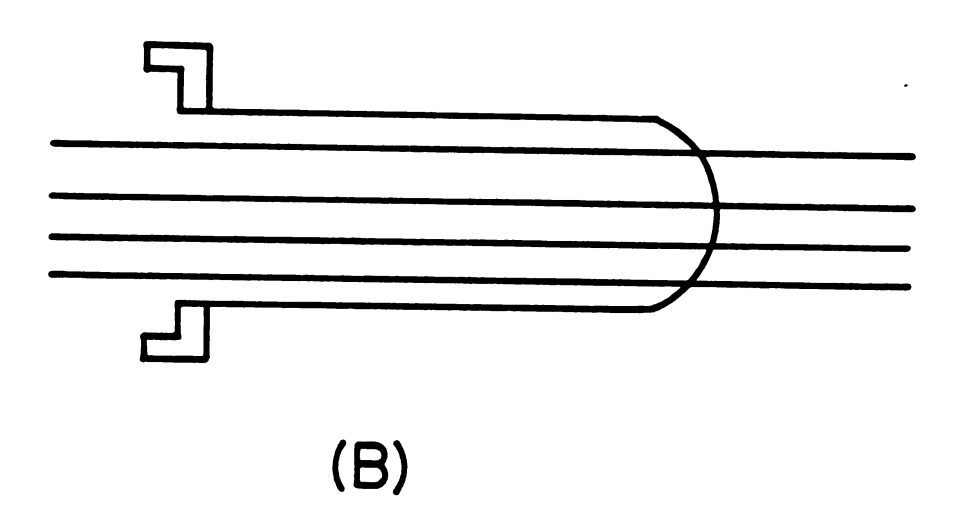


Figure 15. The male and female parts of the vacuum electrical connector. (a) Teflon plug connector which connects the silver lines to the tungsten wire. (b) 9 mm Fisher-Porter cap with four tungsten wires sealed in its glass which plugs into the teflon plug.

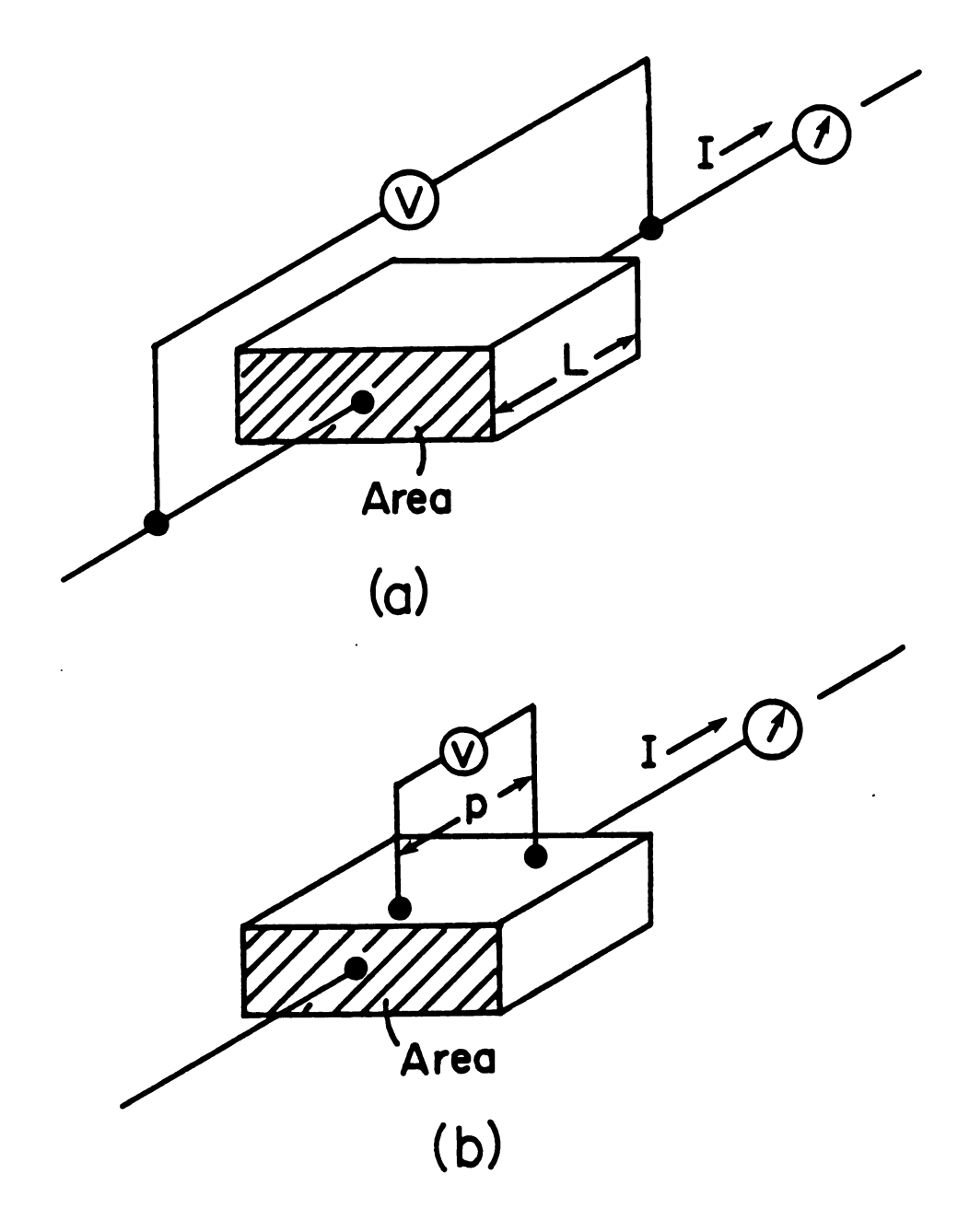


Figure 16. (a) Arrangement for resistance measurement by potential-probe method. (b) Arrangement for resistance measurement by V-I method.

## II.E.4. Pressed Powder Conductivity

Powdered samples of (Na<sup>+</sup>C222)Na<sup>-</sup>, (K<sup>+</sup>C222)Na<sup>-</sup>, (Rb<sup>+</sup>-C222)Na<sup>-</sup>, (Cs<sup>+</sup>18C6)e<sup>-</sup>, (Li<sup>+</sup>C211)e<sup>-</sup> and (Cs<sup>+</sup>18C6)Na<sup>-</sup> were prepared as described earlier for (Na<sup>+</sup>C222)Na<sup>-</sup> (see Section II.E.1). Some of the powdered samples were supplied by other researchers in our group (90). The D.C. conductivity and band gap of the pressed powders were determined by the voltmeter-ammeter method (V-I).

Two similar pieces of apparatus were used in the determination of the conductivity and band gap of the various powdered samples. The first apparatus (referred to as the pressed powder cell or cell A) is shown in Figure 17. pressed powder cell was basically a brass tube with a screw cap which pressed two electrodes together. The electrodes were round aluminum plates, 2.54 cm in diameter and 0.64 cm thick, with a copper post which protruded outside the brass tube. One electrode had a cylindrical post 0.32 cm high and 0.475 cm in diameter. The other had a cylindrical depression, 0.30 cm deep, into which the post fit tightly. The sides of the depression were lined with Teflon to prevent shorts between the two electrodes. The depression was loaded with powder and the cell assembled in an inert atmosphere box at ambient temperature. The sample area of the assembled cell was rendered air tight by Teflon plugs fitted with Neoprene "O"-rings. The cell was removed from the inert atmosphere box and placed in an

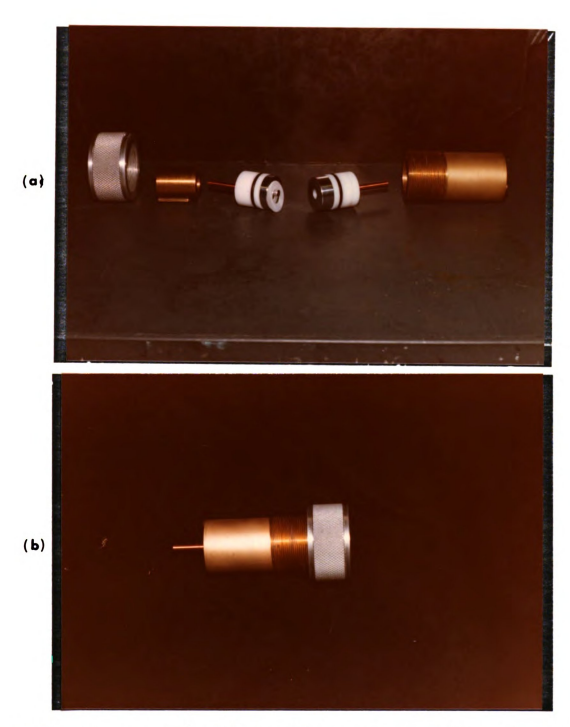


Figure 17. The pressed powder cell or cell A. (a) Open cell. From left to right the parts are: Cap: used to apply pressure to electrodes by screwing it tightly on the body. First electrode: with cylindrical post and its teflon and "o" ring seals. Second Electrode: with cup for powder sample. Brass body: into which all the rest fit. (b) Closed cell.

Po

Th ce

c.

e1,

Th

mak

Was

insulated container, which was cooled by dry ice. Leads from the copper posts were attached to a Heathkit variable voltage supply and a Keithley 610 BR electrometer. The temperature of the sample was determined with a copperconstantan thermocouple attached to one of the copper posts as close to the aluminum plate as possible.

This first pressed powder cell had three drawbacks:

- (1) The size of the powdered sample was unnecessarily large.
- (2) The inert atmosphere box had no provisions for keeping the sample and apparatus below ambient temperature during assembly. This made the system impractical for most samples which were less stable than (Na<sup>+</sup>C222)Na<sup>-</sup>.
- (3) The pressure applied to the sample by the screw cap was unknown.

It was therefore necessary to design a second pressed powder cell and companion inert atmosphere cooling jacket. This pressed powder cell (referred to as the cold jacket cell, c.j.c., or cell B) is pictured in Figure 18. The c.j.c. confined the powder between two stainless steel electrodes inside a 2 mm I.D. heavy wall quartz capillary. This greatly reduced the amount of powder necessary to make a voltage-current measurement. Also the pressure was applied to the powder by means of a steel spring. By

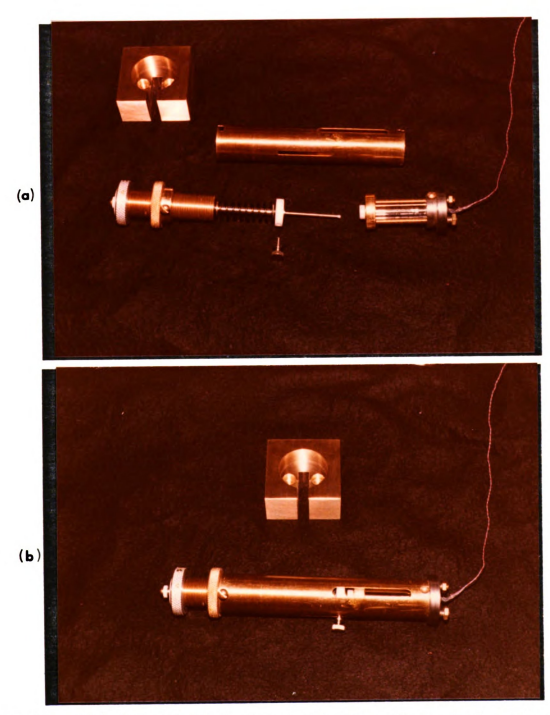


Figure 18. (a) Open cold jacket cell or cell B showing the stainless steel plunger in the top assembly and the quartz capillary in the bottom assembly.

Above these is the cylindrical outer body and brass stand. (b) Closed cell B with brass stand above it.

measuring the spring constant and the compression of the spring the force applied to the powder could be calculated.

The cooling jacket (Figures 19 and 20) was designed to do two things. First, to control the temperature of the sample from 50°C to -100°C, and second to bathe the cell in an inert atmosphere. The temperature was maintained or changed by changing the temperature of the nitrogen gas flowing through the cooling jacket (Figure 19). nitrogen temperature was controlled by a Varian V-4540 variable temperature controller. The nitrogen flowing over the Pt temperature sensor and the heater was a variable mixture of compressed tank N2 and cold N2 boiled-off from a pool of liquid nitrogen. The temperature controller was needed to stabilize the more temperature-sensitive compounds and to obtain data for the log R vs 1/T plots. The inert atmosphere sheath was necessary because the cell was not gas tight. The flow of nitrogen in the cooling jacket was such that the jacket could be opened to the room atmosphere so adjustments to the cell could be made.

Since the powders are air sensitive and the cell was not air tight the loading of the sample, assembly of the cell and the placing of the cell into the cooling jacket had to be done under an inert atmosphere. The cooling jacket was too large to be conveniently used in the argon inert atmosphere box, so a glove bag, using dry nitrogen gas, was used instead. The glove bag had the added advantage that



Figure 19. Cooling jacket for Cell B. Picture looking down the inside of the cooling jacket and top.

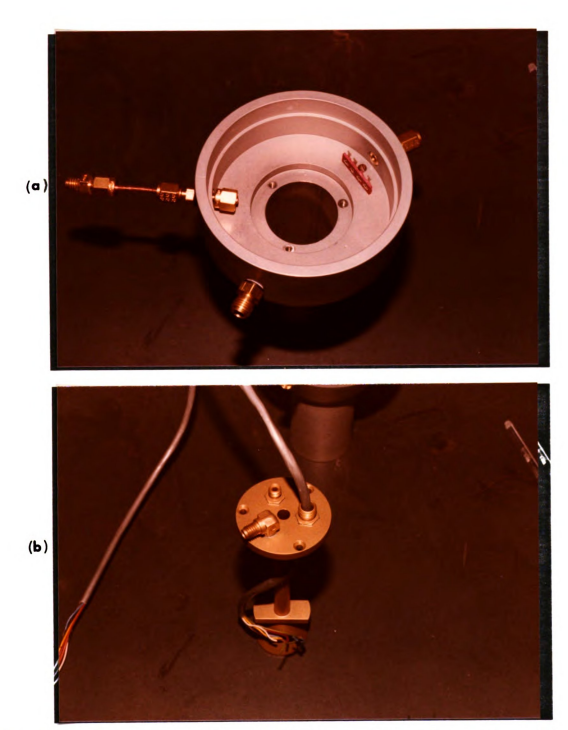


Figure 20. (a) The base on which the cooling jacket sets.
(b) Insert which fits in the center hole in the base. Through this insert the cooling gas passes by a platinum temperature sensor and a small heater.

lig

ter

col

tha

liquid nitrogen could be used to keep the powdered sample cold. This allowed measurements to be made on the more temperature sensitive sodides and electrides. Thus the cold jacket cell could be used with a wider range of salts than could the pressed powder cell.

#### OPTICAL SPECTRA

The bright metallic "gold" color of (Na<sup>+</sup>C222)Na<sup>-</sup> solid and films which formed on the vessel walls during preparation of the solid prompted a great deal of interest in obtaining the optical spectra of this compound. As other films were observed while preparing other compounds of the general types (M<sup>+</sup>C)M<sup>-</sup>, (M<sup>+</sup>C)N<sup>-</sup> and (M<sup>+</sup>C)e<sup>-</sup> their color also increased interest in the optical absorption spectra. The absorption spectra of the various compounds were obtained by preparing a thin film of the compound on the side of an optical cell. The films were formed by rapid evaporation of solutions splashed onto the sides of the optical cell (a more detailed description of the method used is given in Section II.E.2).

This method of obtaining an absorption spectrum had some limitations. First a thin reasonably stable film has to form when the solvent is evaporated. The film must be thin enough to allow the analyzing beam to pass through, with best results achieved when the maximum absorption is less than about 1.5. Another limitation is the distortion of the absorption peak shapes by the inability to form films of uniform thickness across the optical cell face (see Appendix B).

## III.A. M/C222 Films

Most of the optical studies described here are of solvent-free (dry) films made from amine solutions containing M<sup>+</sup>C222 (abbreviated as M<sup>+</sup>C) and M<sup>-</sup> where M is Na, K, Rb, or Cs. The solvent was removed by evaporation into a side-arm trap kept at liquid nitrogen temperatures.

# III.A.1. Na/C222 Films From Ethylamine Solutions

Films made from ethylamine solutions containing sodium and 222-cryptand were blue in color by transmission and gold-bronze by reflection. The (Na<sup>+</sup>C)Na<sup>-</sup> film spectrum, shown as the solid line in Figure 21, has three features: the main absorption at 15,400 cm<sup>-1</sup> (~650 nm), a shoulder at 18,900 cm<sup>-1</sup> (~530 nm), and a small but distinct peak at 24,500 cm<sup>-1</sup> (~410 nm). In contrast, the three spectra of (K<sup>+</sup>C)K<sup>-</sup>, (Rb<sup>+</sup>C)Rb<sup>-</sup>, and (Cs<sup>+</sup>C)Cs<sup>-</sup> from methylamine solutions, exhibit only one main band as shown in Figure 22. These bands are tabulated and compared to M<sup>-</sup> bands in ethylenediamine, EDA, (99) in Table 2. The EDA M<sup>-</sup> band positions are marked by arrowheads in Figure 22.

It was of interest to determine whether the shoulder and high energy peak (18,900 cm<sup>-1</sup> and 24,500 cm<sup>-1</sup>) observed with Na<sup>+</sup>C·Na<sup>-</sup> were characteristic only of Na<sup>-</sup> or whether they depend upon the counterion, Na<sup>+</sup>C222. It was expected that a solution of K<sup>+</sup>C222 and Na<sup>-</sup> could be prepared

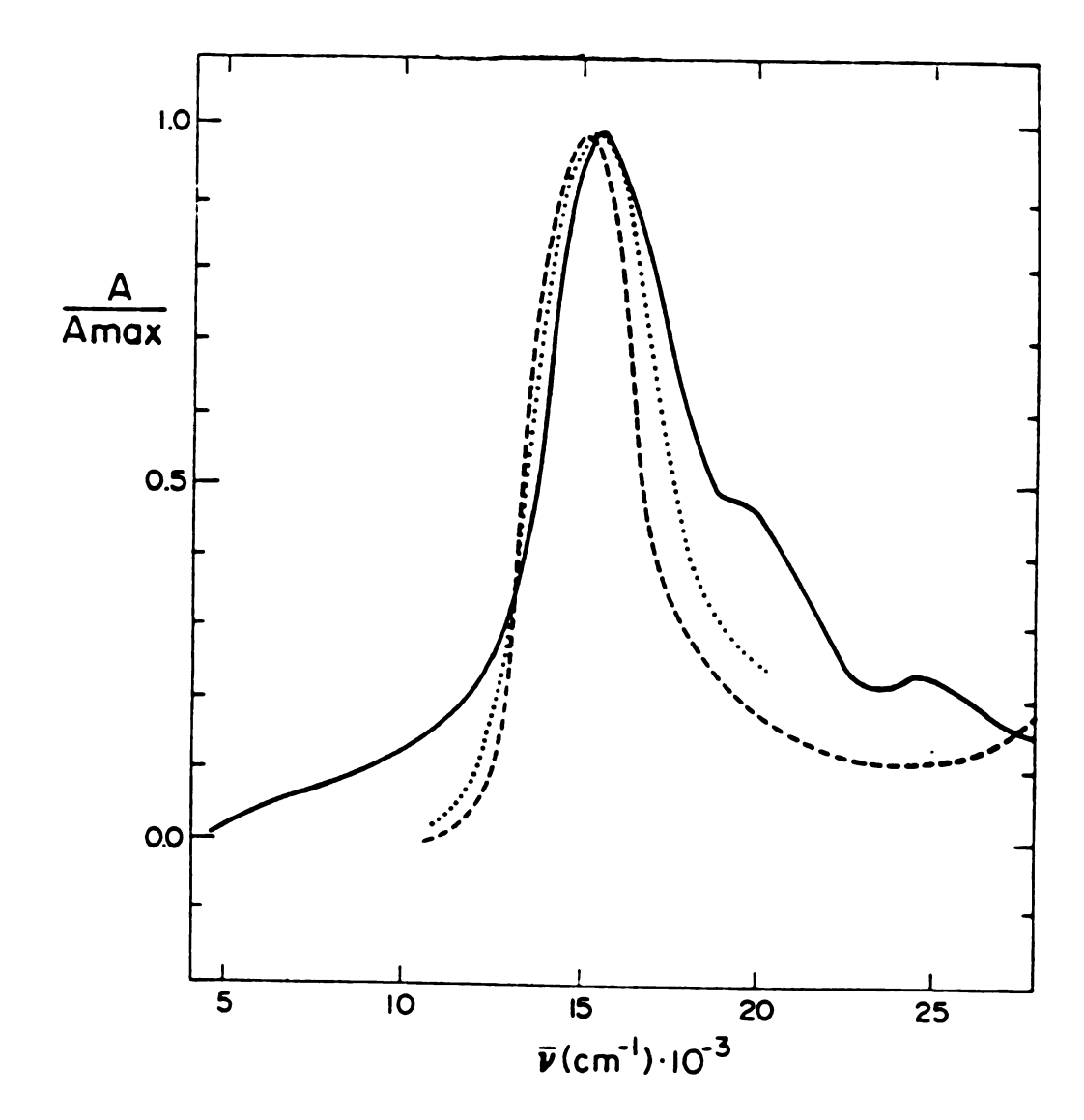


Figure 21. Baseline-corrected normalized spectra of the sodium anion under various conditions: solid line, (Na+C222)Na- film from ethylamine; dashed line, (K+C222)Na- film from methylamine; dotted line, Na- in ethylenediamine.

7

ire

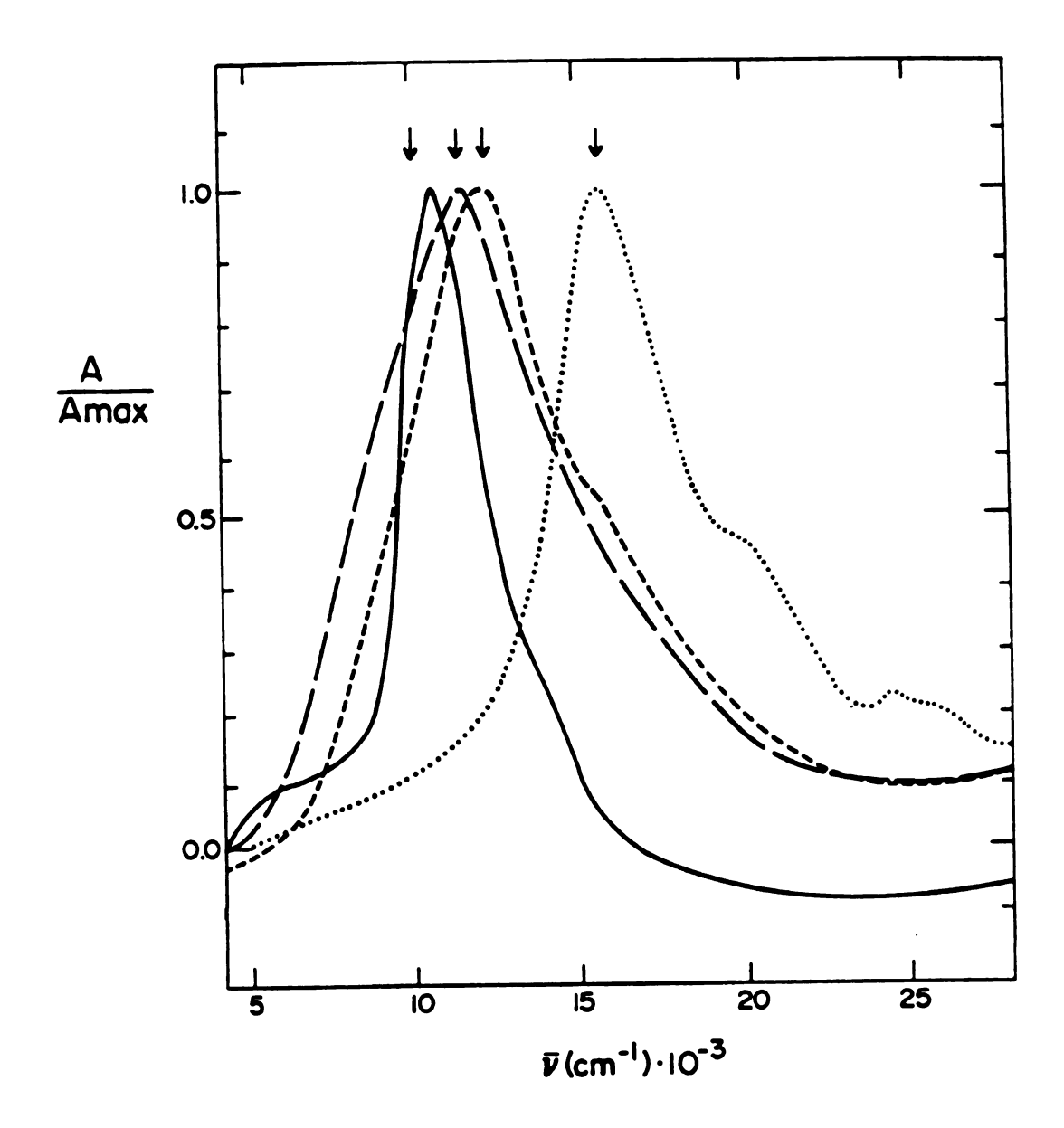


Figure 22. Spectra of films prepared by evaporation of methylamine solutions which contain M+C222 and M-: from left to right (peak positions) M = Cs, Rb, K, Na, respectively. The arrows indicate the position of the absorption maxima for the corresponding anions in ethylenediamine.

Tabl			
Idbi			
=			

Table 2. Comparison of Alkali Metal Anion Peak Positions in Solid Films from Methylamine and in Metal-EDA Solutions.

	Solid Film	EDA Solution (20)
Na T	15,400 cm <sup>-1</sup> (650 nm)	15,400 cm <sup>-1</sup> (650 nm)
к <sup>-</sup>	11,900 cm <sup>-1</sup> (840 nm)	12,000 cm <sup>-1</sup> (833 nm)
Rb	11,600 cm <sup>-1</sup> (860 nm)	$11,200 \text{ cm}^{-1}$ (893 nm)
Cs <sup>-</sup>	10,500 cm <sup>-1</sup> (950 nm)	$9,800 \text{ cm}^{-1}$ (1,020 nm)

by allowing a C222 solution to contact Na and K metals. The reasoning was as follows:

- (1) The addition of Na<sup>+</sup> to a solution of K<sup>-</sup> causes

  Na<sup>-</sup> and K<sup>+</sup> formation; i.e., Na<sup>-</sup> is thermodynamically
  favored over K<sup>-</sup> (28,33).
- (2) Cryptand C222 binds K<sup>+</sup> more strongly than Na<sup>+</sup> (101).
- (3) A C222 solution upon prolonged contact with both Na and K, shows only the Na signal and no Na C222 signal in the 23Na NMR spectrum (115).

The film absorption spectra of  $(K^+C)Na^-$  and  $(Na^+C)Na^-$  are shown in Figure 21. For  $(K^+C)Na^-$  the Na $^-$  peak was red-shifted by  $\sim 300$  cm $^{-1}$  from the Na $^-$  peak in  $(Na^+C)Na^-$  and the shoulder and high energy peak were absent. The Na $^-$  spectrum of sodium dissolved in ethylenediamine is also shown (91).

The position of the Na¯ maximum and the peak width at half-height for Na¯tc·Na¯ were slightly temperature-dependent. The position of the maximum shifted to the red with increasing temperature with  $d\bar{\nu}/dT \approx -1.6$  cm $^{-1}$  deg $^{-1}$ . The width at half-height increased by  $\sim 1.1$  cm $^{-1}$  deg $^{-1}$ .

# III.A.2. M/C222 Films from Methylamine Solutions

The same spectrum was observed for (Na<sup>+</sup>C222)Na<sup>-</sup> films formed by evaporating methylamine solutions as for the films from ethylamine solutions (Figure 21). Also, the same spectrum was observed with films from methylamine solutions prepared by dissolving (Na<sup>+</sup>C222)Na<sup>-</sup> crystals rather than forming the solution over a sodium mirror.

Equimolar potassium metal and C222 in methylamine yield solutions of stoichiometry  $K^+C$  and  $e^-_{solv}$ . Solvent evaporation yielded films which were blue both by reflected and by transmitted light. The absorption spectrum of a film made from such a solution is shown as spectrum A in Figure 23. The maximum absorbance at 7,400 cm<sup>-1</sup> ( $\sim$ 1350 nm) is assigned to the trapped electron. When the potassium to C222 mole ratio in solution is between one and two, both the absorption of trapped electrons and of  $K^-$  are observed as shown in spectrum B of Figure 23. At K/C222 mole ratios of two or greater, spectrum C of Figure 23 is seen, in which only the  $K^-$  band appears at 11,900 cm<sup>-1</sup> (840 nm).

A somewhat more complex spectral dependence on metal to C222 ratio was observed for the rubidium system, as shown by the solid and dashed lines in Figure 24. The dotted line spectrum was that of a film from a rubidium solution prepared in a sodium borosilicate glass apparatus. The main peak is assigned to Rb while the shoulder is presumably that of Na, which results from the reaction

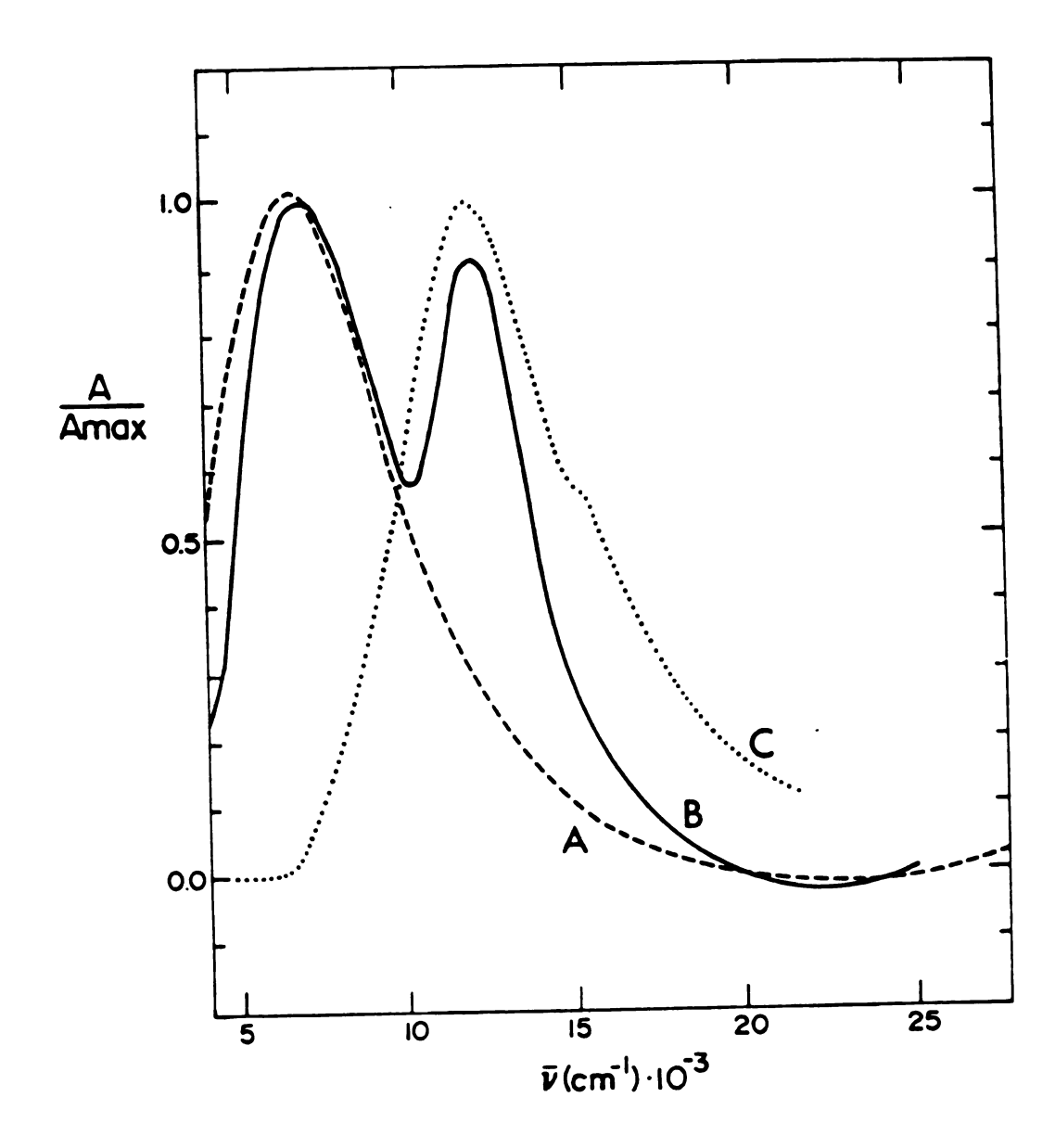


Figure 23. Spectra of films produced by evaporation of methylamine from solutions containing cryptand (2,2,2) and various relative amounts of potassium: spectra of films produced from solutions containing progressively lower concentrations of solvated electrons and higher concentrations of K are in the order A, B, C.

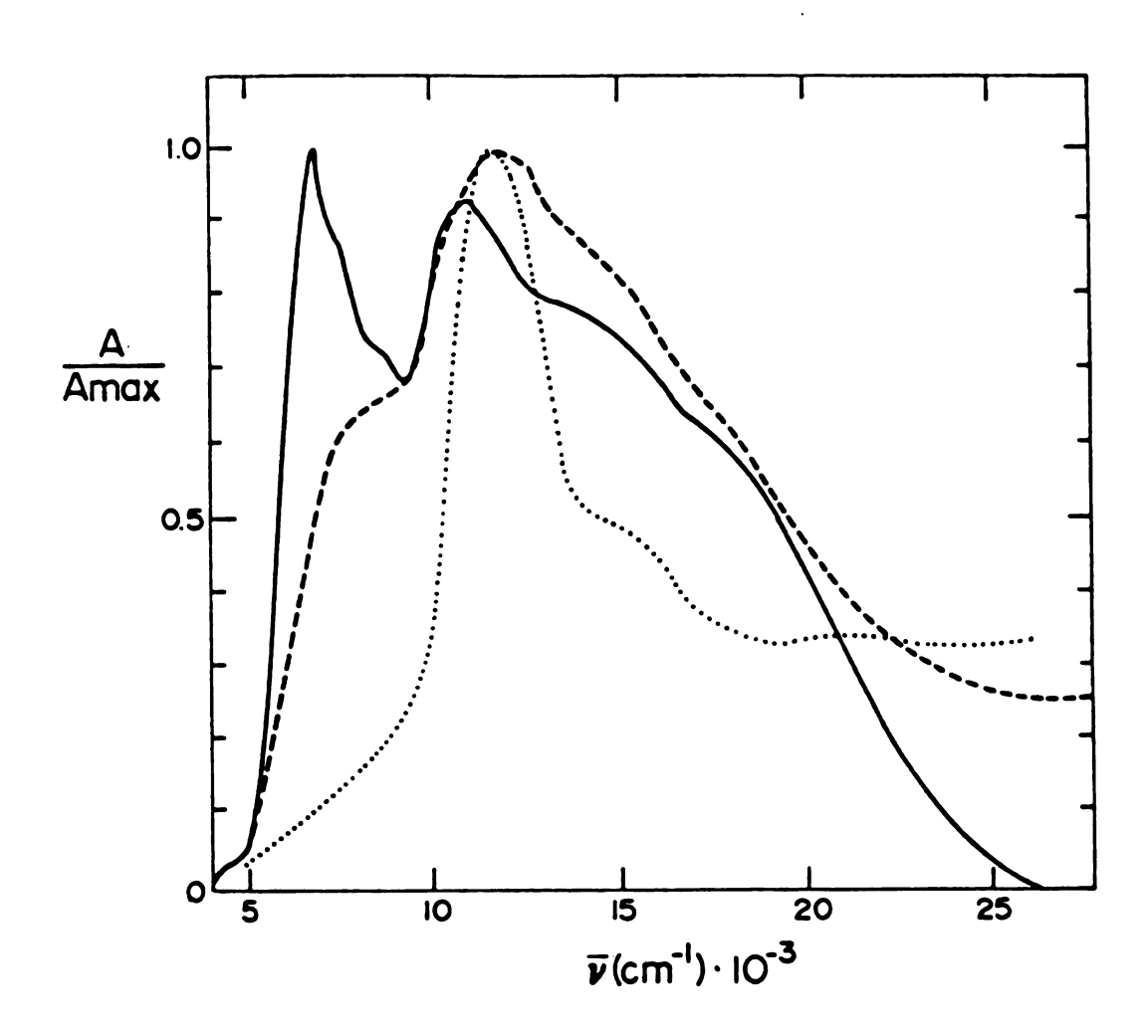


Figure 24. Spectra of films produced by evaporation of methylamine solutions containing cryptand (2,2,2) and various relative amounts of rubidium anions and solvated electrons (solid and dashed lines). The dotted line spectrum is from a film prepared from a sodium borosilicate glass apparatus; the solution presumably contained some Na.

(28,33):

$$Rb_{sol}^- + Na_{wall}^+ \rightarrow Rb_{wall}^+ + Na_{sol}^-$$
 (7)

Note that even in an all-quartz apparatus there is considerable absorption in the 500-600 nm region. These high energy peaks seem to be characteristic of mixed M - e systems and are of unknown origin.

In contrast to the potassium and rubidium cases, spectra of films from sodium or cesium-cryptand methylamine solutions do not show the near-IR absorption of the trapped electron regardless of the metal to C222 ratio.

By far the most stable films were those obtained from solutions of Na<sup>+</sup>C and Na<sup>-</sup>. One such film showed only a 20% decline in the absorption maximum after 48 hours at room temperature. The stability series seems to be Na<sup>-</sup> > Cs<sup>-</sup> > Rb<sup>-</sup> > K<sup>-</sup>. Films of K<sup>-</sup> are the least stable and the half-life of a (K<sup>+</sup>C)K<sup>-</sup> film at room temperature was about four minutes. Stability also varied from one solution preparation to another of the same composition. The spectra of films from fresh and decomposing solutions displayed the same qualitative features. If the solutions and films were handled at low temperatures (-30°C and below) decomposition slowed considerably and was negligible below -50°C.

# III.A.3. Discussion

The spectra of films of Na, K, Rb, and Cs salts of M<sup>+</sup>C are strikingly similar to those obtained in solution. The bands are at nearly the same position and are of comparable width as indicated in Figures 21 and 22. Even the spectra of the presumed electride salts are not very different from the infrared absorption band which is characteristic of e<sub>solv</sub> in amine solvents in the presence of cations and cryptands (92). The persistence of charge transfer to solvent, "ctts", absorption bands from solution to crystalline solids has also been observed with more conventional "ctts" bands. For example, the absorption band of I has been observed in a number of solvents as well as in crystalline RbI and CsI (93). The absorption band of I in the crystals lies at lower energies than in hydroxylic solvents but at higher energies than in amine and ether solvents. In the present work, the spectra of films produced by evaporating methylamine from solution of both RbI and (Rb+C)I were examined. The peak position for  $I^-$  in an RbI film (44,000 cm<sup>-1</sup>) is in reasonable agreement with the results reported by Fox and Hayon (93) for crystalline RbI (43,400 cm<sup>-1</sup>). The I transition was shifted to the red by 2400 cm<sup>-1</sup> when a film of (Rb<sup>+</sup>C)I<sup>-</sup> was used. We conclude that the absorption bands of  $M^-$  in solid films are related to those in solution just as the iodide "ctts" bands persist from solutions to crystals.

In the (Na<sup>+</sup>C)Na<sup>-</sup> spectrum, the origin of the shoulder at  $18,900 \text{ cm}^{-1}$  and the high energy peak at  $24,500 \text{ cm}^{-1}$ is uncertain. These features are not present in all films which show the Na band, as shown by the spectrum of (K<sup>+</sup>C)Na<sup>-</sup>. A possible simple explanation of these features is the presence of sodium metal, since thin films of alkali metals show complex spectra (94). However, the optical spectrum of a film consisting of DABCO (see Reagents) and sodium metal showed no absorption bands. The bicyclic diamine DABCO was chosen as a noncomplexing diluent which is similar in size and shape to C222. A second explanation is that one or both bands result from a charge transfer from Na to Na C222 (95). This is partially supported by the absence of the two bands in the (K+C)Na spectrum. However, the absence of the two bands in the latter spectrum could also be due to an expected change in crystal structure from (Na<sup>+</sup>C)Na<sup>-</sup> to (K<sup>+</sup>C)Na<sup>-</sup>. In (M<sup>+</sup>C)I<sup>-</sup>, the cryptand strands twist from antiprismatic to a prismatic arrangement when Na is replaced by K (96). There is another possible explanation for the shoulder. The electrical conductivity band gap for (Na<sup>+</sup>C)Na<sup>-</sup> is 2.2-2.5 eV (see D.C. powder conductivity) which corresponds to 17,800 cm<sup>-1</sup> to 20,200 cm<sup>-1</sup>. The shoulder could be a transition from the valence band to the conduction band in the semiconductor.

The band of Na in the films is very similar to that in solution. The band of Na in solution has been attributed

to a bound-bound transition (3s + 3p) with some contribution from a bound-continum band (97). The bound to excited state transition may autoionize into the continuum. Alkali metal anions in the gas phase exhibit photodetachment through autoionization (98). The increased gap between the ground state and the conduction band compared with the gas phase shows that the solution transition for Na and other alkali metal anions in solid films is modified by crystal field effects.

A longstanding question has concerned the origin of the metallic appearance of alkali metal anion salt crystals. The spectra show absorption bands with high intensity in the near-infrared and a sharp cutoff in the visible, behavior similar to the plasma absorption of metals. This can lead to a strikingly metallic appearance even for non-conducting crystals (99).

The thickness of the  $(M^+C)M^-$  films is not known. However, estimates can be made if a total oscillator strength of about two is assumed, as has been shown for Na in solution (100). The total area under the absorption spectrum of  $(Na^+C)Na^-$  and the density of the solid (101) yielded a thickness of  $\sim 500$  Å for a film with an absorbance of 1.0.

The band assigned to trapped electrons in films from K/C222 solutions, with a K:C222 ratio of 1:1, is very similar to optical bands of trapped electrons in both crystalline and glassy solids. The optical spectra of the

trapped electron in more than forty organic and aqueous glasses have been reported by Shieda (102). These bands are in the near-infrared and visible and exhibit a high energy tail similar to that of the solvated electron.

In crystalline solids the color center or F-center in alkali halides (103) is a trapped electron which has been extensively studied. The F-center is an electron localized in an anion vacancy defect in the crystal. If the dark blue solid, which forms from a solution of  $K^+C$  and  $e^-_{solv}$ , is  $(K^+C)e^-$ , then it can be considered a system of F-centers in which all anions are replaced by trapped electrons.

The energy of maximum absorption, E<sub>max</sub>, for F-centers in alkali halides is closely related to the size of the anion vacancy. Ivey and Mollwo (103) expressed this in a semi-empirical equation:

$$E_{\text{max}} = 17.4 \text{ a}^{-1.83}$$

where  $\underline{a}$  is the interionic (cation - anion) distance in units of  $10^{-8}$  cm and  $\underline{E}_{max}$  is in electron volts. The Ivey-Mollwo equation holds for alkali halides with the NaCl structure (face-centered cubic). The simplest structural model for  $(K^+C)e^-$  is a closest-packed structure of cryptated potassium cations with trapped electrons in the octahedral interstices. This would give an interionic distance, a, of  $\sim 7.8$  Å. The Ivey-Mollwo equation predicts an absorption

maximum in the infrared at  $3300 \text{ cm}^{-1}$  (3000 nm).

Although the equation obviously fails quantitatively for (K<sup>+</sup>C)e<sup>-</sup>, the prediction is in the correct spectral region. Since the two systems present different environments for the trapped electron the lack of quantitative agreement is not surprising. In F-centers the electron is surrounded by cations which are small compared to the anions. For example in NaCl the radius ratio, r+/r-, is 0.53. Even for the alkali halide CsF, with the largest cation and the smallest anion the radius ratio is 1.24. In contrast the radius ratio for (K<sup>+</sup>C)e<sup>-</sup> in the proposed model is 2.4. The trapped electrons are surrounded by cations which are of large size. This environment is opposite to that in most alkali halides. If the Ivey-Mollwo equation is recast using the anion radius instead of the interionic distance, the predicted absorption energy is in the visible region of the spectrum.

Another model is that of a particle in a spherical well with an infinite potential outside and zero potential inside. If a sphere of radius 2.3 Å is assumed for the trapped electron in both the ground and excited states, the model predicts an s to p transition at 3190 cm<sup>-1</sup> (3100 nm) (104). Both the prediction of the Ivey-Mollwo equation and the prediction of the spherical well model are in qualitative agreement with experiment. However, these simple models do not accurately represent the more complex physical

situation and a better model is needed.

Shoulders occur on the high energy side of the K<sup>-</sup> and Rb<sup>-</sup> bands when trapped electrons, e<sup>-</sup>t, are also present. These shoulders are not observed for films which contain only trapped electrons or only M<sup>-</sup>. Shoulders on the e<sup>-</sup>t and M<sup>-</sup> peaks may represent different environments or sites for these species. Different environments for e<sup>-</sup>t and M<sup>-</sup> could result from heterogeneous film formation, occurrence of more than one crystalline phase, or grain boundary effects. For example, the trapped electron in glasses is sensitive to its local environment as found in mixed solvent glasses (105). Mixtures of similar solvents cause shifts in the absorption maximum. Mixtures of two dissimilar solvents can result in two separate trapped electron absorptions.

#### III.B. M/18C6 Spectra from Methylamine Solutions

The success in obtaining optical absorption spectra of thin films containing cryptated alkali cations and either alkali metal anions or trapped electron prompted the study of films prepared from solutions of Na, K, Rb, and Cs and 18-crown-6, 18C6, in methylamine. It is known that the crown ethers, in particular 18-crown-6, complex alkali metal cations. The 18C6 alkali metal cation complex is open to solvent on two sides, whereas the 222-cryptand entirely encloses the alkali metal cation. It was thought

that this open nature of the complex might result in precipitation of the alkali metal if the M<sup>+</sup>18C6 were not capped by two solvent molecules. Because of this, the liquid nitrogen used in preparing the M/C222 films was replaced with a dry-ice/isopropanol bath. (See the section on preparing films in the experimental chapter.) It was hoped that this would not "dry out" the film entirely, but allow enough methylamine to remain in the film to cap the M<sup>+</sup>18C6.

# III.B.l. Na/18C6 Films from Methylamine

when sodium solutions with R = (Na)/(18C6) = 2 were evaporated, the films were gold colored by reflectance as long as some methylamine was present. The color changed to a light purple when all the methylamine was removed by immersing the side-arm reservoir in liquid nitrogen. The gold-color would remain indefinitely if the film temperature was -10°C or lower and the solution temperature was -78°C or higher. The transmission spectrum of such a film is shown in Figure 25 as spectrum A. The strong absorption peak at 16,000 cm<sup>-1</sup> (625 nm), characteristic of Na<sup>-</sup> (106,107), was present as well as a small broad peak at 25,000 cm<sup>-1</sup> (400 nm) but the prominent shoulder at ~19,000 cm<sup>-1</sup> (525 nm) observed with films of (Na<sup>+</sup>C222)Na<sup>-</sup> was absent (107).

When the methylamine was completely removed the color changed from gold to purple. This color change was

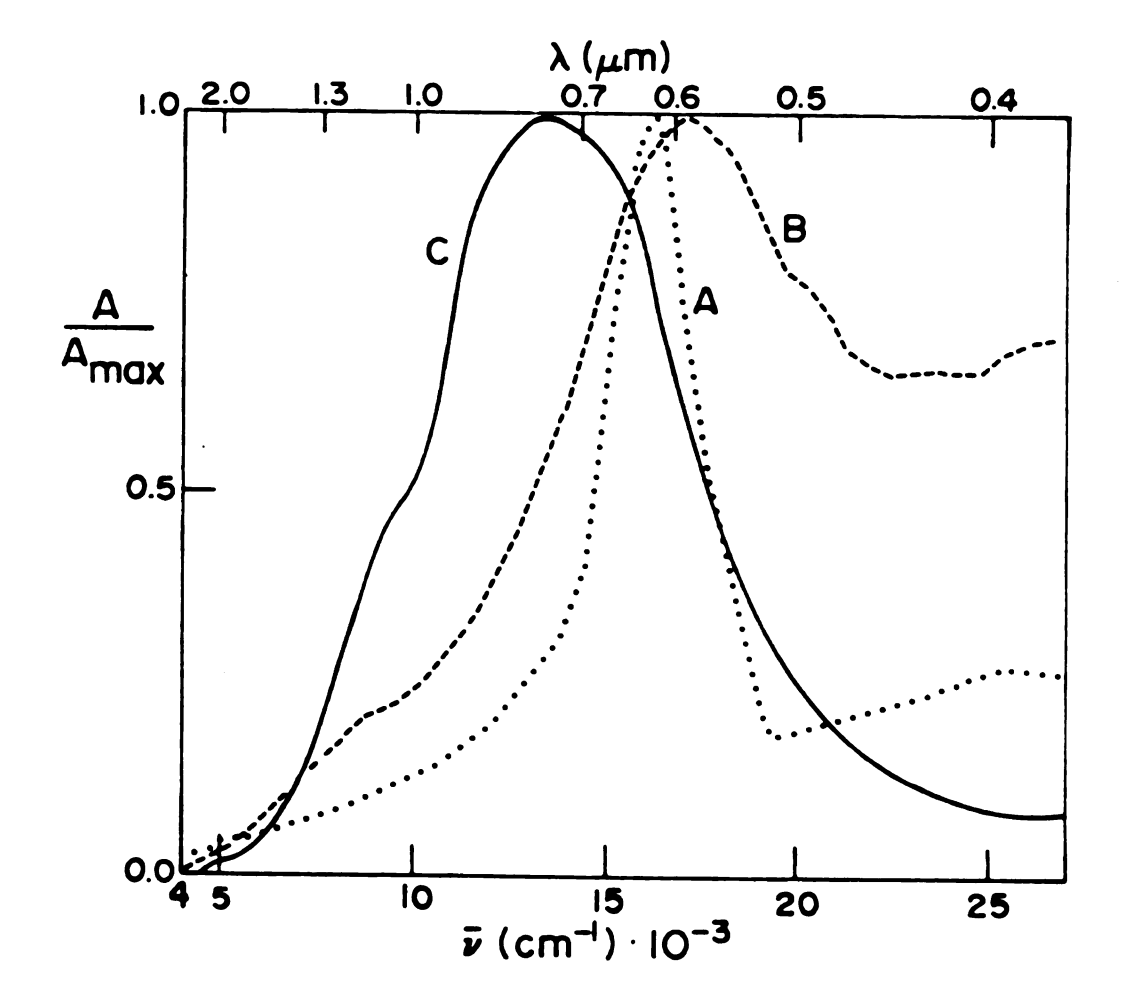


Figure 25. Spectra of metal-18-crown-6 films from methylamine. A (····) sodium film, R=2, with methylamine vapor present; B (---) dry sodium film, R=2; C (——) dry film from Na-K-18C6 solution.

accompanied by pronounced spectral changes as shown by spectrum B of Figure 25. The band at 16,700 cm<sup>-1</sup> (600 nm) could be a perturbed band of Na but the pronounced shoulder at 20,000 cm<sup>-1</sup> (500 nm) and the small peak at 26,000 cm<sup>-1</sup> (380 nm) are not present in the other Na/18C6 spectra. Although films of this type could be dissolved and reformed via the intermediate gold-film, it was not possible to convert purple films directly to gold films by the introduction of methylamine vapor. Films prepared in a similar way were used to prepare samples for methylamine analysis by proton NMR. The "gold" film had a ratio of MA:18C6 of 20-30:1 while the purple film had a ratio of

In the gold-colored film the trapped sodium cation probably remains isolated from Na by intervening solvent molecules. Removal of the methylamine permits direct Na+Na-interaction in purple-colored film, which greatly alters the spectrum of Na by interaction with neighboring ions. Another film was obtained by preparing a film from a solution containing equimolar Na, K, and 18C6 in methylamine. The resulting spectrum, spectrum C of Figure 25, has a peak at 13,300 cm-1 (750 nm) and a shoulder at 9,000 cm-1 (1100 nm). If the major absorption is due to Na, the presence of K+18C6 causes a red shift of 2700 cm-1. If it is due to K-, the presence of Na+18C6 causes a blue shift of 1100 cm-1. In contrast, the Na-peak in the

(K<sup>+</sup>C222)Na<sup>-</sup> film (107) is shifted by only 300 cm<sup>-1</sup> from that of Na<sup>-</sup> in (Na<sup>+</sup>C222)Na<sup>-</sup>. Unlike films made from Na and 18C6, the spectrum of Na-K/18C6 films does not change when all of the methylamine is removed by cooling the sidearm reservoir with liquid nitrogen. Therefore the mixed Na-K/18C6 films can be considered as dry films.

# III.B.2. K, Rb, and Cs/18C6 Films From Methylamine Solutions

A number of "dry" films were prepared from K, Rb, and Cs solutions with 18C6 present. Potassium films with R = (K)/(18C6) = 2 (spectrum A, Figure 26) have a strong absorption band at 12,200 cm<sup>-1</sup> (820 nm) and a pronounced shoulder at 9000 cm<sup>-1</sup> (1100 nm). Films made with R = 1 (spectrum B, Figure 26) have bands at 12,000 cm<sup>-1</sup> (830 nm) and 6500 cm<sup>-1</sup> (1550 nm). The peak at 12,000 cm<sup>-1</sup> is probably that of K while those at 9000 cm<sup>-1</sup> and 6500 cm<sup>-1</sup> are probably caused by trapped electrons. The higher energy band may result from strong interaction of the trapped electron with the cation as occurs in solvated electron-cation contact pairs in amine and ethers (108-110).

Films of Rb with 18C6 (spectrum B, Figure 27) show absorptions at 12,000 cm<sup>-1</sup> (830 nm) and 9100 cm<sup>-1</sup> (1100 nm) (111). These peaks are assigned to Rb and  $e_t$ , respectively.

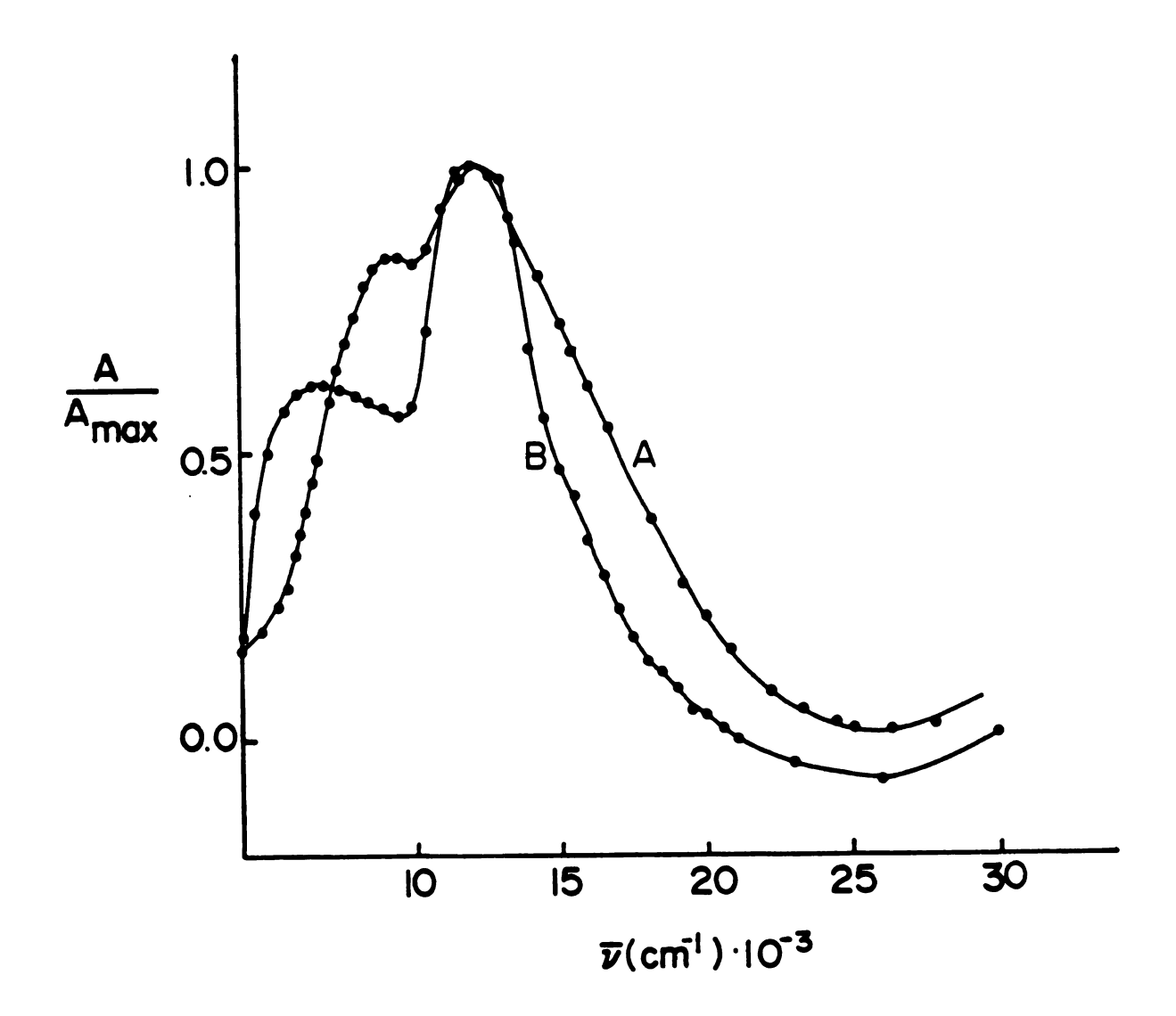


Figure 26. Spectra of potassium/18-crown-6 films with different ratios of K/18-C-6. Curve A is the spectrum of potassium film with R=2, and curve B is the spectrum of potassium film with R=1.

The band of  $e_t^-$  is shifted to higher energies by interaction with Rb<sup>+</sup>18C6 or Rb<sup>-</sup>. The behavior of cesium films with 18C6 is very different. Cesium-18C6 films formed from solutions with R values of 2, 1, 0.5 and 0.1 all show a single strong band at 6400-6700 cm<sup>-1</sup> (1560-1500 nm) and a weak absorption at 15,400 cm<sup>-1</sup> (650 nm). The spectrum obtained with R = 2 is shown as Curve C in Figure 27. The small band at 15,400 cm<sup>-1</sup> was probably caused by Na<sup>-</sup> present as an impurity. The low energy band probably originates from a trapped electron which is isolated from Cs<sup>+</sup>. The Cs<sup>+</sup> may be effectively isolated from  $e_t^-$  by formation of sandwhich-type complexes with 18C6 (112-114). Cs/18C6 films behave very differently from Cs/C222 films which show only the band of Cs<sup>-</sup> at 10500 cm<sup>-1</sup> (950 nm) both for R = 2 and R = 1 (107).

A notable feature of films containing 18C6 is their stability. Except for (Na<sup>+</sup>C222)Na<sup>-</sup>, films containing cryptands and either M<sup>-</sup> or e<sub>t</sub> are very unstable above about -20°C. In contrast films prepared with 18C6 are stable for long periods at 0°C and some are even stable at room temperature.

## III.C. Summary of Optical Spectra

Table 3 summarizes the peak positions for the films studied. The optical spectrum in the systems observed depends on the metal and the cation-complexing agent used.

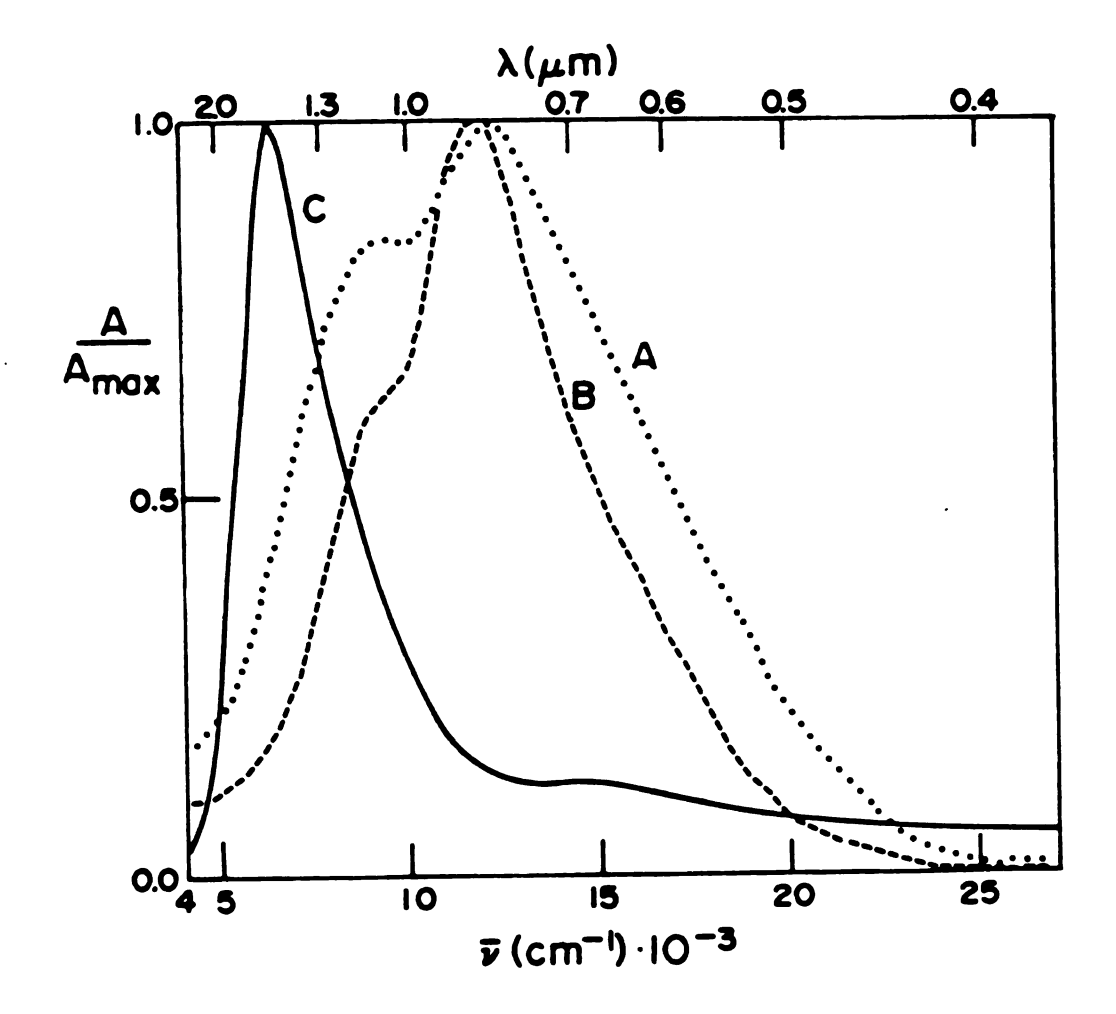


Figure 27. Dry film spectra of metal-18-crown-6 films from methylamine with R=2. A (····) potassium; B (----) rubidium; C (——) cesium. With R=1, 0.5 and 0.1 spectra of dry cesium films are essentially identical with curve C.

Summary of Peak Positions in Optical Spectra of Films. Table 3.

Main   Solvent   Ligand   R   Condition <sup>a</sup>   M   e <sup>-</sup> / <sub>L</sub>   Others   Others   Others     Na   CH <sub>3</sub> NH <sub>2</sub>   C222   2   dry   15,400(m)     18,900(s),24,500(sp)   No     CH <sub>3</sub> CH <sub>2</sub> NH <sub>2</sub>   C222   2   dry   15,400(m)     25,000(sp)   No     CH <sub>3</sub> CH <sub>3</sub> NH <sub>2</sub>   C222   2   dry   16,000(m)     20,000(sp)   No     Na   CH <sub>3</sub> NH <sub>2</sub>   C222   2   dry   11,900     20,000(sp)   No     Na   CH <sub>3</sub> NH <sub>2</sub>   C222   2   dry   11,900     20,000(sp)   No     Na   CH <sub>3</sub> NH <sub>2</sub>   C222   2   dry   12,000(m)   15,000(sp)   No     Na   CH <sub>3</sub> NH <sub>2</sub>   C222   2   dry   12,000(m)   15,000(sp)   15,000(sp)   No     Na   CH <sub>3</sub> NH <sub>2</sub>   C222   C22   dry   12,000(m)   15,000(sp)   15,000(sp)   No     Na   CH <sub>3</sub> NH <sub>2</sub>   C222   C22   dry   C220   C220					Film	14	Peak Positions <sup>b</sup> (cm <sup>-1</sup> )	$^{ m b}$ (cm <sup>-1</sup> )	Plasma
H <sub>2</sub> C222 2 dry 15,400(m) 18,900(s),24,500(sp) 18C6 2 dry 15,400(m) 25,000(sp) 18C6 2 dry 16,000(m) 20,000(sp)  C222 2 dry 11,900 7400 1 dry 12,200(m) 9,000(s)  C222 2 dry 12,200(m) 9,000(s)  C222 2 dry 11,000 7000(m) 15,000(s)  C222 2 dry 11,000 7000(m) 15,000(s)  C222 2 dry 11,000 7000(m) 15,000(s)  C222 2 dry 10,500 6400-6700 15,400(sp)  C222 2 or 1 dry (Na <sup>-</sup> )15100 6400-6700 15,400(sp)  C222 2 dry 11,000 6400-6700 15,400(sp)  C222 2 dry (Na <sup>-</sup> )15100 9,000(s)	Σ	Solvent	Ligand	<b>X</b>	Conditiona	Σ	l d	Others	Character?
H <sub>2</sub> C222 2 4ry 15,400(m) 18,900(s),24,500(sp) 18C6 2 4ry 16,000(m) 25,000(sp) 2 2,000(sp) 2 2 4ry 11,900 20,000(s),26,000(sp) 2 222 2 4ry 11,900 9,000(s) 18C6 2 4ry 12,200(m) 9,000(s) 2 18C6 2 4ry 11,600 1 4ry 11,600 9,000(s) 18C6 2,1, 4ry 12,000(m) 9100(s) 1 8C6 2 4ry 11,600 6400-6700 15,400(sp) 2 222 2 0r 1 4ry 10,500 6400-6700 15,400(sp) 2 222 2 or 1 4ry (Na <sup>-</sup> )15100 6400-6700 15,400(sp) 2 222 2 or 1 4ry (Na <sup>-</sup> )15100 6400-6700 15,400(sp) 2 222 2 or 1 4ry (Na <sup>-</sup> )15100 6400-6700 15,400(sp)	Na	CH <sub>3</sub> NH <sub>2</sub>	C222	2	dry	*15,400(m)		18,900(s),24,500(sp)	No
18C6 2 dry 16,000(m) 25,000(sp)  2 wet 16,700(m) 20,000(s),26,000(sp)  C222 2 dry 11,900 7400  1 dry 7400 9,000(s)  18C6 2 dry 12,200(m) 9,000(s)  C222 2 dry *11,600  18C6 2,1, dry *11,000 7000(m) 15,000(s),18,000(s)  18C6 2,1, dry 12,000(m) 9100(s)  C222 2 or 1 dry 10,500 6400-6700 15,400(sp)  C222 2 or 1 dry (Na <sup>-</sup> )15100 9,000(s)  18C6 2,1, dry (Na <sup>-</sup> )15100 6400-6700 15,400(sp)  C222 1:1 <sup>c</sup> dry (Na <sup>-</sup> )15100 9,000(s)		$cH_3cH_2NH_2$	C222	2	dry	15,400(m)		18,900(s),24,500(sp)	No
C222       2       dry       11,900        20,000(s),26,000(sp)         18C6       2       dry       11,900        7400          18C6       2       dry       12,200(m)        9,000(s)         18C6       2       dry       *11,600           18C6       2       dry       *11,000       7000(m)       15,000(s),18,000(s)         18C6       2,1,       dry       12,000(m)       9100(s)          18C6       2,1,       dry       10,500        6400-6700       15,400(sp)         C222       2 or 1       dry       (Na <sup>7</sup> )15100            18C6       1:1 <sup>c</sup> dry       (Na <sup>7</sup> )15100            6222       2 or 1       dry       (Na <sup>7</sup> )15100            6222       2 or 1       dry       (Na <sup>7</sup> )15100            6222       2 or 1       dry       (Na <sup>7</sup> )15100            6222       1:1 <sup>c</sup> dry       (Na <sup>7</sup> )15100        -		CH <sub>3</sub> NH <sub>2</sub>	1806	7	dry	16,000(m)		25,000(sp)	No
C222         2         dry         11,900          7400            18C6         2         dry         12,200(m)          9,000(s)           18C6         2         dry         *11,600             1         dry         *11,600             18C6         2         dry         *11,000         7000(m)         15,000(s),18,000(s)           18C6         2,1,         dry         12,000(m)         9100(s)          6400-6700         15,400(sp)           C222         2 or 1         dry         10,500          6400-6700         15,400(sp)            C222         2 or 1         dry         (Na <sup>7</sup> )15100              C222         1:1°         dry         (Na <sup>7</sup> )15100              C222         1:1°         dry         (Na <sup>7</sup> )15100              C222         1:1°         dry         (Na <sup>7</sup> )15300(m)		,		2	wet	16,700(m)	!!!	20,000(s),26,000(sp)	No
18C6       2       dry        7400          18C6       2       dry       12,200(m)        9,000(s)         1       dry       12,000       6500          12       dry       *11,600           18C6       2       dry       *11,000       700(m)       15,000(s),18,000(s)         18C6       2,1,       dry       12,000(m)       9100(s)          18C6       2,1,       dry        6400-6700       15,400(sp)         18C2       2 or 1       dry       10,500           18C6       1:1 <sup>c</sup> dry       (Na*)13300(m)          18C6       1:1 <sup>c</sup> dry       (Na*)13300(m)       9,000(s)	×	$CH_3NH_2$	C222	2	dry	11,900	-		No
18C6         2         dry         12,200(m)          9,000(s)           1         dry         *11,600             1         dry         *11,600             18C6         2         dry         12,000(m)         9100(s)            18C6         2,1,         dry          6400-6700         15,400(sp)           2222         2 or 1         dry         10,500             2222         1:1 <sup>c</sup> dry         (Na <sup>-</sup> )15100             18C6         1:1 <sup>c</sup> dry         (Na <sup>-</sup> )15300(m)         9,000(s)		) )		-	dry		7400		Yes
C222       2       dry       *11,600           1       dry       *11,000       7000(m)       15,000(s),18,000(s)         18C6       2       dry       12,000(m)       9100(s)          18C6       2,1,       dry        6400-6700       15,400(sp)         C222       2 or 1       dry       10,500           C222       1:1 <sup>c</sup> dry       (Na <sup>-</sup> )15100           18C6       1:1 <sup>c</sup> dry       (Na <sup>-</sup> )13300(m)       9,000(s)			18C6	2	dry	12,200(m)		9,000(s)	No
C222       2       dry       *11,600           18C6       2       dry       12,000(m)       9100(s)          18C6       2,1,       dry        6400-6700       15,400(sp)         C222       2 or 1       dry       10,500           C222       1:1 <sup>c</sup> dry       (Na <sup>-</sup> )15100           18C6       1:1 <sup>c</sup> dry       (Na <sup>-</sup> )13300(m)       9,000(s)				Н	dry	12,000	9029	-	No
18C6 2 dry *11,000 7000(m) 15,000(s),18,000(s) 18C6 2,1, dry 6400-6700 15,400(sp)  C222 2 or 1 dry 10,500  C222 1:1 <sup>C</sup> dry (Na <sup>-</sup> )15100 9,000(s)	Rb	CH <sub>3</sub> NH <sub>2</sub>	C222	2	dry	*11,600	-		No
18C6       2       dry       12,000(m)       9100(s)          18C6       2,1, 0.5       dry        6400-6700       15,400(sp)         C222       2 or 1       dry       10,500           C222       1:1c dry       (Na^*)15100           18C6       1:1c dry       (Na^*)13300(m)       9,000(s)		1		1	dry	*11,000	7000(m)	15,000(s),18,000(s)	No
18C6 2,1, dry 6400-6700 15,400(sp) 0.5 C222 2 or 1 dry 10,500 C222 1:1 <sup>c</sup> dry (Na <sup>-</sup> )15100 9,000(s)			18C6	2	dry	12,000(m)	9100(s)		No.
C222 2 or 1 dry 10,500 C222 1:1 <sup>c</sup> dry (Na <sup>-</sup> )15100 18C6 1:1 <sup>c</sup> dry (Na <sup>-</sup> )13300(m) 9,000(s)	Cs	$cH_3NH_2$	18C6	2,1, 0.5	dry		9400-6700	15,400(sp)	No
C222 1:1 <sup>c</sup> dry (Na <sup>-</sup> )15100 9,000(s)			C222	2 or 1	dry	10,500	!	1 1	No
18C6 1:1 <sup>c</sup> dry (Na <sup>-</sup> )13300(m) 9,000(s)	K/Ns	1 CH <sub>3</sub> NH <sub>2</sub>	C222	$1:1^{c}$	dry	(Na <sup>7</sup> )15100	-		No
		1	18C6	$1:1^{c}$	dry	(Na <sup>-</sup> )13300(m	(u	6,000(s)	No

b m = major peak, s = shoulder, sp = small peak. aref = re-formed, fr = fresh, ann = annealed.

Three types of solid films form: (1) solids which contain salts of alkali metal anions, (2) solids which contain trapped electrons, and (3) solids which are a mixture of the latter two. In films from ethylamine and methylamine the species found are similar to those in solution, showing that the solution bands persist from solution to solids.

#### D.C. ELECTRICAL CONDUCTIVITY STUDIES

## IV.A. Pressed Powder

Crystals of the salt (Na<sup>+</sup>C222)Na<sup>-</sup>, frequently grow as thin hexagonal plates with shinny metallic-looking faces. The color of the crystals varies from bright yellow-gold at liquid nitrogen temperature to dark bronze at room temperatures. Thus, the physical appearance of (Na<sup>+</sup>C222)Na<sup>-</sup> stimulated interest in measuring the D.C. electrical conductivity of the crystals. It was expected that the solids would be either a metallic conductor or a semiconductor. If it were metallic it would be of extreme interest because of the largely organic nature of the compound.

Initial studies done by M. T. Lok (77) indicated that (Na<sup>+</sup>C222)Na<sup>-</sup> was a semiconductor. Lok used various powder methods in order to determine the magnitude of the conductivity and its temperature dependence, as suitable single crystals were not available. He had varying degrees of success with the different methods, but one method which used conducting glass and aluminum plates as the two electrodes showed that (Na<sup>+</sup>C223)Na<sup>-</sup> is a semiconductor with an energy gap of 2.6-3.0 eV (77). Lok's initial success with pressed powders of (Na<sup>+</sup>C222)Na<sup>-</sup> prompted us to improve the apparatus in order to obtain quantitative data for

(Na<sup>+</sup>C222)Na<sup>-</sup> and to measure the conductivity of other alkali metal anion and electride salts. Two similar pieces of apparatus, described in Section II.E.4, were developed to do this.

# IV.A.l. Pressed Powder Conductivity Cell

The pressed powder cell described in Section II.E.4 was based on Lok's two-probe method (77). The new apparatus was designed to greatly facilitate the loading of the (Na C222) Na powder. To check the loading procedure and to check for electrical shorts the apparatus was loaded with mercuric sulfide, HgS. Mercuric sulfide is an intrinsic semiconductor with a reported band gap of 1.8 eV thermal, 2.0 eV optical, and  $\rho$  at RT equal to  $10^9-10^{10}~\Omega$ cm (118). An Ohm's law plot and the measurement of the current through the HgS at different temperatures showed that the pressed powder apparatus was working correctly. The Ohm's law plot was a straight line and the plot of log R vs 1/T showed that the pressed powder of the sample of HgS used had a band gap of 1.7 eV. The different between the reported value and that measured here was probably caused by the low purity of our HgS, 99%.

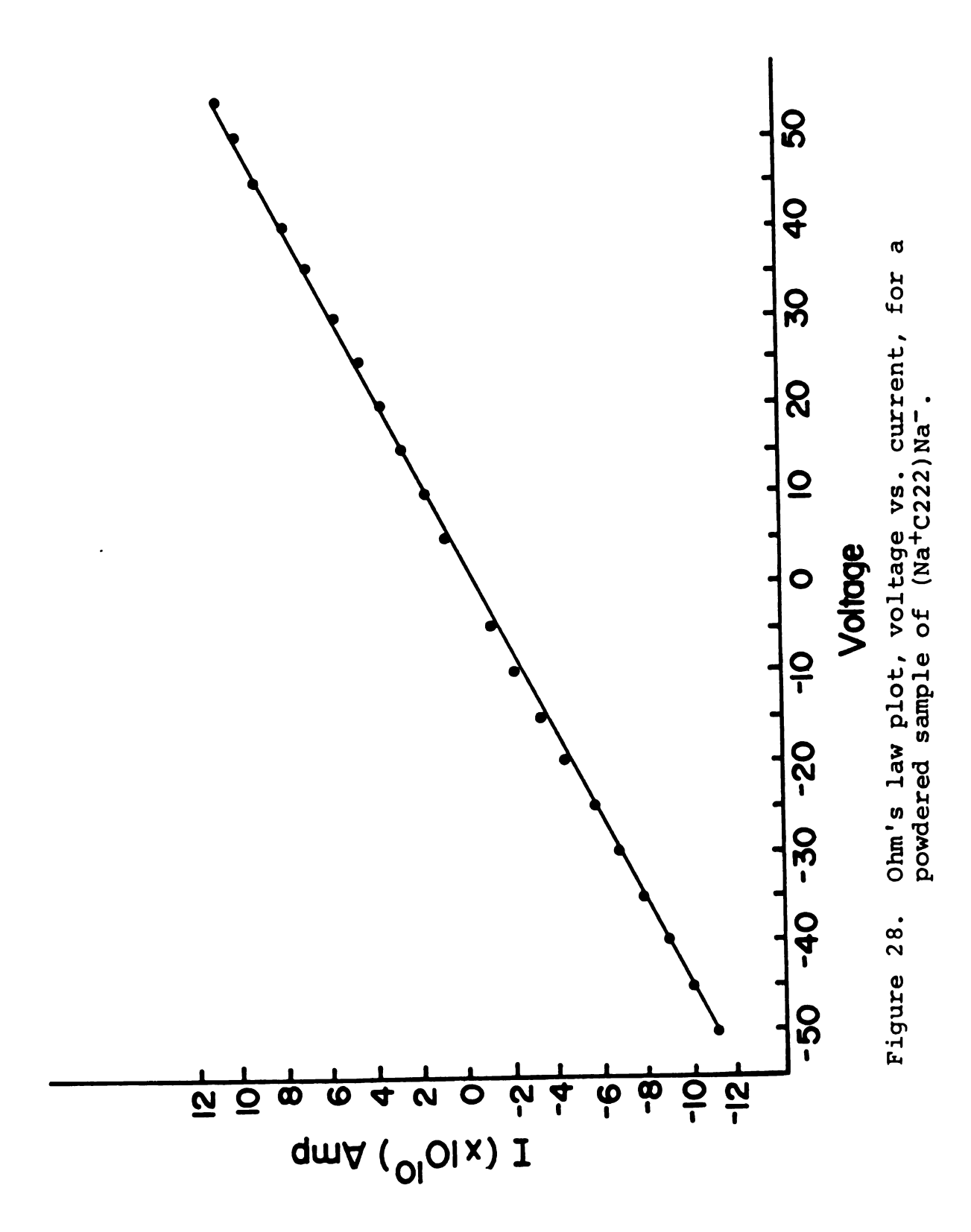
IV.A.l.a. Pressed Powder Conductivity of (Na<sup>+</sup>C222)Na<sup>-</sup> - Packed powder samples of (Na<sup>+</sup>C222)Na<sup>-</sup> gave a straight line Ohm's law plot through the origin, as shown in Figure 28. The temperature-dependent electrical conductivity was that expected for a semiconductor. As shown in Figure 29, a plot of log R vs 1/T gave a straight line over six decodes of resistance. The magnitude of the resistance depended upon the packing pressure and decreased with time as the sample "annealed". The temperature dependence of the conductivity of this salt gives a band gap of 2.4±0.2 eV.

The pin in the top plate and the cup in the bottom plate pressed the (Na<sup>+</sup>C222)Na<sup>-</sup> powder into a disk, 4.7 mm diameter and 0.25 mm thick. Using these dimensions, resistance at 0°C,  $R_{\odot}$ , and resistance at  $\infty$ °C,  $R_{\infty}$ , the conductivity  $\sigma_{\odot}$  and  $\sigma_{\infty}$  can be calculated (119)

$$\rho = \frac{R A}{\ell}; \qquad \text{where A = cross section area} \\ \ell = length$$

$$\sigma = 1/\rho$$

The  $\sigma_{\rm O}$  and  $\sigma_{\rm \infty}$  for pressed powder of (Na<sup>+</sup>C222)Na<sup>-</sup> equals 1.6 x 10<sup>-9</sup> ohm<sup>-1</sup> cm<sup>-1</sup> and 1.3 x 10<sup>11</sup> ohm<sup>-1</sup> cm<sup>-1</sup>, respectively. In some instances the entire disk could be removed from the cup. The compact (Na<sup>+</sup>C222)Na<sup>-</sup> disc reacted slowly with air. The surface of the disk would first turn black



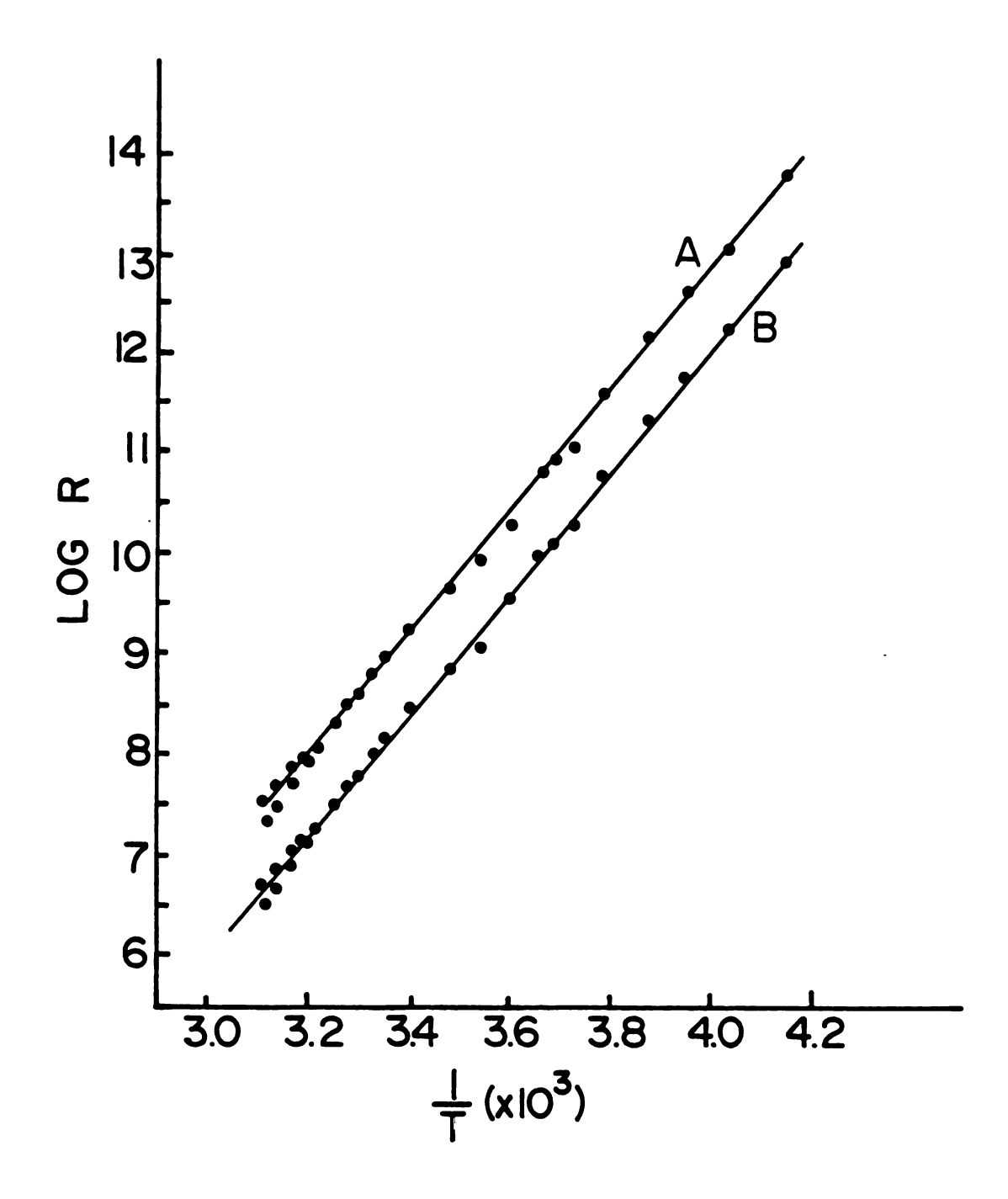


Figure 29. Semi-log plot of the resistance of powdered samples of (Na<sup>+</sup>C222)Na<sup>-</sup> versus the reciprocal of the temperature. Sample A was relatively loosely-packed. The data shown for the tightly-packed sample B were measured at both increasing and decreasing temperatures. Final dimensions of the sample were 4.7 mm dia. and 0.25 mm thick.

(finely divided metal?) and then white (metal oxide and hydroxide?). If the disk was then broken into two pieces, "gold" (Na<sup>+</sup>C222)Na<sup>-</sup> was found still remaining in the center. Upon exposure to air this center region would also decompose.

# IV.A.1.b. Pressed Powder Conductivity of Other Sodide Salts - The success of the pressed powder method with (Na<sup>+</sup>C222)Na<sup>-</sup> prompted us to attempt to measure the conductivity of other sodide (Na<sup>-</sup>) salts. Two other salts were prepared for measurement in the pressed powder apparatus, (K<sup>+</sup>C222)Na<sup>-</sup> and (Rb<sup>+</sup>C222)Na<sup>-</sup>. The resistance of these salts was measured with varying degrees of success.

Powdered (K<sup>+</sup>C222)Na<sup>-</sup> was loaded into the pressed powder apparatus in the same manner as the (Na<sup>+</sup>C222)Na<sup>-</sup> powder.

(For a detailed description see Section II.E.4.) This meant that the (K<sup>+</sup>C222)Na<sup>-</sup> powder was subjected to temperatures near room temperature (22-25°C) for different periods of time. The first exposure to room temperature took place in the inert atmosphere box while the powder was being loaded into the apparatus. This first exposure lasted approximately one half hour, depending on difficulties encountered in loading the sample. The sample thus loaded gave a linear Ohm's law plot and the log R vs 1/T curve shown in Figure 30, curve A, which corresponds to a band gap of 1.58 eV. After three days at room temperature the same

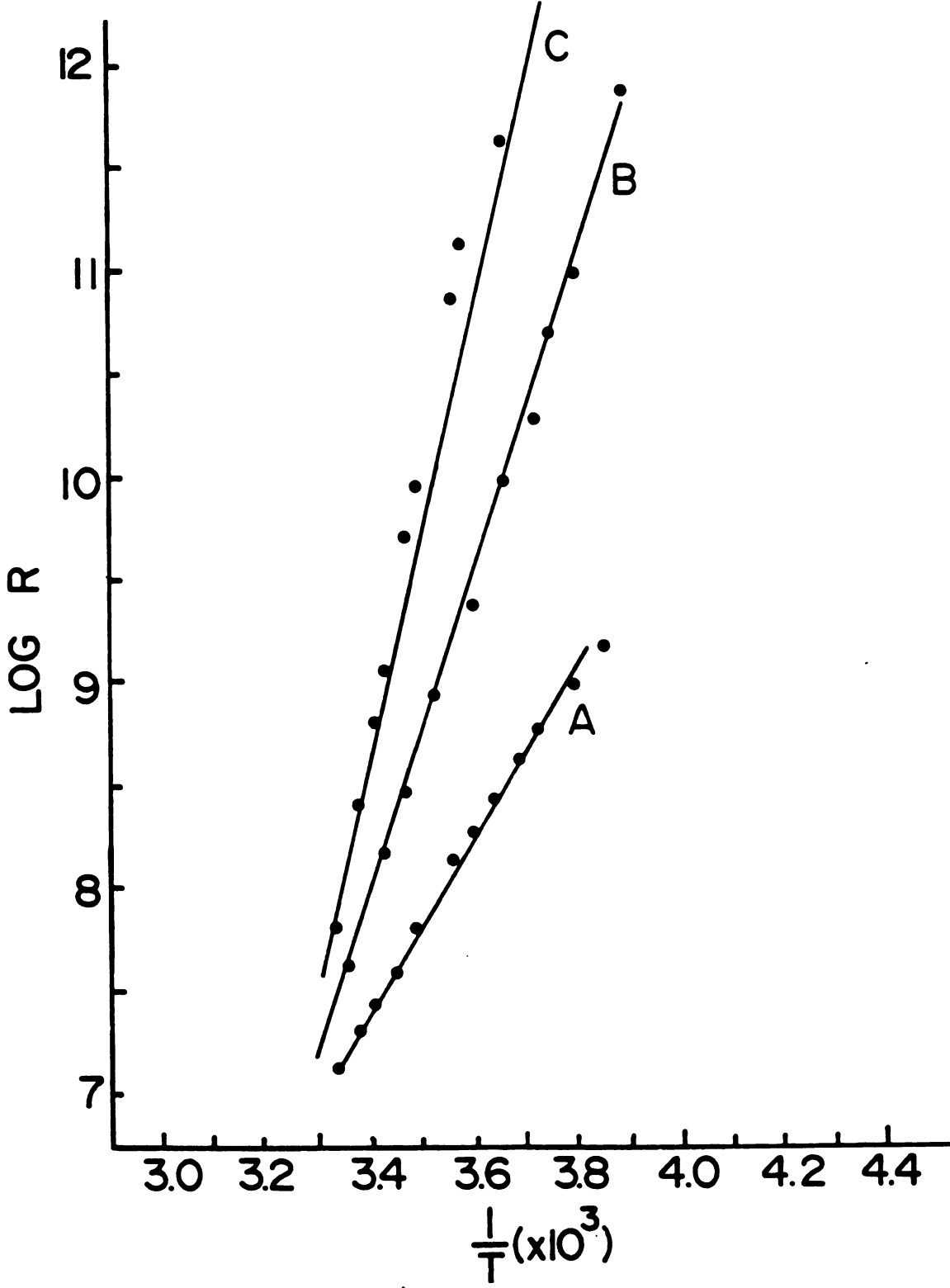


Figure 30. Curve A is (K<sup>+</sup>C222)Na exposed to high temperature for approximately one-half hour. Curve B is (K<sup>+</sup>C222)Na exposed to high temperature longer than A (1 to 3 days). Curve C is (K<sup>+</sup>C222)Na exposed to high temperature for over thirty days.

sample gave the log R vs 1/T curve shown in Figure 30, curve B, which gives a band gap of 3.06 eV. The sample was then allowed to stand at ambient temperature for one month which gave a log R vs 1/T plot similar to curve C, Figure 30, with a band gap of 3.64 eV. A second sample of (K+-C222) Na was prepared for measurement, but because of difficulties in loading the sample, it was exposed to room temperature initially for two hours. The sample was Ohmic and gave a log R vs 1/T curve similar to Figure 30, curve B with a band gap of 3.13 eV. This sample was again allowed to stay at room temperature and a final log R vs 1/T curve was obtained as shown in Figure 30, Curve C. The final band gap reached by this sample was 3.74 eV. Upon opening both apparatuses the original dark bronze powder was found to have turned to a white pressed powder. It is believed that the slow thermal decomposition of the (K+C222)Napowder is the source of the band gap change from 1.58 eV to 3.74 eV. The band gap value, 1.58 eV for the sample which was kept at room temperature for a shorter period of time is believed to be more indicative of the true pressed powder band gap of (K+C222)Na-. These results show that even the decomposition products mimic the semiconductor behavior of undecomposed sodide salts so that all powder Conductivity results should be interpreted with caution.

The reduction in the band gap from 2.4 eV for (Na<sup>+</sup>C222)Na<sup>-</sup> to 1.58 eV for (K<sup>+</sup>C222)Na<sup>-</sup> may be due to changes in the

rystal structure between the two. Although the anion,

Na, is the same in both salts, the cations are different (K<sup>+</sup>C222 vs Na<sup>+</sup>C222). The C222 has a cavity which is optimum for K<sup>+</sup> and must twist down to make the cavity smaller for the sodium cation. This change in the complexed cation configuration could force a change in crystal lattice between the two salts. Alternatively, (K<sup>+</sup>C222)Na<sup>-</sup> might be "contaminated" with trapped electrons which would lower the apparent band gap.

The other salt for which conductivity measurements were attempted was (Rb+C222)Na-. While the sample was evacuated and at dry ice/isopropanol bath temperatures the (Rb+C222)-Na- was a loose powder with a bronze color. When the ampule was placed into the ambient temperature inert atmosphere box, the powder darkened in color to a shiny black Upon opening the ampule in the inert atmosphere box the powder was found to have formed a hard solid black mass in the bottom of the tube. The powder had become a black mass so hard that it could not be removed from the glass tube. It is believed that the thermal decomposition and/or melting occurred at or near room temperature to form the hard black mass.

#### IV.A.2. Cold Jacket Pressed Powder Cell

The pressed powder cell described in the last section (IV.A.1) had three draw backs: (1) unnecessarily large sample size, (2) ambient temperature loading of the powder,

and (3) unknown pressures applied to the powder. Therefore, it was necessary to design a second pressed powder cell and companion inert atmosphere cooling jacket. For a detailed description see Section II.E.4. The "cold jacket pressed powder cell" greatly reduced the sample size by using a 2 mm I.D. heavy wall quartz capillary to contain the powder. The use of a liquid nitrogen pool beneath a cold plate in a nitrogen-filled glove bag, and the cold jacket on the cell, eliminated the need to load the sample at The pressure was applied to the powambient temperatures. der by means of a steel spring. By measuring the spring constant and the compression of the spring, the force applied to the powder could be calculated. The displacement of the spring from equilibrium caused by a known mass was measured and used along with Hookes' law to calculate the spring constant. A value of 2.66 x 10<sup>3</sup> kg sec<sup>-2</sup> was obtained for the condition used in the conductivity experiments.

Temperature readings from two different thermocouples (Figure 31) were compared to check the accuracy of the temperature recorded for the pressed powder during the conductivity experiment. The thermocouple, TCl, embedded in the stainless steel base of the quartz sample chamber was the thermocouple used to measure the temperature of the powder during the experiment. Since the powder and the thermocouple were separated by a short segment of stainless steel,

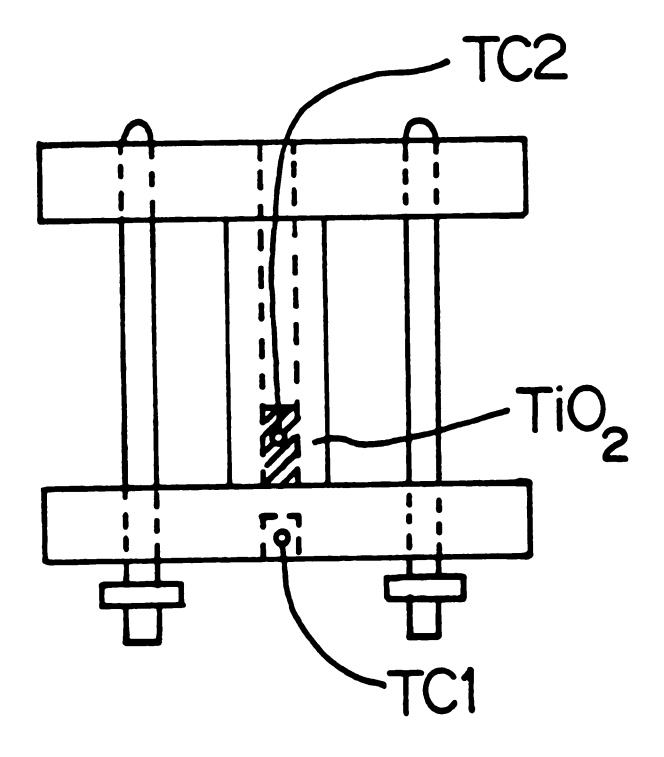


Figure 31. TCl is the thermocouple imbedded in the stainless steel base of the quartz sample chamber. It is used to measure the temperature of the powder in the experiments. TC2 is a thermocouple imbedded in the powdered TiO<sub>2</sub> which is not present in the conductivity experiments.

it was feared that the poor thermal conductivity of stain-less steel might cause a difference in the temperature measured by the thermocouple and the actual temperature of the powder sample. Therefore, a thermocouple, TC2, was embedded in powdered titanium oxide,  $TiO_2$ , to permit comparison of the temperature of the powder with that measured by TC1. It was found that TC2 lagged behind TC1 by  $\pm 0.2^{\circ}$ C when the temperature was continually changing so that there was no time for equilibration. When the temperature of the cell was decreasing, TC1 = TC2 +  $0.2^{\circ}$ C. Conversely, TC1 = TC2 -  $0.2^{\circ}$ C when the temperature of the cell was increasing at the normal rate. The readings of TC1 and TC2 were the same if allowed to equilibrate for five minutes.

IV.A.2.a. Trial Test of the Cold Jacket Pressed Powder

Cell with TiO<sub>2</sub> and HgS - In order to check the electrical

circuit of the cold jacket pressed powder cell, Figure 32,

for shorts, the quartz sample chamber was loaded first with

titanium oxide and then with mercury sulfide. Both of these

compounds are Ohmic semiconductors so a plot of current, I,

vs. voltage, V, provides a good test of the electrical cir
cuit. Ohmic semi-conductors will give a straight line plot

of current vs. voltage. When the cell was loaded with TiO<sub>2</sub>

and the voltage across the sample was varied, the measured

current was a linear function of the applied voltage (Figure

33). The cell was loaded with reagent grade TiO<sub>2</sub> powder

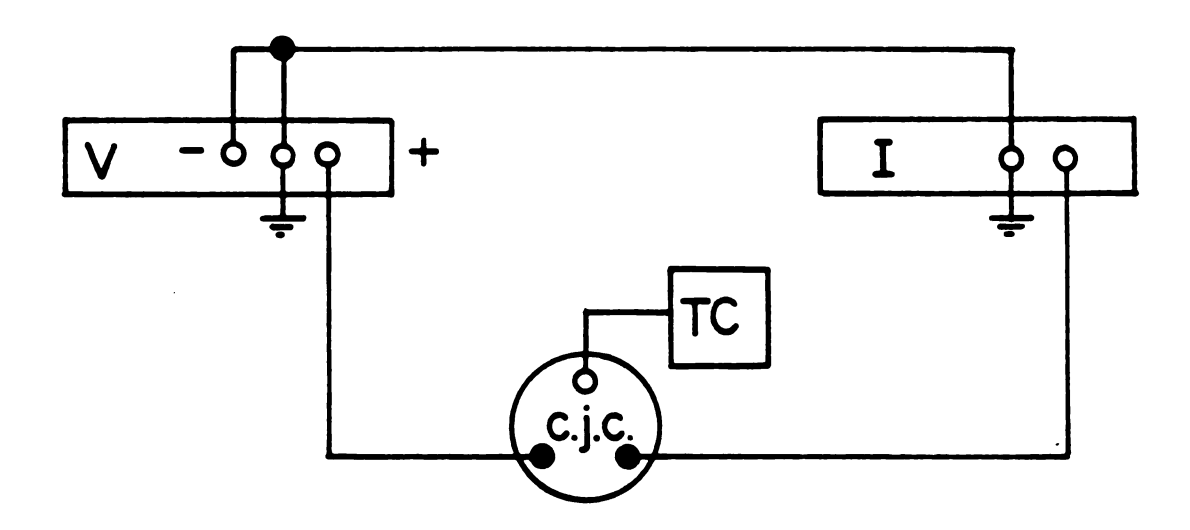


Figure 32. Schematic diagram of the cold jacket pressed powder cell. V, regulated voltage supply. I, Keithly electrometer. C.J.C. cold jacket cell and T.C. is a thermocouple readout.

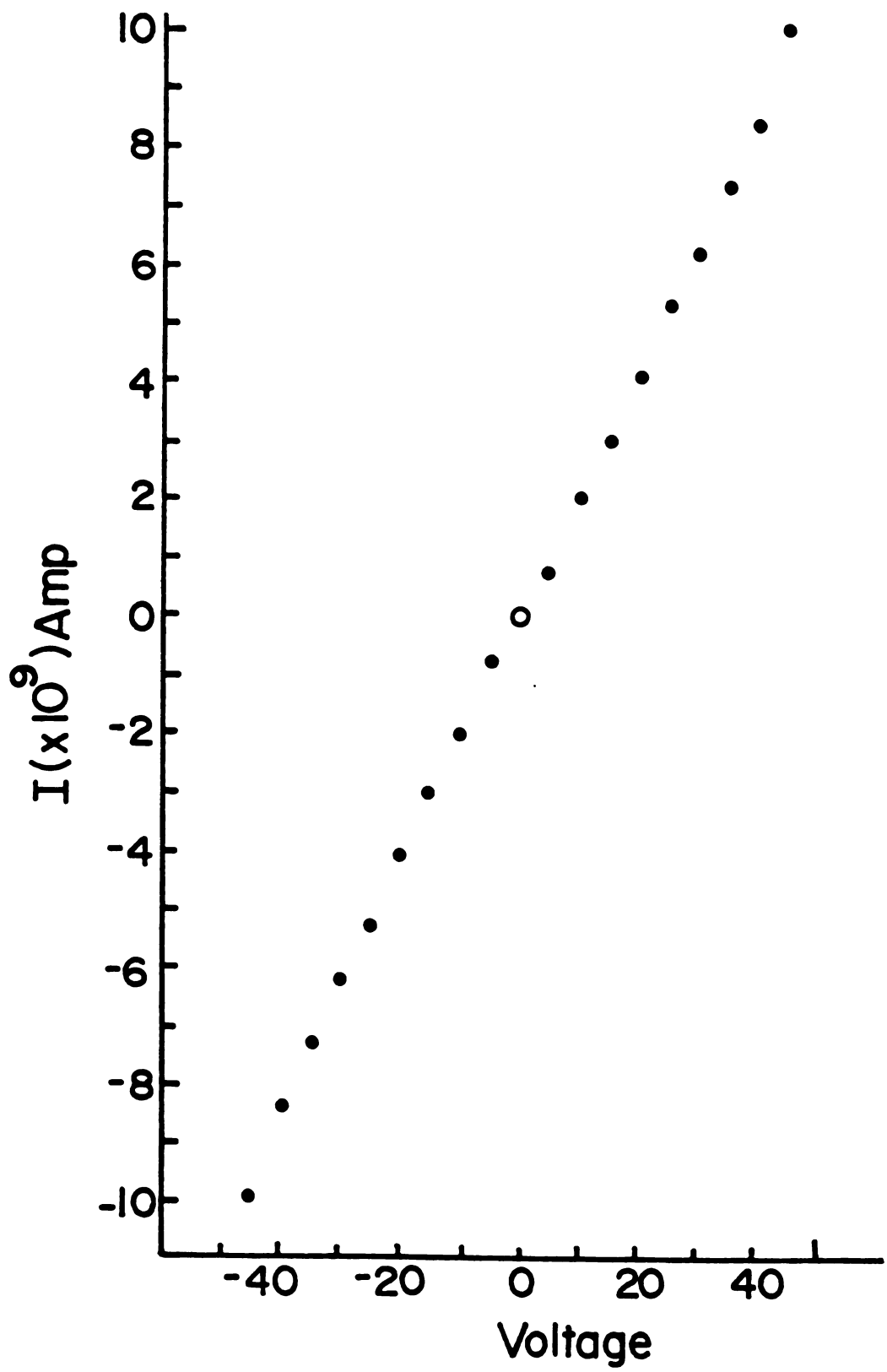


Figure 33. Ohm's law plot for a sample of powdered TiO<sub>2</sub> in the cold jacket pressed powder cell.

and the variation of the current with temperature was measured (Figure 34). The measured band gap for this TiO<sub>2</sub> powder was found to be 1.14 eV. Probably because of impurities in the pressed TiO<sub>2</sub> powder, the calculated band gap energy was much lower than the literature value of 3.05 eV (120) for a single crystal of rutile, TiO<sub>2</sub>.

A check of the intercept of the semi-log plot, Figure 34, at T =  $\infty$  showed that the sample was not an intrinsic semiconductor but was doped with impurities. Mercury sulfide, HgS, was also used to check the cold jacket pressed powder cell's circuit. Although TiO<sub>2</sub> showed that the circuit was operating properly, mercury sulfide was also studied, because it had been used in the previous pressed powder cell and a comparison was desired. The results for both types of apparatus were very similar.

IV.A.2.b. <u>D.C.</u> Conductivity Measurements of Different Salts Containing C222 and the Sodium Anion, Na - D.C. conductivity measurements were made in the "cold jacket pressed powder cell" for the following salts which contained both C222 and the sodium anion; (Na + C222) Na -, (K + C222) Na -, (Rb + C222) Na - and "(Ba + C222) Na - ". (Na + C222) Na - was run in the cold jacket pressed powder cell for two reasons: first, so that the results could be compared to the previous results, and second because the relative stability of (Na + C222) Na - lends itself well to trials of new

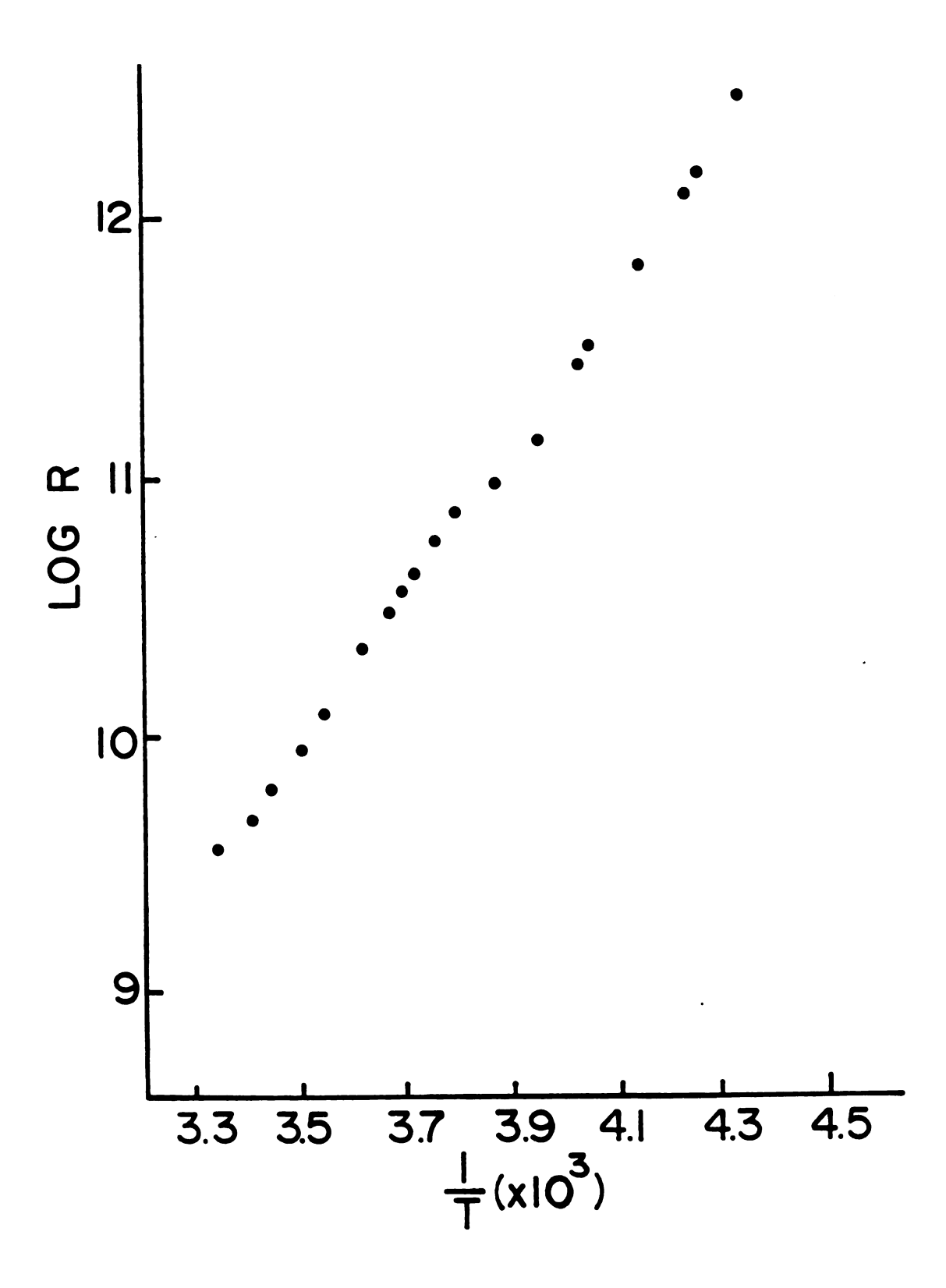


Figure 34. Log R vs 1/T for a sample of powdered TiO<sub>2</sub> in the cold jacket pressed powder cell.

equipment and methods. The Ohm's law plot for (Na +C222) -Na was a straight line and was similar to that obtained in the other pressed powder cell, Figure 28. The plot of log R vs 1/T is shown in Figure 35. The band gap energy calculated for this sample of (Na<sup>+</sup>C222)Na<sup>-</sup> powder was 2.2 The pressure applied to the powdered sample was calculated from the compression of the spring and the spring constant by using Hookes' Law. The powder was packed with a pressure of 25 bar. Doubling the packing pressure on the sample made no measurable difference in the d.c. conduc-Therefore, we can be confident that the highpressure packing limit had been reached. By using the dimensions of the pressed powder sample, 2 mm diameter and 1 mm in length, and the data in Figure 35, the d.c. conductivity at 0°C and  $\infty$ °C,  $\sigma_{\infty}$  and  $\sigma_{\infty}$ , can be calculated,  $\sigma_{o} = 1.0 \times 10^{-13} \text{ ohm}^{-1} \text{ cm}^{-1} \text{ and } \sigma_{\infty} = 1.2 \times 10^{7} \text{ ohm}^{-1} \text{ cm}^{-1}$ .

The next compound to be studied with the cold jacket pressed powder cell was (K<sup>+</sup>C222)Na<sup>-</sup> (121). Two separate samples of (K<sup>+</sup>C222)Na<sup>-</sup> were run in this cell. The samples were loaded into the cell as described in Chapter II. The first sample was dark bronze with a greenish glint (in the tube under vacuum before opening). After opening to the nitrogen atmosphere of the glove bag the sample turned black. The sample was never allowed to reach a temperature greater than -15°C. This sample of (K<sup>+</sup>C222)Na<sup>-</sup> powder was studied under a pressure of 59.3 bar. The

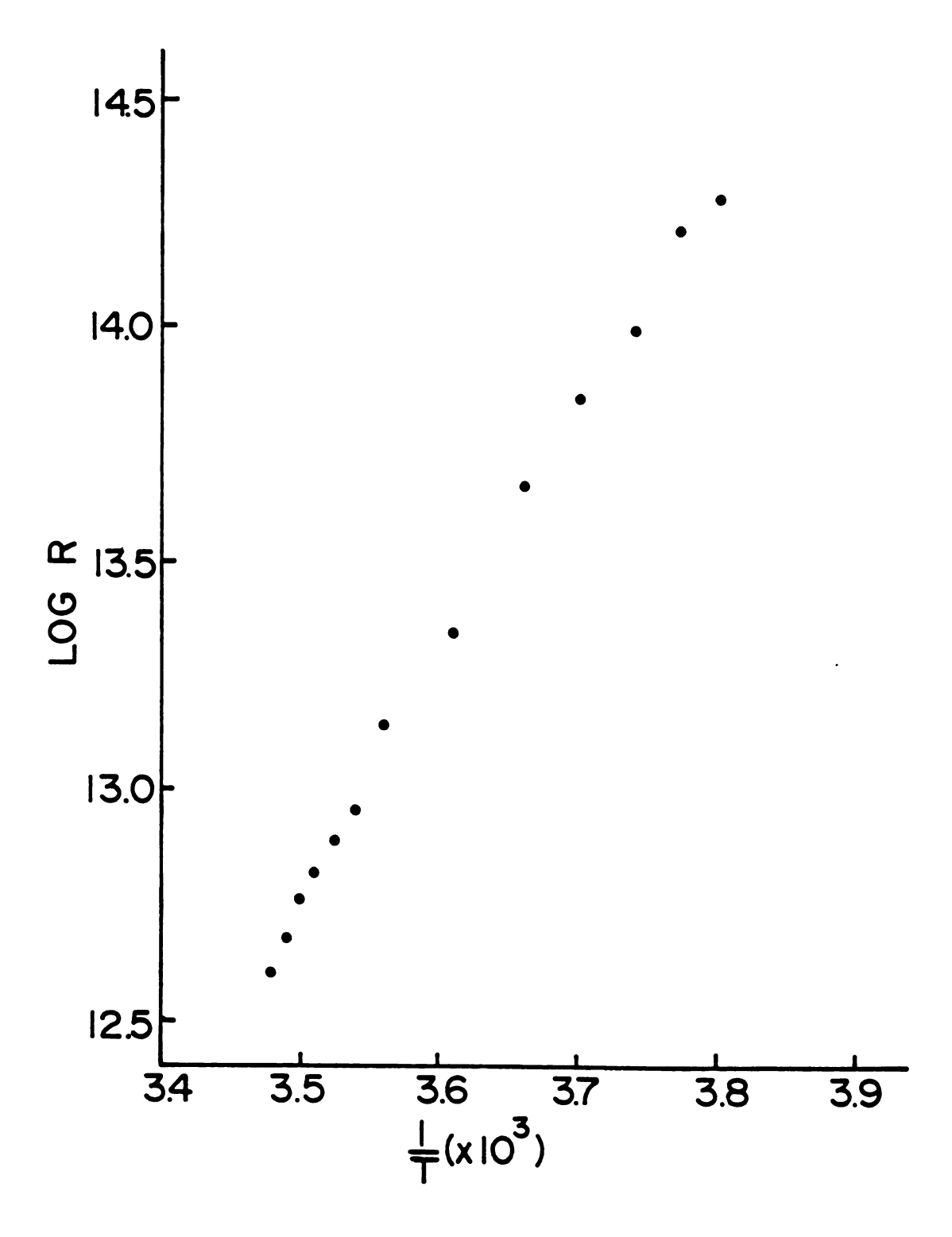


Figure 35. Log R vs 1/T for (Na<sup>+</sup>C222)Na<sup>-</sup> from measurements made with the cold jacket pressed powder cell.

Ohm's law plot of current vs voltage was a straight line for both the first and second pressed powder samples of  $(K^+C222)Na^-$ . Figure 36 shows this plot for the second sample. The plots of log R vs 1/T for both samples are shown in Figure 37. These data give a band gap of 0.87 eV for the first sample. The dimensions of this pressed powder sample, 0.5 mm in length and 2 mm in diameter, and the information from the log R vs 1/T plot were used to calculate  $\sigma_0 = 3.18 \times 10^{-9}$  ohm<sup>-1</sup> cm<sup>-1</sup> and  $\sigma_\infty = 2.8$  ohm<sup>-1</sup> cm<sup>-1</sup>; this low value may suggest conductivity by minor species such as e<sup>-</sup>.

The second powdered sample of (K<sup>+</sup>C222)Na<sup>-</sup> was prepared and loaded into the cold jacket pressed powder cell in the same way as the first, but this time the sample temperature was kept below -50°C during the loading. The second sample went through the same color changes as the first. This sample was pressed under two different pressures, 25.51 bar and then 59.3 bar. This change in the packing pressure had no effect on the band gap energy. A plot of log R vs 1/T for both pressures is shown in Figure 37. From this graph a band gap energy of 0.98 eV was calculated.

The sample dimensions, 1 mm in length and 2 mm in diameter, and the  $R_{o}$  and  $R_{\infty}$  from Figure 37 were used to calculate  $\sigma_{o}$  = 5.0 x 10 $^{-10}$  ohm $^{-1}$  cm $^{-1}$  and  $\sigma_{\infty}$  = 2.0 ohm $^{-1}$  cm $^{-1}$ .

Two salts containing C222 and the sodium anion on

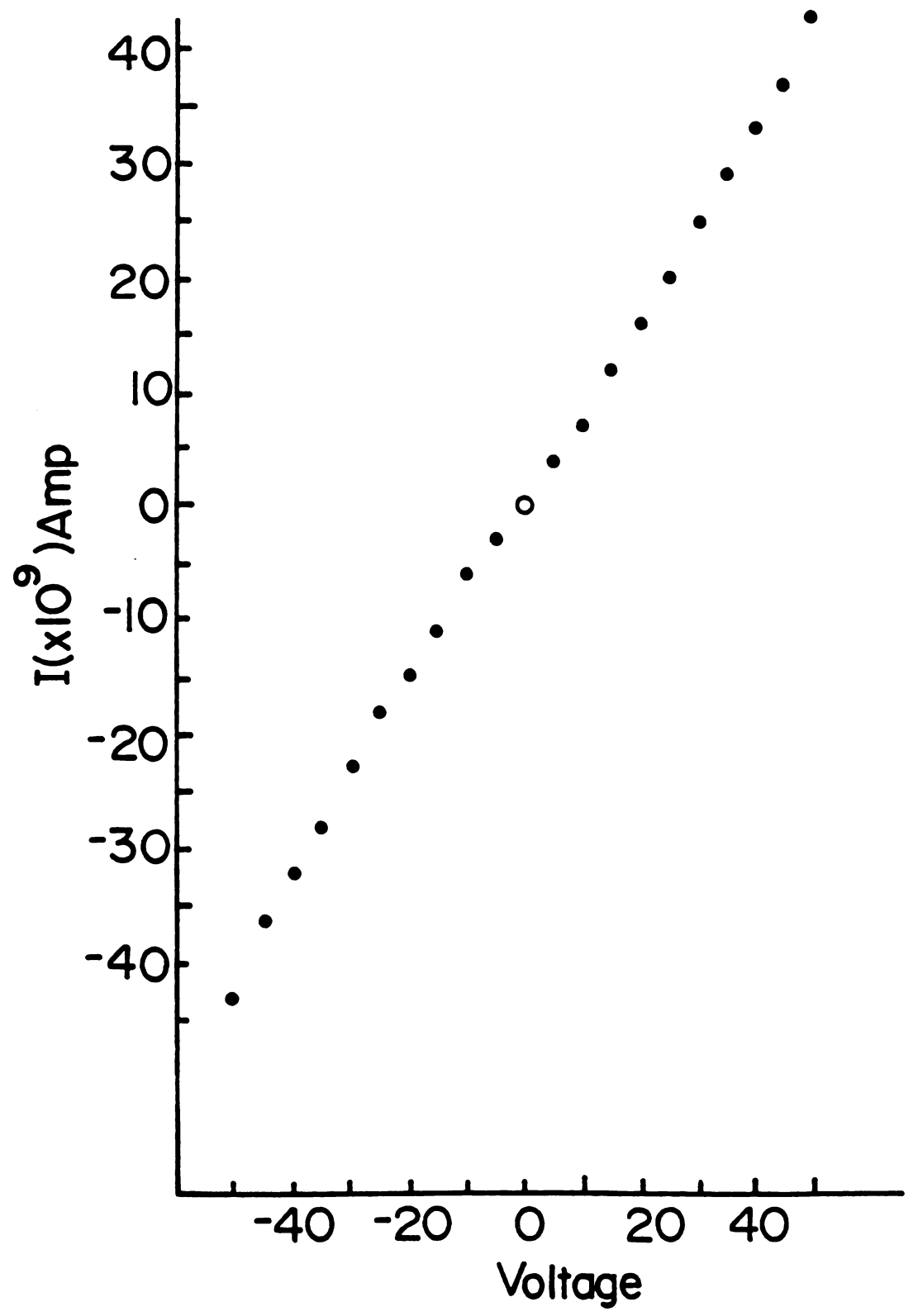
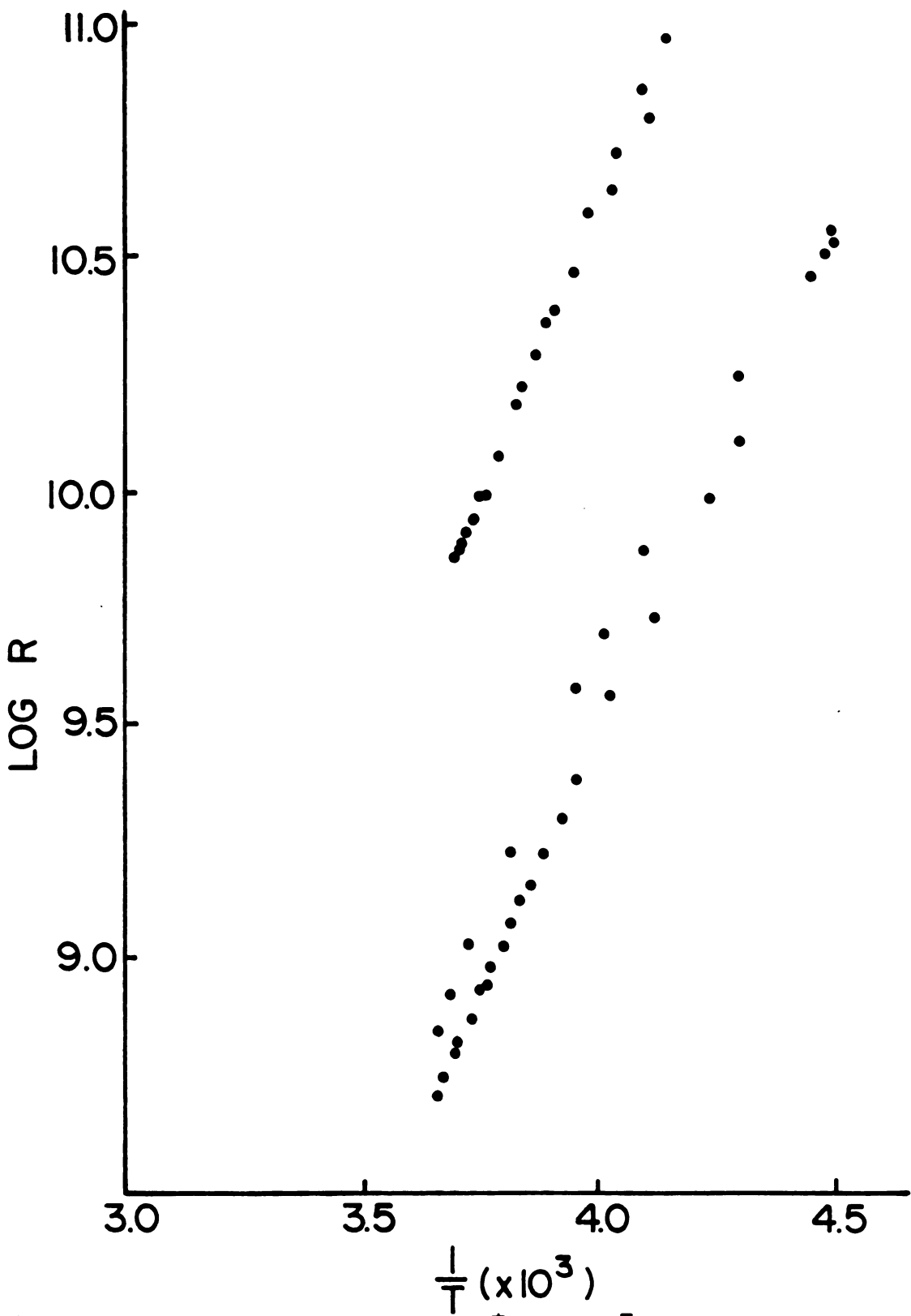


Figure 36. Ohm's law plot for the second sample of (K+C222)Na powder measured in the cold jacket pressed powder cell. The first samples' Ohm's law plot is very similar.



T(x|0<sup>3</sup>)

Figure 37. Log R vs 1/T for (K<sup>+</sup>C222)Na samples. The lower set of points are for the first sample and the upper set of points are for the second sample.

which initial attempts to measure their d.c. conductivity were made in the cold jacket pressed powder cell were  $Rb^{+}C222Na^{-}$  (124) and "Ba<sup>++</sup>C222Na<sub>2</sub>" (122). The one sample of Rb<sup>+</sup>C222Na<sup>-</sup> on which measurements were made was loaded into the cell in the same manner as the previous samples. The highest temperature the bright gold Rb + C222Na powder was exposed to during loading was -15°C. The powder was studied under a pressure of 59.3 bar. After the measurements were made the (Rb + C222) Na sample was removed. showed the same bright gold color that it had at the beginning of the experiment. The (Rb+C222)Na pressed powder sample showed a straight line Ohm's law plot. The plot of log R vs 1/T is shown in Figure 38. The band gap energies which correspond to the square data points and to the round data points outside of the circled area are 2.05 eV and 1.20 eV respectively. Inside the circled area of Figure 38 between -39.9°C and -41.0°C the straight line character of the log R vs 1/T plot is gone and the current seems to "wander". Two possible reasons for this behavior are: (1) the (Rb<sup>+</sup>C222)Na<sup>-</sup> might undergo a phase change in which the structure of the crystalline powder changes irreversibly between -39.9°C and -41.0°C; or (2) even though this effect occurred at the low end of the temperature range of the experiment, the sample might have been undergoing some decomposition. It is possible that this decomposition was caused by the current passing through the sample.

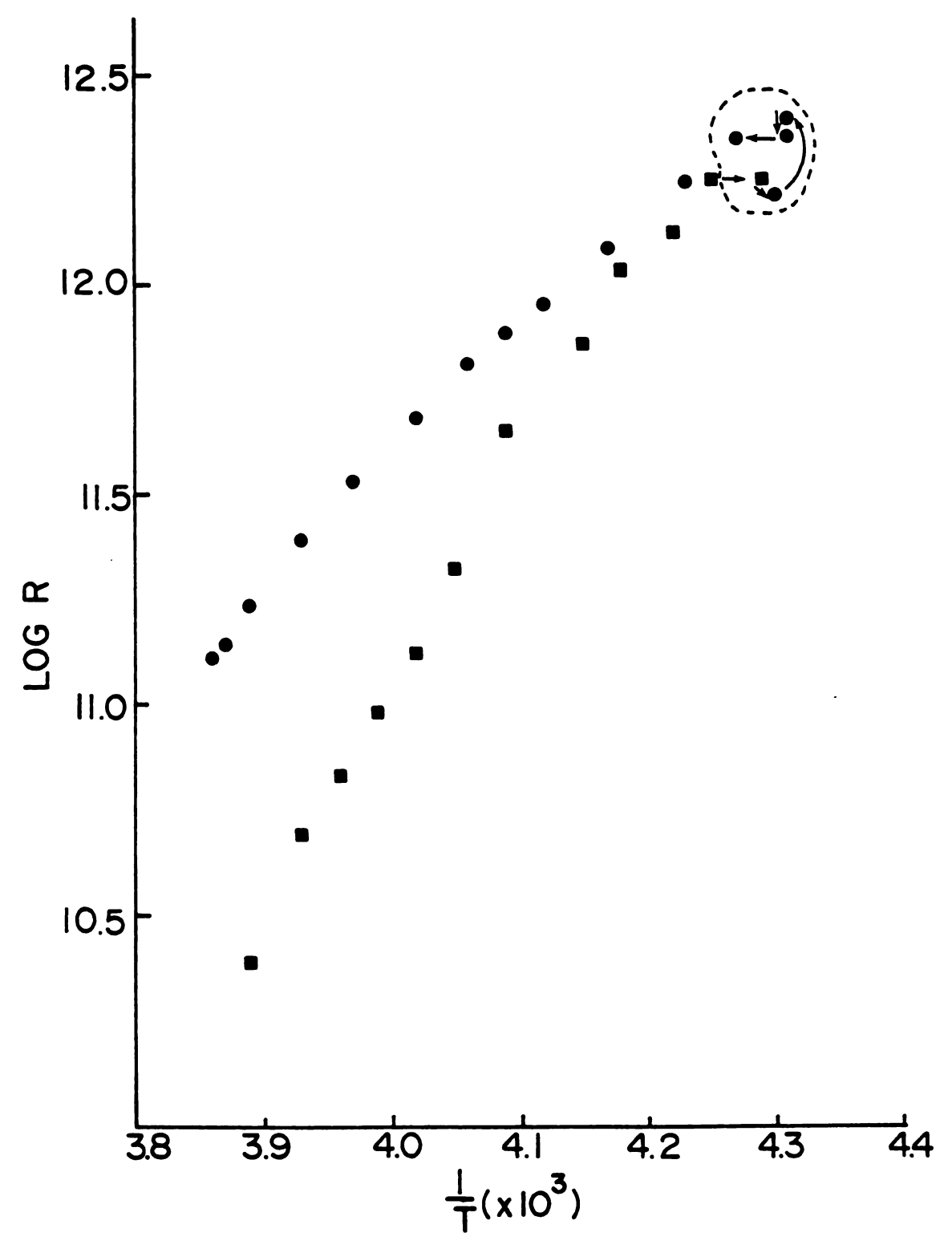


Figure 38. Log R vs 1/T for (Rb<sup>+</sup>C222)Na<sup>-</sup>. The band gap energies for the square data points and the round data points outside of the circled area are 2.05 eV and 1.20 eV. The circled area between -39.9°C and -41.0°C was an area where the current wandered.

It would be necessary to carry out more experiments with (Rb<sup>+</sup>C222)Na<sup>-</sup> to determine the origin of this anomaly.

The last salt which contained both C222 and Na studied in the cold jacket pressed powder cell was a powdered sample which was thought to be (Ba++C222)Na2 (122). The sample of "(Ba++C222)Na2" available for this study was extremely small. The small size of the available sample lead to the failure of this experiment. When the cell was examined, it was found that the powder had been pressed into a very thin and discontinuous disc between the electrodes. Because of this, no reliable current measurements were obtained. After completion of these experiments, it became evident that the sample of "(Ba++C222)Na2" was contaminated with (Na+C222)Na so that any measurements would have been inconclusive.

IV.A.2.c. D.C. Conductivity Measurements of Salts Containing 18C6 and the Sodium Anion, Na - D.C. conductivity measurements were also made on two salts which contained 18C6 instead of C222 as the complexing agent. The measurements were made on samples of (K+18C6)Na and (Cs+18C6)Na prepared by Dheeb Issa. Two samples of (Cs+18C6)Na and one sample of (K+18C6)Na were available for use in powder cell B (cold jacket pressed powder cell).

The two samples of (Cs<sup>+</sup>18C6)Na<sup>-</sup> gave very similar results. The plots of current versus voltage for both

samples were the same and showed both samples to be Ohmic in nature, Figure 39. The first sample of (Cs<sup>+</sup>18C6)Na<sup>-</sup> gave an average band gap energy of 1.7 eV and the second gave an average band gap energy of 1.7 eV. Average band gap energies are reported because under varying conditions both samples gave band gap energies ranging from 1.25 to 1.97 eV for the first sample and 1.40 to 1.80 eV for the second sample. The way in which the change in temperature was being made seemed to have the most effect on the plot of log R versus 1/T and therefore the largest effect on the calculated band gap energies.

Doubling the pressure on the pressed powder sample did not have any effect on the plots of log R versus 1/T, but whether the temperature was being increased or decreased did have an effect as shown in Figure 40. These results should be interpreted with caution since even the decomposition products can mimic the semiconductor behavior of the undecomposed sodide salts. The (Cs<sup>+</sup>18C6)Na<sup>-</sup> was allowed to decompose for three days at room temperature to give a white powder with black bands. This powder gave a straight line Ohm's law plot and a plot of log R versus 1/T which gave a band gap energy of 2.7 eV.

The one sample of (K<sup>+</sup>18C6)Na<sup>-</sup> gave a straight line
Ohm's law plot, as shown in Figure 41. The sample of
(K<sup>+</sup>18C6)Na<sup>-</sup> showed a similar plot of log R versus 1/T to
that for (Cs<sup>+</sup>18C6)Na<sup>-</sup> in that in raising and lowering

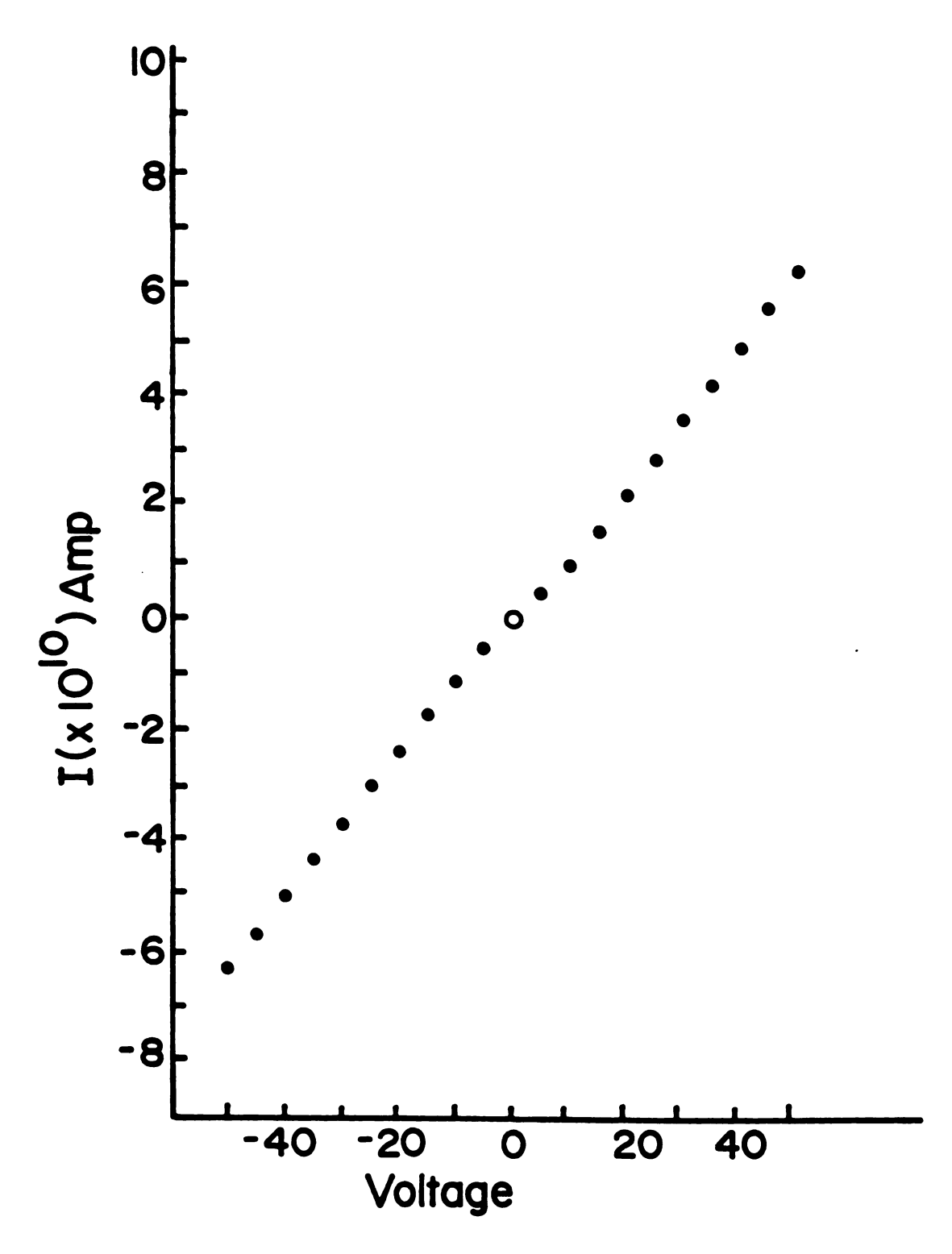


Figure 39. A plot of current versus voltage for a sample of (Cs+18C6)Na- in cold jacket powder cell.

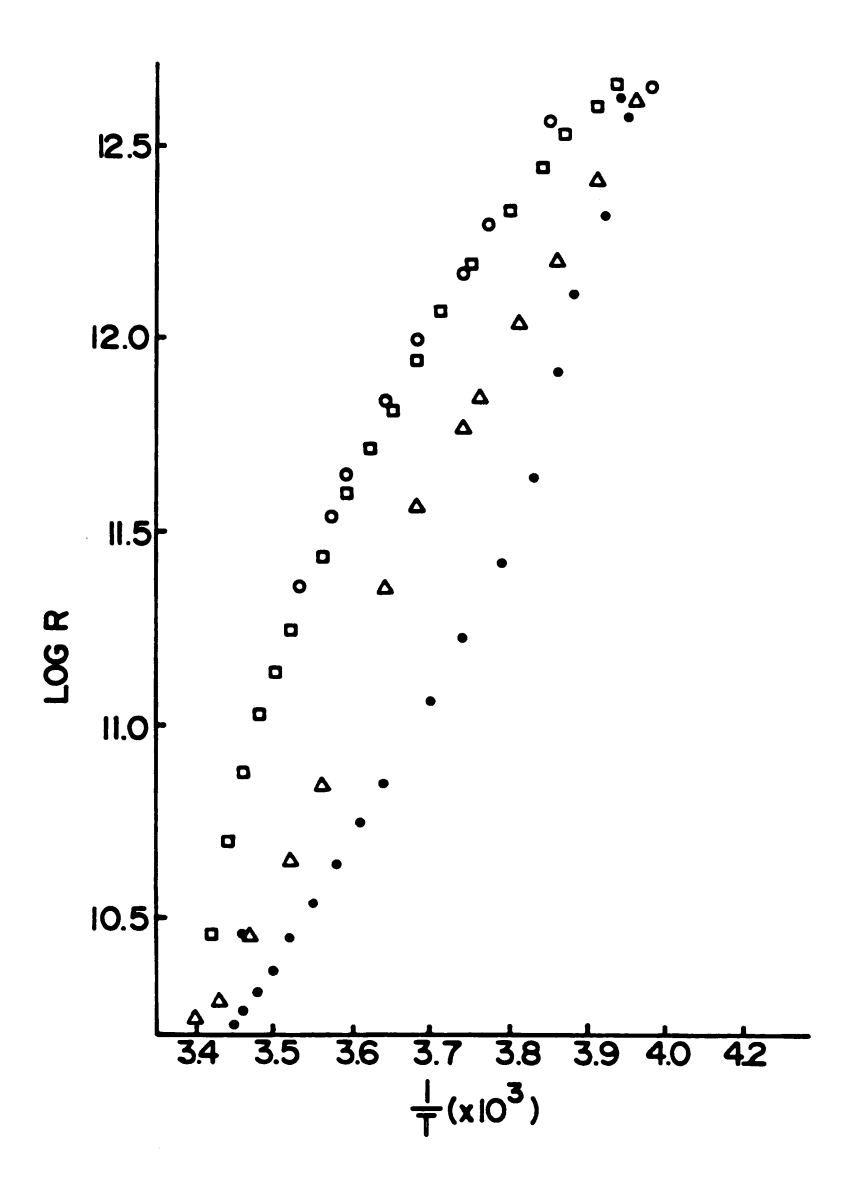


Figure 40. Log R versus 1/T for second sample of (Cs<sup>+</sup>18C6) Na. The round solid dots are data points taken under low pressure, 25.5 bar and decreasing temperature. The square dots were taken under low pressure and increasing temperature. The Triangular dots were taken under high pressure, 59.3 bar and decreasing temperature. The hollow circular dots were taken under high pressure and increasing temperature. The curvature of this line was not due to any possible temperature If it was due to the sample temperature lagging behind the temperature of the thermocouple, the curvature would be in the opposite direction.

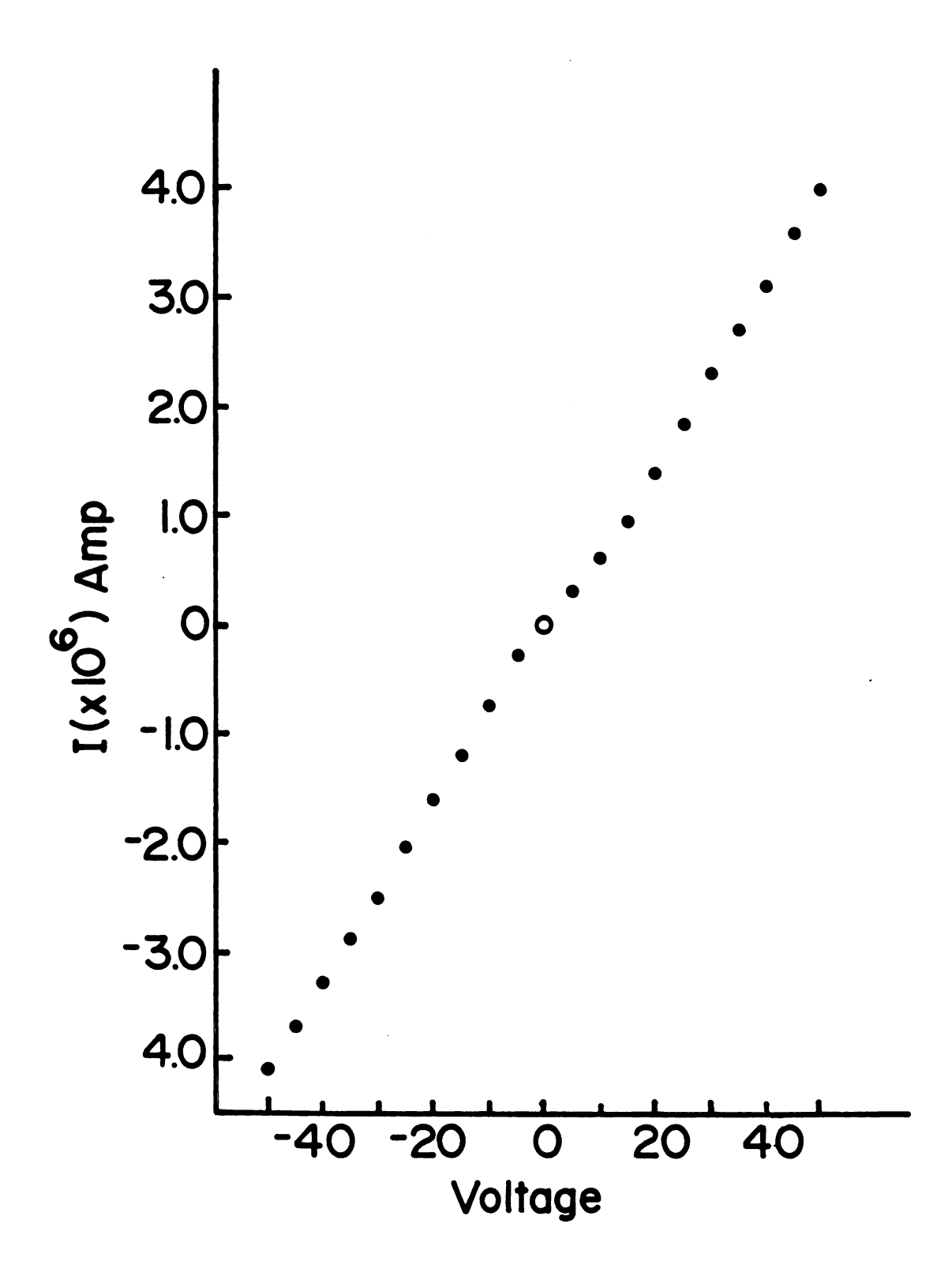


Figure 41. A plot of current versus voltage for a sample of (K+18C6)Na- in powder cell B.

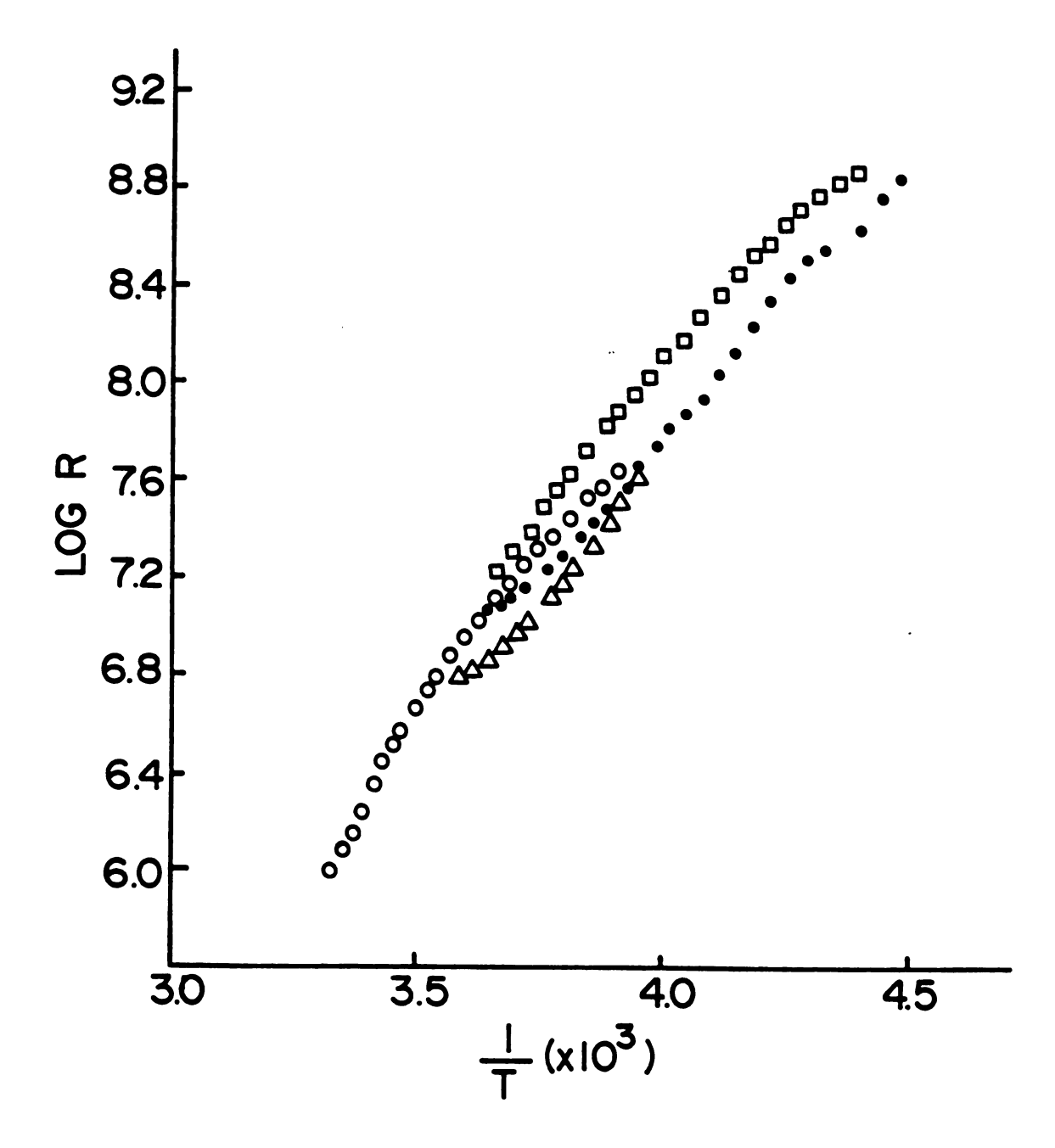


Figure 42. Log R versus 1/T for a sample of (K+18C6)Na in pressed powder cell B. The round dots were taken under decreasing temperature and low pressure, 25.5 bar; band gap energy 1.10 eV. The squares were taken under increasing temperature and low pressure; band gap energy 0.88 eV. The triangles were taken under decreasing temperature and high pressure, 59.3 bar; band gap 0.94 eV. The hollow dots were taken under increasing temperature and high pressure band gap energy 0.98 eV.

the temperatures the data points did not retrace the same curve, Figure 42. The average band gap energy from the curves in Figure 42 was 0.98 eV.

IV.A.2.d. <u>D.C. Conductivity Measurements of (K<sup>+</sup>C222)K<sup>-</sup> and (Li<sup>+</sup>C211)e<sup>-</sup> - D.C. conductivity measurements were made on two salts which did not contain the sodium anion, (K<sup>+</sup>-C222)K<sup>-</sup> (121) and (Li<sup>-</sup>C211)e<sup>-</sup> (123). Most of the measurements and the analyses were done by Long D. Le for (K<sup>+</sup>-C222)K<sup>-</sup> and by J. S. Landers for (Li<sup>+</sup>C211)e<sup>-</sup>. They are reported here to illustrate how complex the plot of log R versus 1/T can become for pressed powder samples of this type.</u>

The sample of (K<sup>+</sup>C222)K<sup>-</sup> was dark bronze in color and was loaded at low temperature, below -20°C. The available sample was small and it was feared that it would not cover the electrode faces when pressed. In fact after the experiment was completed examination of the pressed powder showed that it did not cover the entire surface area of the electrode.

There was, however, no evidence that contact between the electrodes was made except through the sample, although such a thin partial coverage could cause problems with the measurements. The plot of current versus voltage, Figure 43 was not Ohmic. Note the portion of the plot near the origin, where the curve deviates from a straight line.

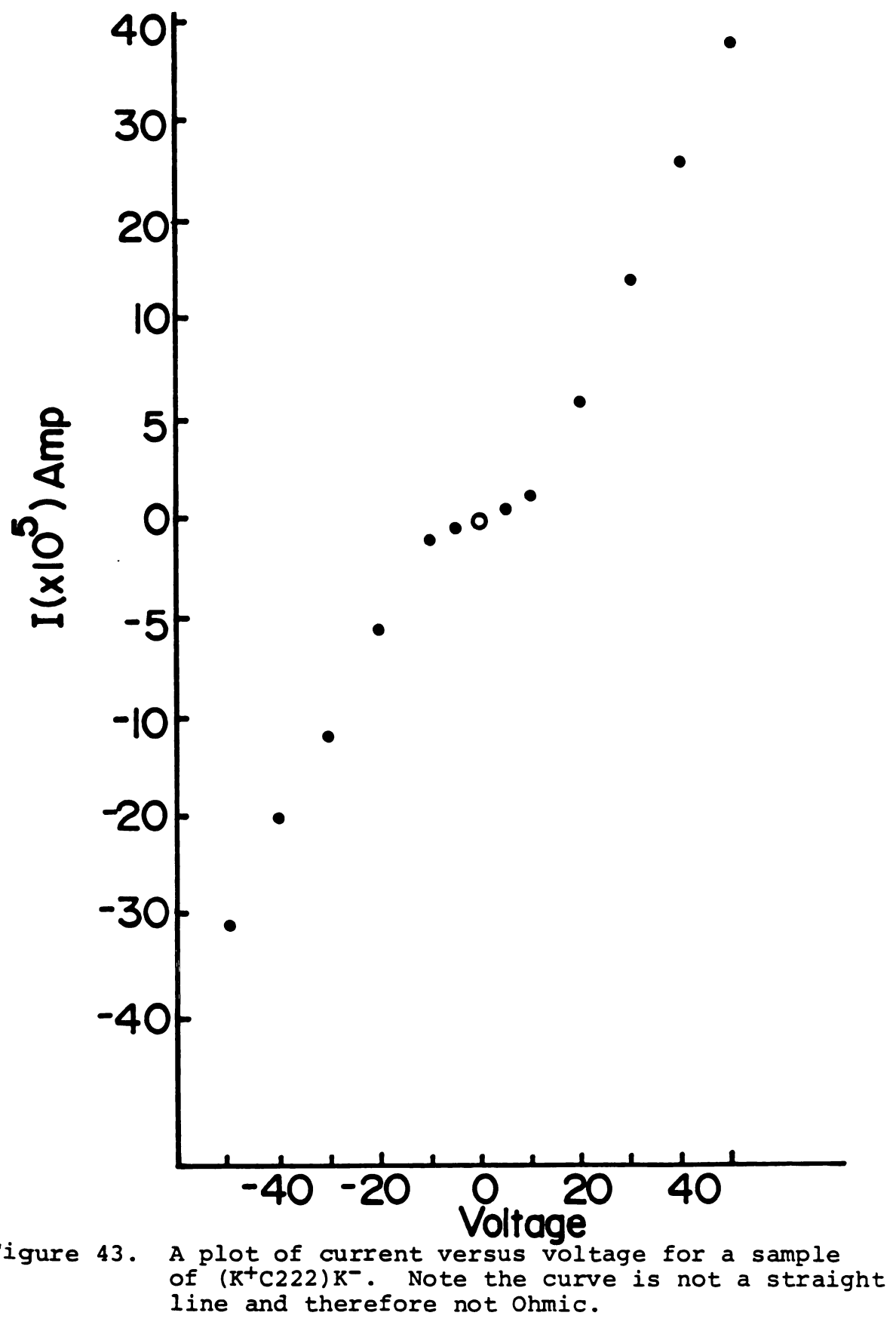


Figure 43.

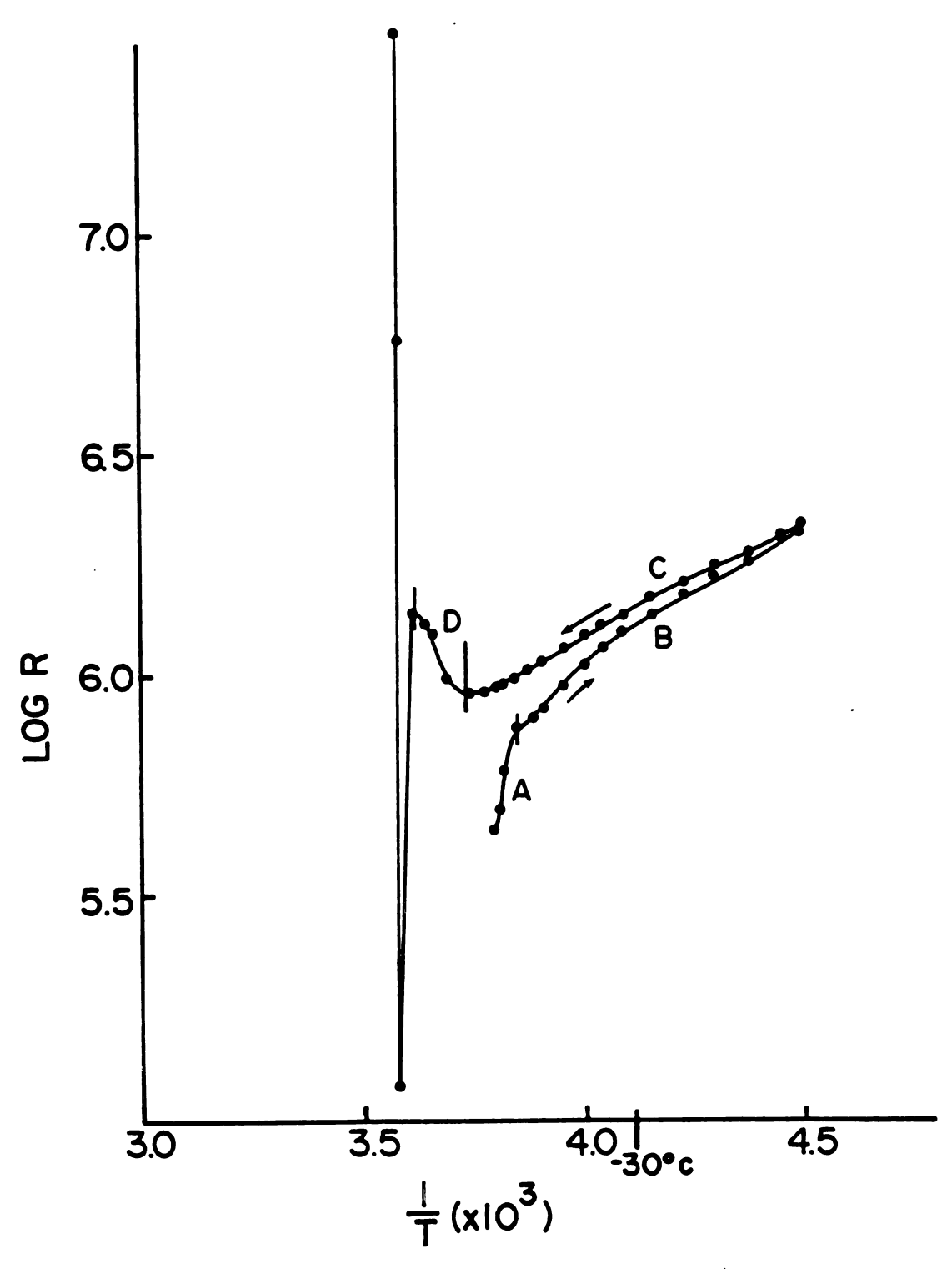


Figure 44. Log R versus 1/T for a sample of (K+C222)K-.
Curve A's band gap energy equals 3.05 eV, curve
B's band gap energy is 0.28 eV, curve C's band
gap energy is 0.22 eV, and curve D shows metallic
character.

The plot of log R versus 1/T is shown in Figure 44. The data were taken at a constant voltage of 30 volts and a constant pressure of 59.3 bar. The different slopes of the curves in Figure 44 may be due to the slow partial decomposition of the (K+C222)K-. A small amount of decomposition can cause a large change in the type and number of carriers in the sample which would greatly change its electrical nature. Alternatively, the different slopes might be caused by structure changes or "annealing" of the sample due to the pressure and/or the current passing through it. Which of these reasons, or whether some other possible cause created the different slopes in Figure 16 is not known.

The D.C. conductivity of a packed powder sample of  $(\text{Li}^+\text{C211})e^-$  was also determined in powder cell B. This material showed a plot of current versus voltage similar to that in Figure 43. The current at various temperatures was read and converted to resistance and a plot of log R versus 1/T was made, Figure 45. The right-hand line yielded a band gap of 0.99 eV and a  $\sigma = 5.1 \times 10^{-5} \text{ ohm}^{-1} \text{ cm}^{-1}$  at  $-45^{\circ}\text{C}$  and at infinite temperature  $\sigma_{\infty} = 3.6 \times 10^{+5} \text{ ohm}^{-1}$  cm<sup>-1</sup>. The band gap for the other straight line is 1.28 eV. The remaining segment of Figure 45 (>-32°C) shows an increasing resistance with increasing temperature. This could be caused by the sample undergoing a metal-nonmetal transition at -33°C or (more likely) by decomposition of

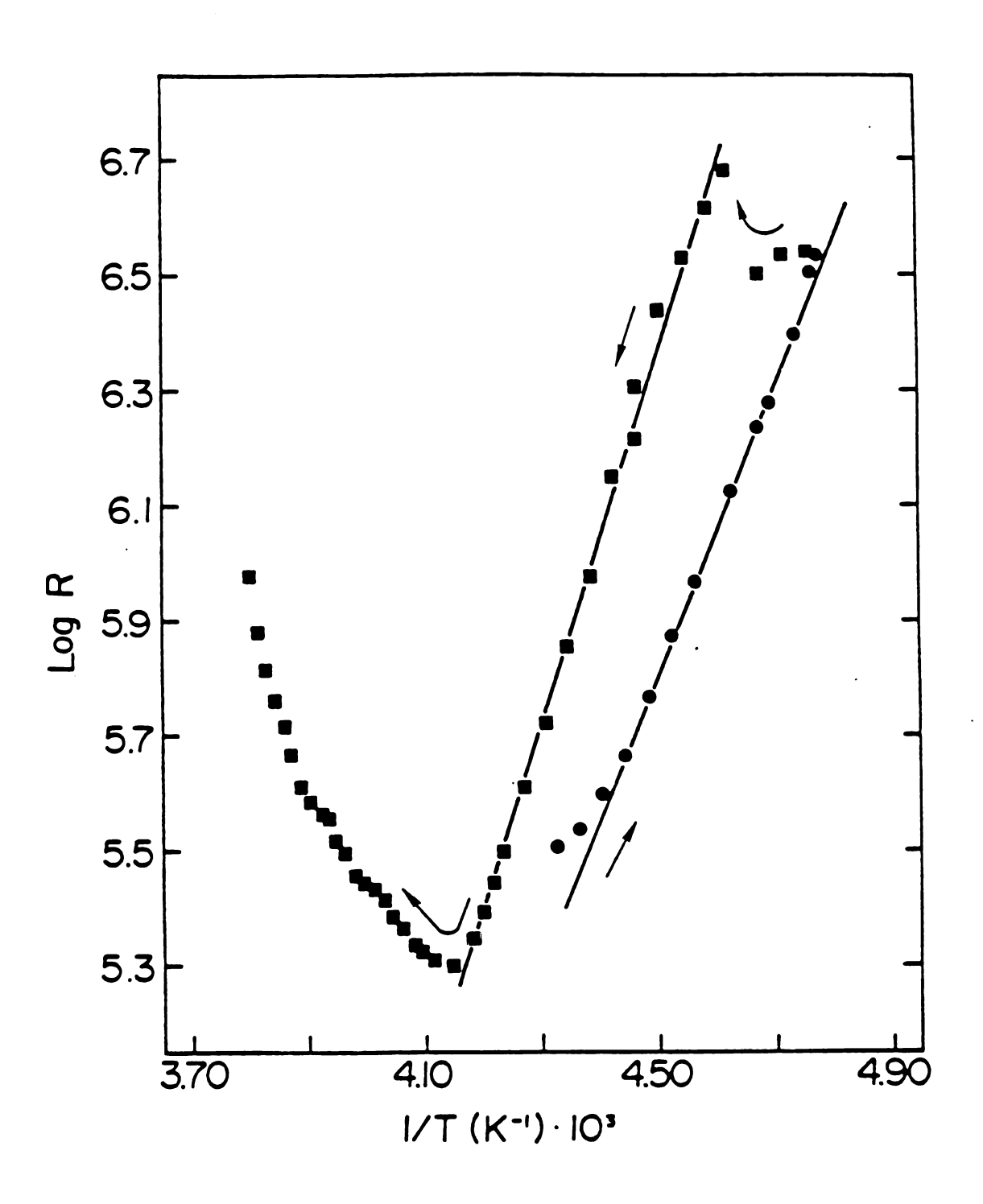


Figure 45. Log R versus 1/T for a sample of (Li<sup>+</sup>C2ll)e as obtained from readings made with powder cell B.

the sample. When the apparatus was opened and the sample was examined at -10°C the sample still appeared to be blue in color, the color of the fresh sample. This does not, however, rule out the presence of sufficient decomposition to raise the resistance less than an order of magnitude. For a more detailed description of the complex properties of (Li<sup>+</sup>C211)e<sup>-</sup> one should refer to J. S. Landers' thesis.

## IV.B. <u>D.C. Conductivity and Photoconductivity of Thin</u> Films of (Na + C222) Na -

Just as the physical appearance of crystals of the salt (Na<sup>+</sup>C222) Na<sup>-</sup> stimulated interest in measuring its D.C. electrical conductivity so did that of thin films formed by rapid evaporation of solutions of sodium and C222 in EA or MA. It was hoped that these films might be less contaminated with decomposition products and more continuous in nature than the powder. Also since the optical spectrum of these films is known, see Section III.A, it might be possible to investigate the change of the conductivity of the film with respect to the wavelength of light passing through it. To accomplish this end, an apparatus which allowed a two probe D.C. conductivity measurement to be made on a film of (Na<sup>+</sup>C222)Na<sup>-</sup> formed on the window of an optical cell was designed and built. electrical measurements were made by means of conducting silver decals, which were fired on the interior of the

optical cell, and connected to the instruments outside by wires through a vacuum seal. (For a detailed description of this apparatus see Section II.E.3.) Each conductivity cell had four conducting silver lines which were used two at a time.

The first few attempts to measure the current passing through a thin film of (Na<sup>+</sup>C222)Na<sup>-</sup> met with failure. failures were caused by the MA or EA dissolving the insulation on the copper wire soldered to the silver decals, which shorted the circuit. A way was devised to use uninsulated copper wire which was kept apart by the Teflon plug. The first film which was not plaqued by shorts gave results which were very different from those obtained with powdered samples. Figure 46 shows the plots of current versus voltage for two different pairs of probes. Note that the curve for probes 1 and 2 is not ohmic while that for probes 1 and 3 is ohmic. It is not known why the behavior of the film differs between the two pairs of silver lines. Perhaps it is that there are areas in the (Na<sup>+</sup>C222)Na<sup>-</sup> film which differ in their structure. Or perhaps what caused the difference was that the readings taken on the first pair of probes were made before the film annealed and that the film annealed in the time between readings with probes 1 and 2 and probes 1 and 3. An important point was that the fluorescent room lights were on during the entire experiment and for the first time the (Na<sup>+</sup>C222)Na<sup>-</sup> sample was

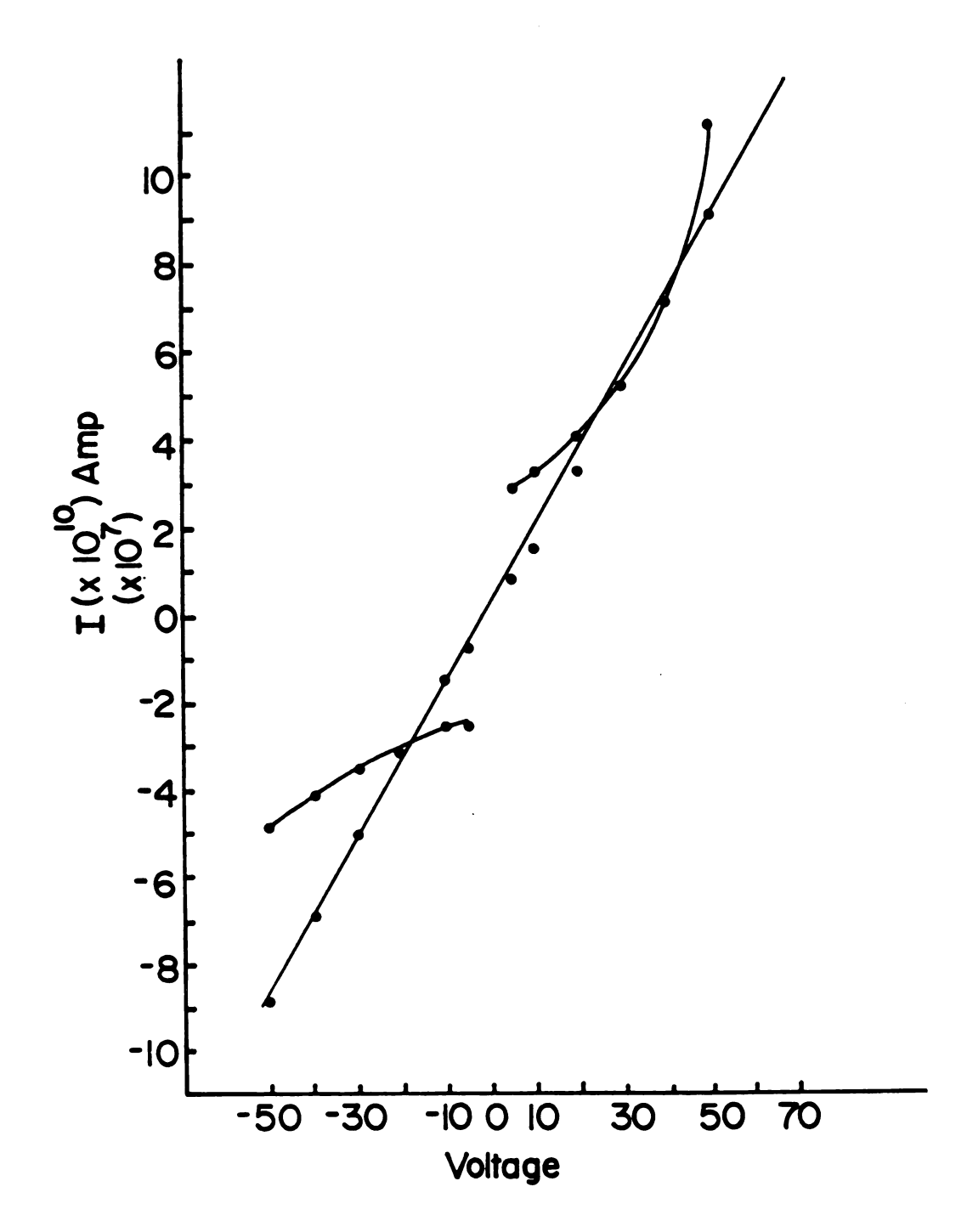


Figure 46. A plot of current versus voltage for two different pairs of probes for a film of (Na<sup>+</sup>C222) Na<sup>-</sup>. The straight line was for probes 1 and 3 and was later in time than the two curved lines, which were for probes 1 and 2.

in an apparatus which did not shield it from light. So it might have been that the difference between the pressed powder results and the above film results for (Na<sup>+</sup>C222)Na<sup>-</sup> resulted from action of the light on the sample. Possibly the light excited electrons into traps closer to the conduction band. This would help account for the apparent decrease in the band gap energy from 2.4 eV for the powder to 0.24 eV for the film. The band gap for the film was calculated from the plot of log R versus 1/T, Figure 47, which is for probes 1 and 3.

The next experiment explored the possibility that light might have an effect on the electrical properties of a film of (Na<sup>+</sup>C222)Na<sup>-</sup>. A new solution was made in an apparatus identical to the first one used except that the quartz optical cell was replaced by Pyrex tubing. This time the plots of current versus voltage remained nonohmic with the passage of time, Figure 48. Although the amount of current passing through the sample increased by an order of magnitude when the film was exposed to the room lights, both plots remained nonohmic. The probe pair with the greatest separation was used for these measurements, probe 1 and 4. An interesting observation was made about this film while the current versus voltage datawere being taken. When the room lights were turned off the current did not instantly fall to the dark current value. At a constant voltage of 5 volts the current only fell at a rate of

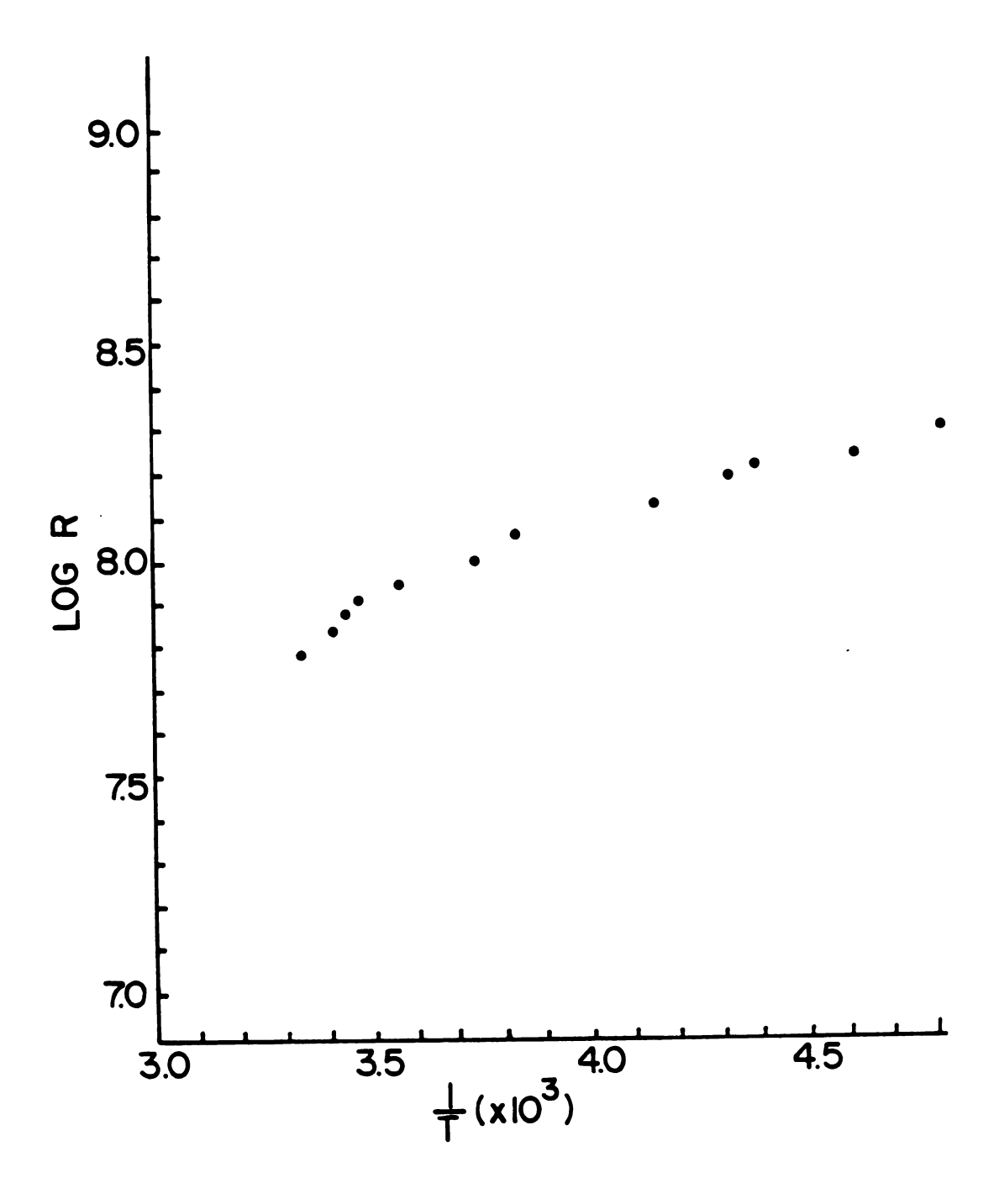


Figure 47. Log R versus 1/T for a film of (Na<sup>+</sup>C222)Na<sup>-</sup> exposed to fluorescent room light.

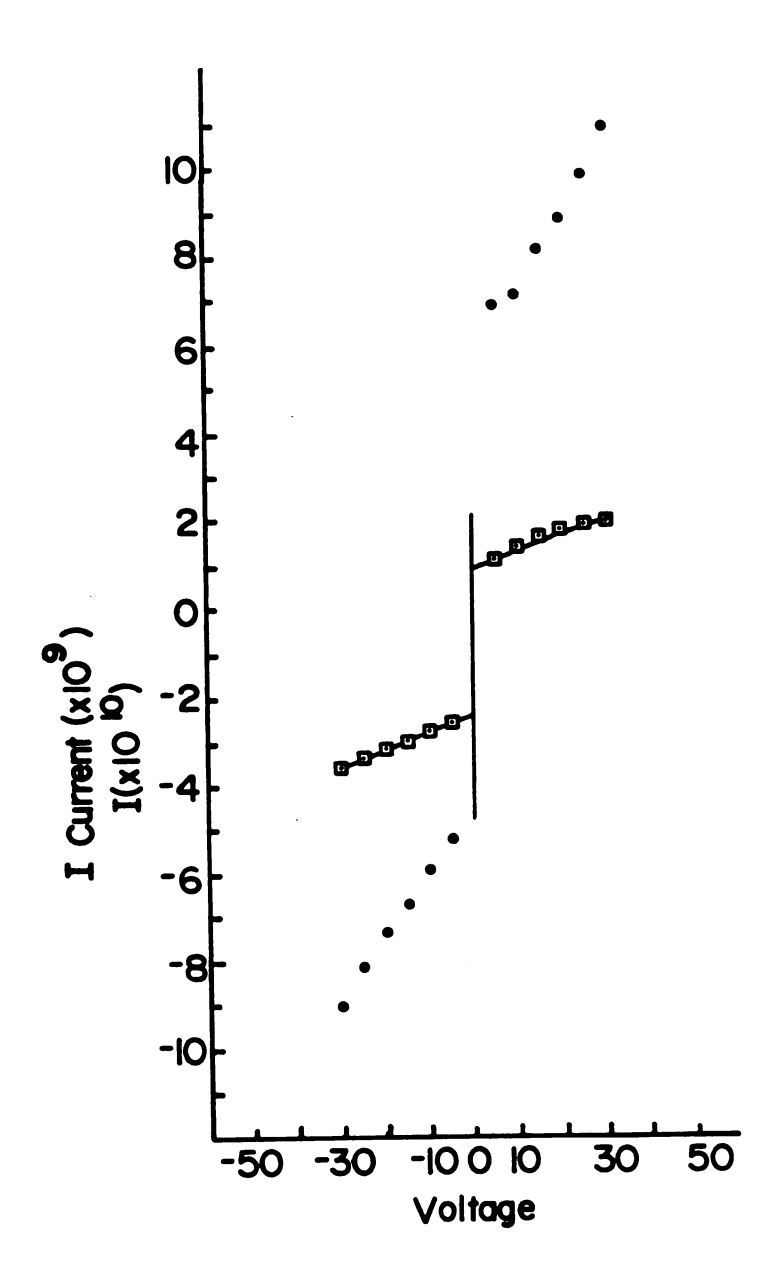


Figure 48. Plots of current versus voltage for a film of  $(Na^+C222)Na^-$ . The squares are for a film of  $(Na^+C222)Na^-$  in the dark between probes 1 and 4, whereas the round points are for the same film exposed to fluorescent room lights. The current scale is y x  $10^{-10}$  amps for the square points and y x  $10^{-9}$  amps for the round.

about 0.2 x 10<sup>-10</sup> amp per min. when the lights were turned off. When the lights were turned on the Keathly electrometer registered an immediate rise in the current to the light value. This indicates that the light promotes electrons in the (Na<sup>+</sup>C222)Na<sup>-</sup> film to traps which are reasonably long lived and more effective in carrying current through the sample. A plot of log R versus 1/T is shown in Figure 49 for this film of (Na<sup>+</sup>C222)Na<sup>-</sup> in the dark. The band gap energy calculated from this plot was 0.33 eV. It must be remembered that powders of (Na<sup>+</sup>C222)Na<sup>-</sup> had a band gap energy of 2.4 eV, and were ohmic in nature, whereas the films have a much smaller band gap energy, ~0.3 eV, or less, and show either ohmic or nonohmic behavior. This was true both for films exposed to light and in the dark.

The reaction of the (Na<sup>+</sup>C222)Na<sup>-</sup> film to a stronger light source and the dependence of current on wavelength were examined. When the film was illuminated with a 50 watt xenon lamp, the current increased as with the room lights but to an even greater extent. When a Bausch and Lomb grating monochrometer, 350 nm to 800 nm, was placed between the xenon lamp and the sample a small increase in current with some wavelengths could be seen, Figure 50. The small response to the light coming through the monochrometer was probably simply due to the fact that now only one wavelength region was exciting the sample at a

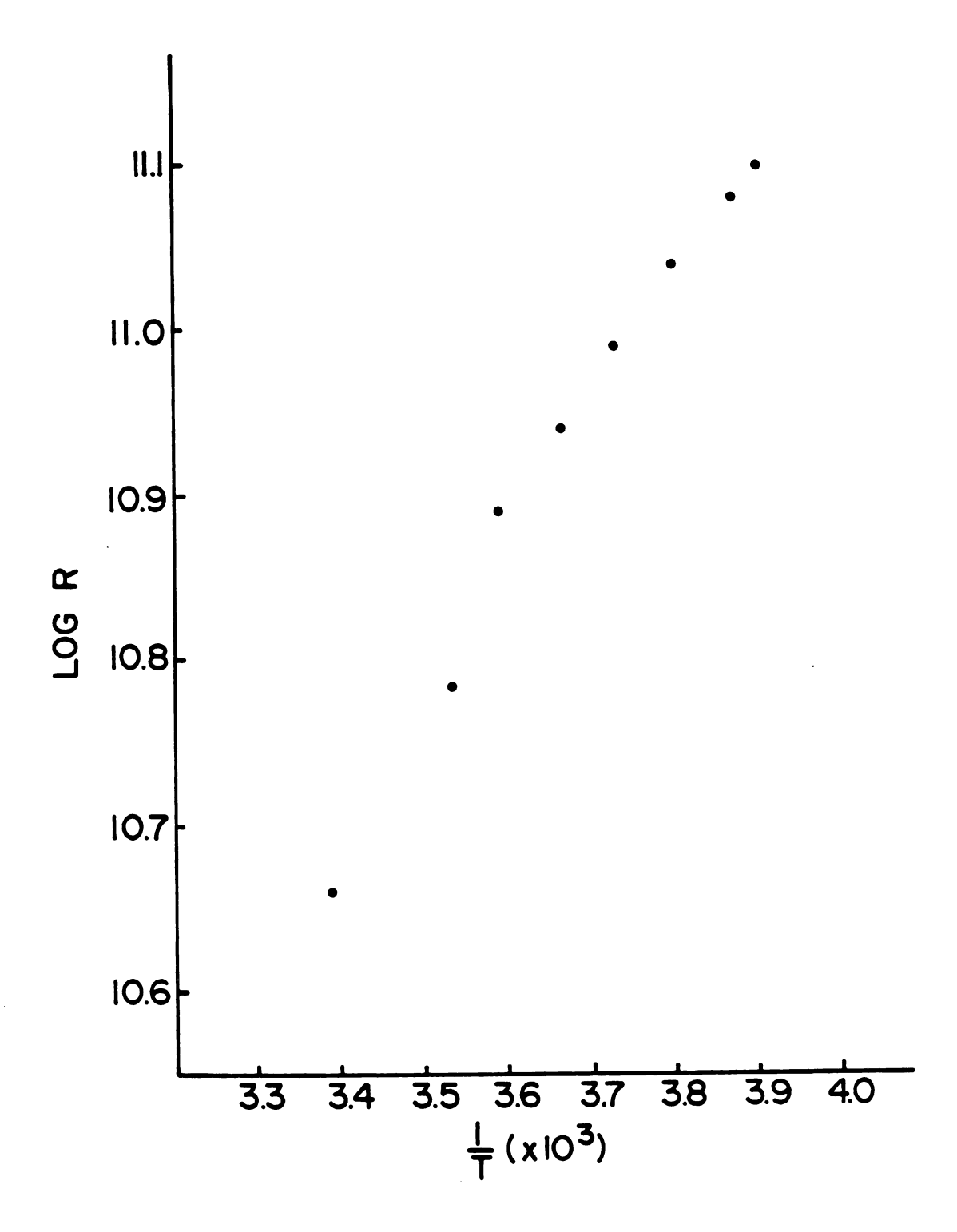


Figure 49. Log R versus 1/T for a film of (Na<sup>+</sup>C222)Na<sup>-</sup> in the absence of light.

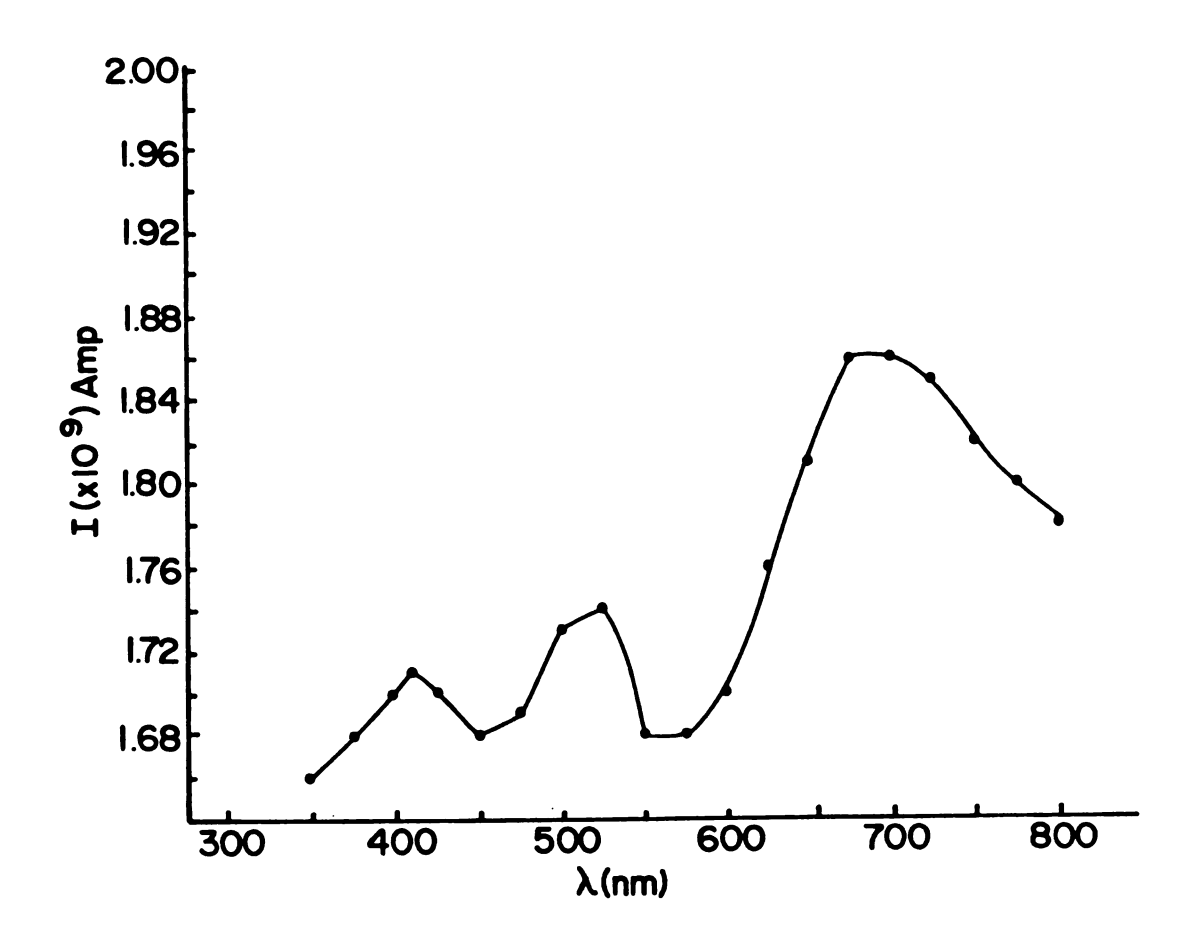


Figure 50. A plot of current versus wavelength at a constant voltage, 5 V. The light source was a 50 watt xenon lamp shown through a Bausch and Lomb grating monochrometer, 350 to 800 nm.

Table 4. Current Flow in a Film of (Na<sup>+</sup>C222)Na<sup>-</sup>.

Light Source on/off	v	I(Amp)	T(°C)
0.17, 0.11			1(0)
Xe/off; RL/off	5	$1.0 \times 10^{-10}$	2
Xe/off; RL/on	5	$3.5 \times 10^{-9}$	2
Xe/on; RL/off	5	$3.3 \times 10^{-8}$	0

time and the intensity of that light was greatly reduced. This same solution was used to make another film about a week later. The solution had been stored in a dry-ice-isopropanol bath during this time. For this experiment the light from the monochrometer was collected and channeled to the film by a Lucite rod which helped increase the light intensity falling on the sample. The results are shown in Figure 51. The first curve (A) was similar to Figure 50 but showed less structure and the response beyond the peak was not studied. As the light continued to shine on the film, the current response to wavelength changed as shown in Curve B. With more exposure to light the film gave a response similar to the dark current, An interesting thing to note was that when the film no longer responded to the light it had an ohmic current -

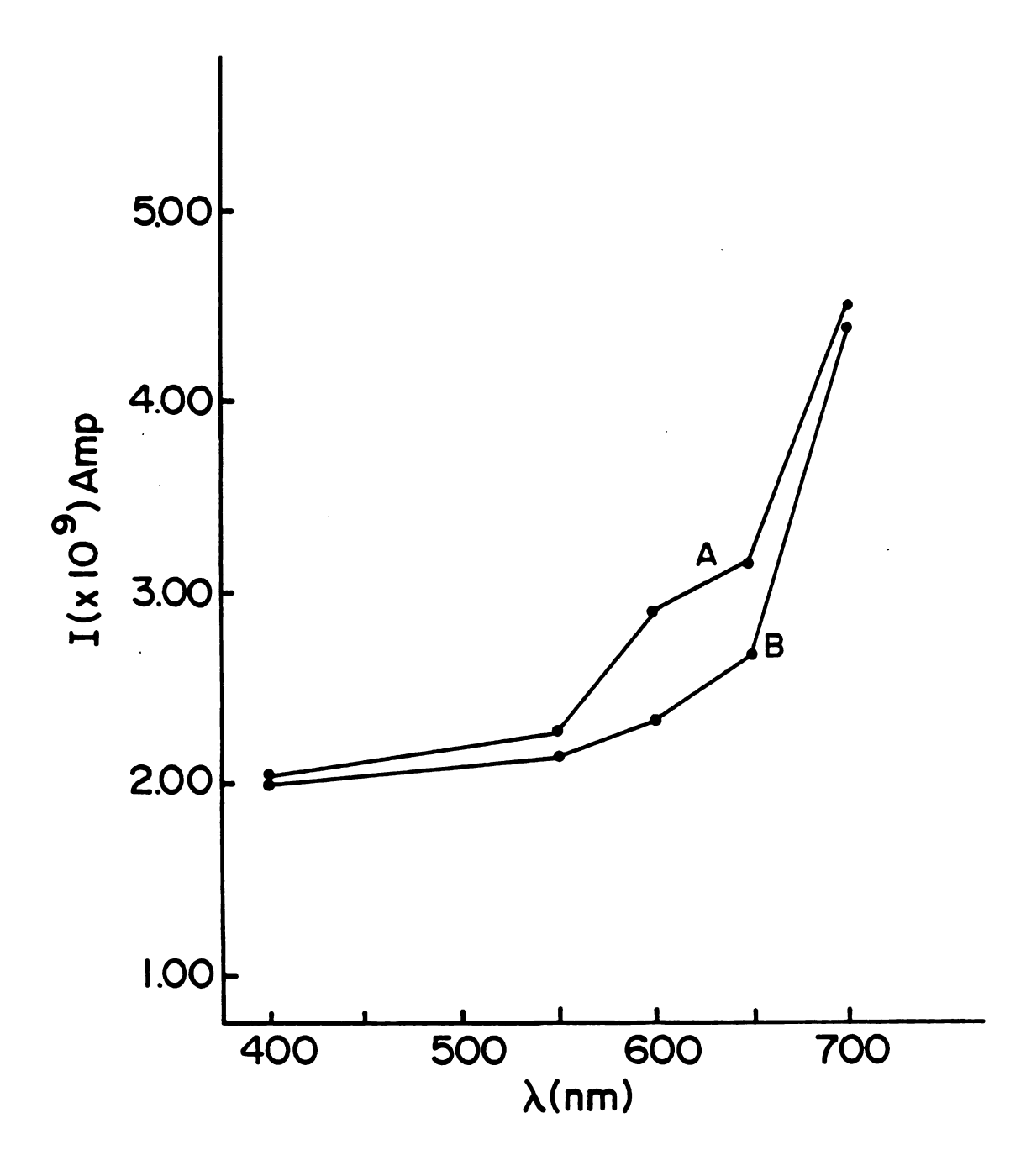


Figure 51. A plot of current versus wavelength for a film made from the same solution as made the film in Figure 50, but a week later. Curve A was a freshly made film. Curve B was for the film ~30 min later.

voltage curve.

A question was raised that perhaps the change in current flow with light was due to electron injection from the silver lines to the film. The first thing that was checked was whether it made any difference which side was illuminated. One side of the film was in contact with the glass and the silver lines so that the silver lines were exposed to the light while on the other side the film covered the silver lines. It was found that the current readings were essentially independent of which side was illuminated. Finally, the current flow across the glass between the silver lines was measured in the absence of a (Na<sup>+</sup>C222)Na<sup>-</sup> film. The well washed silver lines gave the results shown in Table 5 at room temperature.

Table 5. Current Characteristics of the Silver Lines.

Light Source on/off	v	I	(Blank I/Film I) %
dark	5	0.6 x 10 <sup>-11</sup>	6%
Xe/off; RL/on	5	$5.6 \times 10^{-11}$	1%
Xe/on; RL/on	5	$0.6 \times 10^{-9}$	1.5%

These results showed that the background current of the apparatus was a very small part of the readings taken with a

film of (Na<sup>+</sup>C222)Na<sup>-</sup> in place.

The next two solutions which were made in this apparatus gave (Na<sup>+</sup>C222)Na<sup>-</sup> films which were ohmic in nature and for which light had no effect on the current flow.

These films had a band gap of about 0.5 eV. The fourth solution made in the conductivity cell showed some change in current when light was passed through it for a short time. This film of (Na<sup>+</sup>C222)Na<sup>-</sup> was nonohmic with the lights on and ohmic in the dark. With the room lights on, this film showed the one order of magnitude increase in current flow as had been seen before, but before the wavelength dependence could be measured the film stopped responding to light. This film was probably a mixture of the two forms, nonohmic and ohmic, which soon became irreversible and totally the ohmic form.

All films of (Na<sup>+</sup>C222)Na<sup>-</sup> ohmic or nonohmic seemed to have a smaller band gap energy than the pressed powders of (Na<sup>+</sup>C222)Na<sup>-</sup>. Also the less stable nonohmic films have a current flow which was dependent on the wavelength of light passing through the film. The photoconductive behavior of these films is complex and is not understood at present. Studies are being continued by Dr. Long D. Le and Dr. Stephan Jaenicke to try to understand this behavior. The presence of photoconductivity has been clearly demonstrated in the present study but it is not a simple phenomenon. It is important to note that films which no

longer exhibit photoconductivity are nevertheless still gold-colored with no visual evidence of decomposition.

## CONCLUSIONS AND SUGGESTIONS FOR FUTURE WORK

## V.A. Conclusions

The species present in solids prepared by evaporating amine solutions depend on the metal, cation complexing agent, and solvent. The species contained in solids from methylamine and ethylamine are similar to those in solution.

Several types of solids can be isolated. Their properties indicate the existence of three classes of compounds. The first class consists of salts of the alkali metal anions, (M+C)M- and (M+C)N-. The second class consists of electride salts, (M+C)e-. The third class appears to consist of an expanded metal in which the cation is (KC222) (104) or (Li+C211) (123). Mixtures of these three classes also appear to exist. The electride salt and expanded metal can appear together and, appear to be interconvertible in some cases. Electrides and the corresponding expanded metals were studied in detail in both M. H. DaGue's and J. S. Landers' Theses (104 and 123). These possible expanded metals represent new examples in that class of materials and electrides represent a new class of compounds.

The compounds examined in this work by optical spectra

and D.C. conductivity were mostly of the first class with a few of the second class also studied. The compounds of the first class were gold to bronze in color with optical absorbances in the visible spectrum and were semiconductors. The compounds of the second class, electrides, absorbed in the near infrared and were more complex in their electrical behavior.

## V.B. Suggestions for Future Work

The study of the (M<sup>+</sup>C222)M<sup>-</sup>, (M<sup>+</sup>C222)N<sup>-</sup> and (M<sup>+</sup>C222)e<sup>-</sup> systems should be continued in order to further characterize them and to determine the factor(s) which influence such behavior as the photoconductivity of (Na<sup>+</sup>C222)Na<sup>-</sup>. To this end it will probably be necessary to study the x-ray structure and the optical and electrical properties of several compounds of the above types. These studies would be invaluably enhanced if single crystals can be produced.

More work on the D.C. conductivity should be done on the electride salts (K+C222)e- and (Li+C211)e-. The (Li+C211)e- apparently undergoes a MNM transition and the (K+C222)e- seems to be metallic, depending upon annealing conditions, and may be another system which is near the MNM transition. The D.C. conductivity should be expanded to four probe conductivity measurements of pressed powders and single crystals if possible. The mixed alkalides,

(Li<sup>+</sup>C211)Na<sup>-</sup> and (Cs<sup>+</sup>C322)Na<sup>-</sup> and more recently (Cs<sup>+</sup>18C6)Na<sup>-</sup> are quite stable in their bronze-colored films formed from methylamine solutions. These systems should be good candidates for producing single crystals and thereby answering questions about structure and optical and electrical properties.



### APPENDIX A

# THERMODYNAMIC STABILITY OF (Na<sup>+</sup>C222)Na<sup>-</sup> AT 273 K

A longstanding question has been whether (Na<sup>+</sup>C222)Na<sup>-</sup> is thermodynamically or just kinetically stable. One experimental observation suggested that the compound is only kinetically stable. Crystals of the compound were stored in sealed tubes under vacuum at 243 K. After about one year of storage, the samples contained gray lumps which were presumably sodium metal. The samples with gray lumps could be dissolved to give stable blue solutions, which indicates that the lumps were probably not pieces of decomposed organic matter.

If the lumps were sodium metal, then the compound could have decomposed according to the reverse of reaction (A-1).

$$C222_{(s)} + 2Na_{(s)} \stackrel{?}{\leftarrow} (Na^{+}C222)Na_{(s)}^{-}$$
 (A-1)

The compound is thermodynamically stable with respect to  $C222_{(s)}$  and  $Na_{(s)}$  if the free energy change for (A-1) is negative. The chemical potential of solid C222 must be greater than or equal to the chemical potential of the cryptand in solution (in the absence of supersaturation).

Thus, the free energy change for Equation (A-1) will be negative if the free energy change for Equation (A-2) is negative.

$$C222_{(sol)} + 2Na_{(s)} \stackrel{?}{\downarrow} (Na^{+}C222)Na_{(s)}^{-}$$
 (A-2)

This equilibrium is the sum of the following two reactions:

$$C222_{(sol)} + 2Na_{(s)} \stackrel{?}{\leftarrow} (Na^{+}C222)_{(sol)} + Na_{(sol)} - (A-3)_{(sol)}$$

$$(Na^{+}C222)_{(sol)} + Na_{(sol)}^{-} \stackrel{?}{\leftarrow} (Na^{+}C222)Na_{(s)}^{-}$$
 (A-4)

Therefore, if a C222 solution over sodium metal isothermally gives crystals of (Na<sup>+</sup>C222)Na<sup>-</sup>, the compound is stable with respect to sodium metal and cryptand at that temperature. This spontaneous growth of (Na<sup>+</sup>C222)Na<sup>-</sup> was observed in this work at 273 K.

Using the apparatus in Figure 11, an ethylamine solution of 0.04 M C222 was stirred at 273 K over a sodium mirror which contained twice as many moles of sodium as there was C222 in solution. Before all the sodium had dissolved, many gold-colored (Na<sup>+</sup>C222)Na<sup>-</sup> crystals formed in the blue solution.

This experiment proves that (Na<sup>+</sup>C222)Na<sup>-</sup> is thermodynamically stable with respect to cryptand and sodium metal at 273 K. However, it is possible that the compound may slowly decompose, perhaps according to the following scheme:

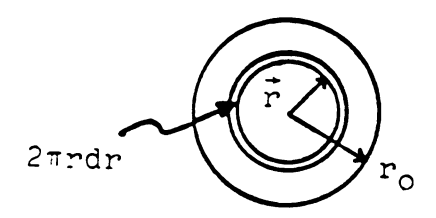
This decomposition may be initiated by absorption of light. Several observations support the hypothesis that the compound is photosensitive. A thin blue film of (Na<sup>+</sup>C222)Na<sup>-</sup> was formed in a tube from a tetrahydrofuran solution of the crystals. The tube was stored at room temperature in a dark drawer and showed little decomposition over an eight week period. At the end of that period, the tube was exposed to ordinary fluorescent lighting of the room and the blue film bleached in 2 to 3 hours. During the photographing of some of the crystals at room temperature under light from a tungsten lamp, some of the gold-colored single crystals turned dark green irreversibly while others were unchanged.

## APPENDIX B

## EFFECT OF OPTICAL FILM NON-UNIFORMITY

A study was conducted to determine the effect on spectral band shape of films of variable thickness and of films partially covering the beam cross section as it passes through the optical cell. Professor J. L. Dye derived the spectral effect of non-uniform film thickness and Mr. Jim Anderson provided much of the computational effort.

Suppose there is a circular light beam of radius  $r_0$  with total intensity  $I_0(\lambda)$  and local intensity  $i_0(\lambda)$ :



Then  $I_O(\lambda) = i_O(\lambda)$  · S where S is the beam cross section and

$$I_{o}(\lambda) = \int_{0}^{r_{o}} i_{o}(\lambda) 2\pi r dr = i_{o}\pi r_{o}^{2}$$
 (B-1)

Let  $I(\lambda)$  be the total light intensity passing through the sample, such that

$$I(\lambda) = \int_{0}^{r_{0}} (\dot{r}, \lambda) 2\pi r dr$$
 (B-2)

Bouguer-Lambert or Beer's law states that, for a sample of uniform thickness x and a light beam of uniform cross section,

$$I = I_o e^{-\alpha x}$$

where  $\alpha$  = absorptivity (cm<sup>-1</sup>) = 2.303· $\epsilon$ ( $\lambda$ )·c where  $\epsilon$ ( $\lambda$ ) is the molar extinction coefficient and c is the molar concentration. Then

2.303 log 
$$\frac{I_O(\lambda)}{I(\lambda)} = A = \alpha x$$

However, for a non-uniform thickness, x(r),

$$i(\lambda) = i_{O}(\lambda) e^{-\alpha(\lambda) \mathbf{x}(\vec{r})}$$
 (B-3)

and

$$I(\lambda) = 2\pi i_{o}(\lambda) \int_{o}^{r_{o}} re^{-\alpha (\lambda) x (\overrightarrow{r})} d\overrightarrow{r}$$
 (B-4)

For simplicity, assume initially that the non-uniform film fills the light beam cross section and  $x(r) = a + b(r/r_0)$ 

Using this model, equation B-4 becomes

$$I(\lambda) = 2\pi i_{o}(\lambda) \int_{o}^{r_{o}-\alpha(\lambda)[a+(\frac{r}{r_{o}})b]} d\vec{r}$$

After performing the integration with a table of integrals and using Equation B-1 for  $I_O(\lambda)$ :

$$\frac{I(\lambda)}{I_{O}(\lambda)} = 2e^{-\alpha(\lambda) \cdot a} \left[ \frac{1 - e^{-\alpha(\lambda)b}(1 + (\lambda)b)}{(\alpha(\lambda)b)^{2}} \right]$$
 (B-5)

If the film were of uniform thickness <  $\ell$  > then  $\frac{I(\lambda)}{I_0(\lambda)} = e^{-\alpha < \ell >}$  and  $\alpha < \ell > = 2.303 \log \frac{I_0}{I}$ . Call  $\log \frac{I_0}{I}$  the nominal absorbance  $A_{nom}$ . Therefore

$$2.303A_{nom} = \alpha < \ell >$$
 (B-6)

But the film is not of uniform thickness and the "area weighted" or average film thickness <1> is calculated by

$$<\ell> = \frac{\int_{0}^{r_{O}} drx(r) 2\pi r dr}{\int_{0}^{r_{O}} dr 2\pi r dr} = \frac{2}{r_{O}^{2}} \int_{0}^{r_{O}} rx(r) dr$$
 (B-7)

For the model chosen,  $x(r) = a + b(r/r_0)$ , so

$$\langle \ell \rangle = \frac{2}{r_0^2} \int_0^{r_0} r[a+b(\frac{r}{r_0})] dr$$

$$< \ell> = \frac{2a}{r_0^2} \int_0^{r_0} r dr + \frac{2b}{r_0^3} \int_0^{r_0} r^2 dr$$

$$\langle l \rangle = \frac{2a}{r_0^2} (\frac{r_0^2}{2}) + \frac{2b}{r_0^3} (\frac{r_0^3}{3}) = a + \frac{2}{3}b$$
 (B-8)

The relationship of a to b can assume any value. If b =  $-\frac{a}{2}$  is arbitrarily chosen, then Equation B-6 becomes

$$2.303A_{\text{nom}} = a(a + \frac{2}{3}b) = \alpha a(\frac{2}{3})$$

Then

$$\alpha a = \frac{3}{2}(2.303) A_{\text{nom}}$$
 (B-9)

and

$$\alpha b = -\frac{3}{4}(2.303) A_{nom}$$
 (B-10)

These values can now be used in Equation B-5 to compute  $\frac{I}{I_0}$ . But first make this specific case more general by allowing the film to cover a variable portion of the optical beam cross section. If

T = (area of beam covered)/(total beam area) = 
$$(\frac{r}{r_o})^2$$

then

$$I(\lambda) = TI(\lambda)_{spot} + (1-T)I_{o}(\lambda)$$
 (B-11)

Thus, Equation B-5 becomes

$$\frac{I(\lambda)}{I_{O}(\lambda)} = T2e^{-\alpha(\lambda)\cdot a} \left[\frac{1-e^{-\alpha(\lambda)\cdot b}(1+\alpha(\lambda)b)}{(\alpha(\lambda)b)^{2}}\right] + (1-T) \quad (B-12)$$

Now, apply the following conditions:

$$\left(\frac{r}{r_0}\right)^2 = T = 1.00$$

$$A_{nom} = 1.50$$

as well as the previously selected b = -a/2. This calculation is for a film which covers the whole beam cross section. If the film were of uniform thickness, the nominal absorbance would be 1.5. However, the film is conical:

$$\frac{1}{a} = \frac{b}{a} - a/2$$

Using Equations B-9 and B-10, a = 5.18 and b = -2.59. Therefore Equation B-12 is

$$(I/I_o)_{max} = (1.00)(2)e^{-5.18}\left[\frac{1-e^{2.59}(1-2.59)}{(2.59)^2}\right] - (1-1.00)$$
 $(I/I_o)_{max} = .0329 \text{ and } (I_o/I)_{max} = 26.9$ 

$$A_{max} = \log(I_o/I)_{max} = 1.43$$

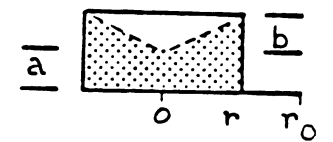
But  $A_{\text{nom}} = 1.50$ , so for this very specific case, the nominal absorbance is decreased 4.7% due to the non-uniform film thickness.

The results of a series of such calculations are tabulated in Tables B-1 through B-5 for various geometries and displayed in Figures B-1 and B-2 for the first two geometries.

Table B-1. Film Shape Effects:  $A_{max}$  for b = -a/2

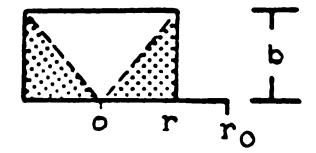
						_		
							ó	r r
			7	Anominal				
		.500	.750	1.000	1.250	1.500	1.750	2.000
	.50	.123	.125	.125	.125	.125	.125	.125
	.75	Anominal  .500 .750 1.000 1.250 1.500 1.750 2  0 .123 .125 .125 .125 .125 .125  5 .288 .330 .348 .354 .357 .358  0 .327 .390 .419 .433 .439 .441  0 .407 .534 .615 .663 .689 .704	.359					
$\frac{r}{r_o}$	.80	.327	.390	.419	.433	.439	.441	.443
-0	.90	.407	.534	.615	.663	.689	.704	.712
	1.00	.491	.731	.967	1.200	1.429	1.656	1.880

Table B-2. Film Shape Effect:  $A_{max}$  for b = a/2



				Anom				
		.500	.750	1.000	1.250	1.500	1.750	2.000
r	.50	.123	.125	.125	.125	.125	.125	.125
	.75	.291	.333	.349	.355	.358	.358	.359
	.80	.330	.393	.422	.434	.440	.442	.443
	.90	.412	.541	.622	.669	.694	.707	.714
	1.00	.498	.745	.991	1.236	1.479	1.721	1.962

Table B-3. Film Shape Effect:  $A_{max}$  for a = 0, b 0



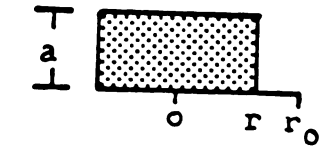
				Anom				
		.500	.750	1.000	1.250	1.500	1.750	2.000
r r <sub>o</sub>	.50	.119	.122	.123	.124	.124	.124	.125
	.75	.272	.312	.331	.341	.346	.349	.352
	.80	.308	.365	.395	.411	.421	.427	.431
	.90	.383	.493	.565	.610	.640	.660	.673
-	1.00	.462	.662	.842	1.001	1.143	1.269	1.381

Table B-4. Film Shape Effect:  $A_{max}$  for b = -a

a			b	-0-
	ö	r	To.	

	.500	.750	A <sub>nom</sub>	1.250	1.500	1.750	2.000
.50	.106	.112	.115	.117	.118	.119	.120
.75	.228	.263	.115	.296	.305	.312	.317
.80	.257	.302	.330	.349	.362	.372	.380
.90	.317	.394	.447	.485	.513	.536	.554
1.00	.380	.506	.606	.689	.759	.819	.872

Table B-5. Film Shape Effect:  $A_{max}$  for b = 0; uniform thickness.



				Anom				
		.500	.750	1.000	1.250	1.500	1.750	2.000
$\frac{r}{r_o}$	.50	.123	.125	.125	.125	.125	.125	.125
	.75	.292	.334	.350	.356	.358	.359	.359
	.80	.332	.395	.423	.435	.440	.442	.443
	.90	.414	.594	.625	.671	.696	.709	.715
	1.00	.500	.750	1.000	1.250	1.500	1.750	2.000

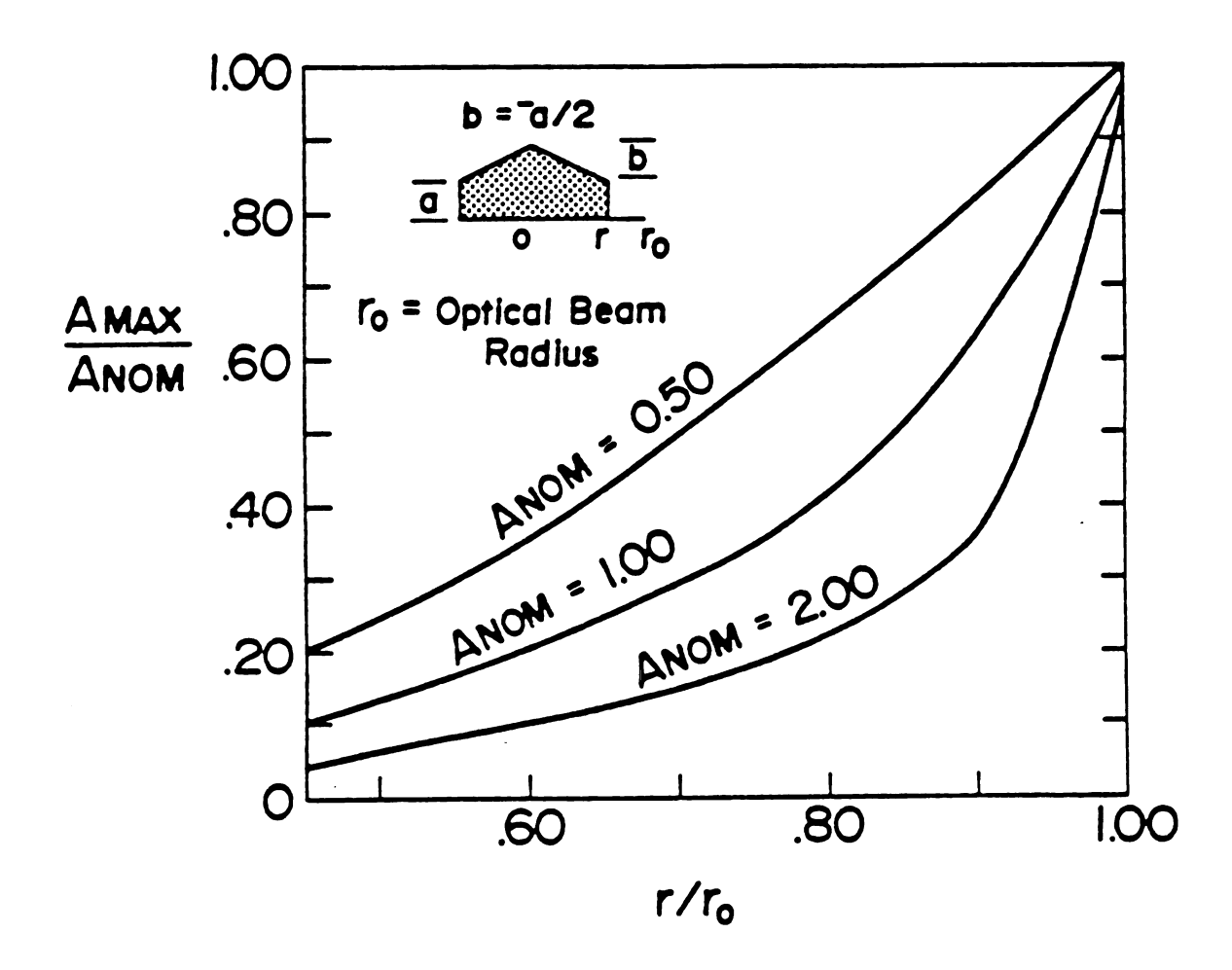
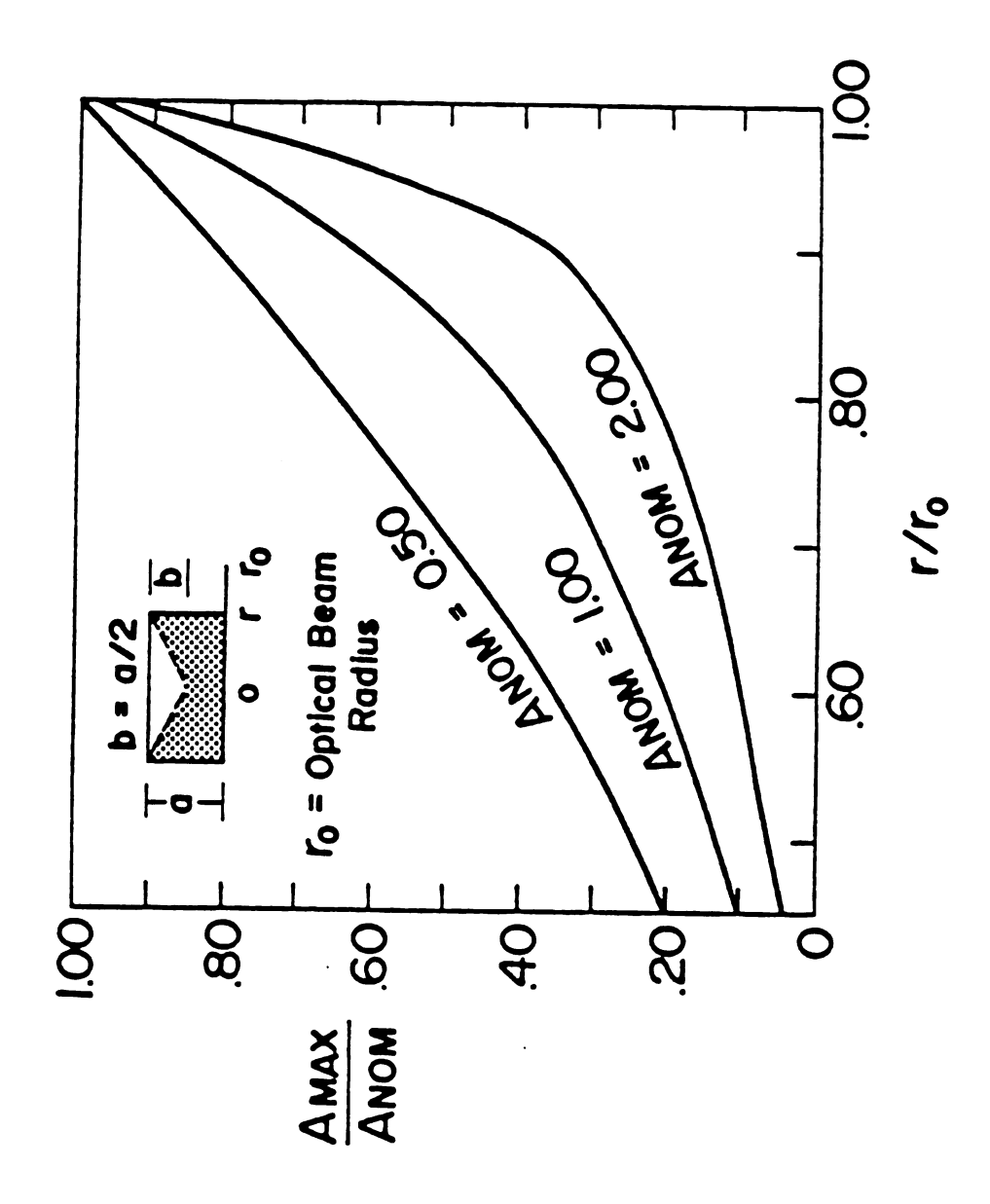


Figure B-1. Effect on the peak amplitude of an optical film which is of non-uniform thickness (shape as indicated) and which fills various amounts of the optical beam.



Effects on the peak amplitude of an optical film which is of non-uniform thickness (shape as indicated) and which fills various amounts of the optical beam. Figure B-2.

It is informative to observe the effect of a film of non-uniform thickness on a complete line shape, not just upon the maximum peak amplitude as in the previous tables and figures. An absorption curve of Lorentzian shape can be described by ( ):

$$g(\omega - \omega_0) = \frac{T_2/\pi}{1 + (\omega - \omega_0)^2 T_2^2}$$
 (B-13)

where  $\omega_0$  is the angular frequency of the radiation at resonance and  $T_2$  is the spin-spin relaxation time. For the purposes here, the line shape function can be simplified considerably:

$$Y = Y_{\text{max}} \frac{c}{d^2 + (\omega - \omega_0)^2}$$
 (B-14)

where  $Y_{max}$  equals  $A_{nom}$  when c=d=1. For each incremental step of  $(\omega-\omega_0)$  in Equation B-14, Equation B-12 is employed to determine  $A_{max}$  for the desired  $A_{nom}$  and chosen film geometry. The results are displayed graphically in Figures B-3 and B-4 for nominal absorbances of 1.50 and 2.00, respectively.

The results show that the highest nominal absorbances are affected the most by both irregular film thickness and incomplete coverage of the beam cross section. Films not filling the entire optical beam cross section cause a significant peak broadening with a reduction in amplitude.

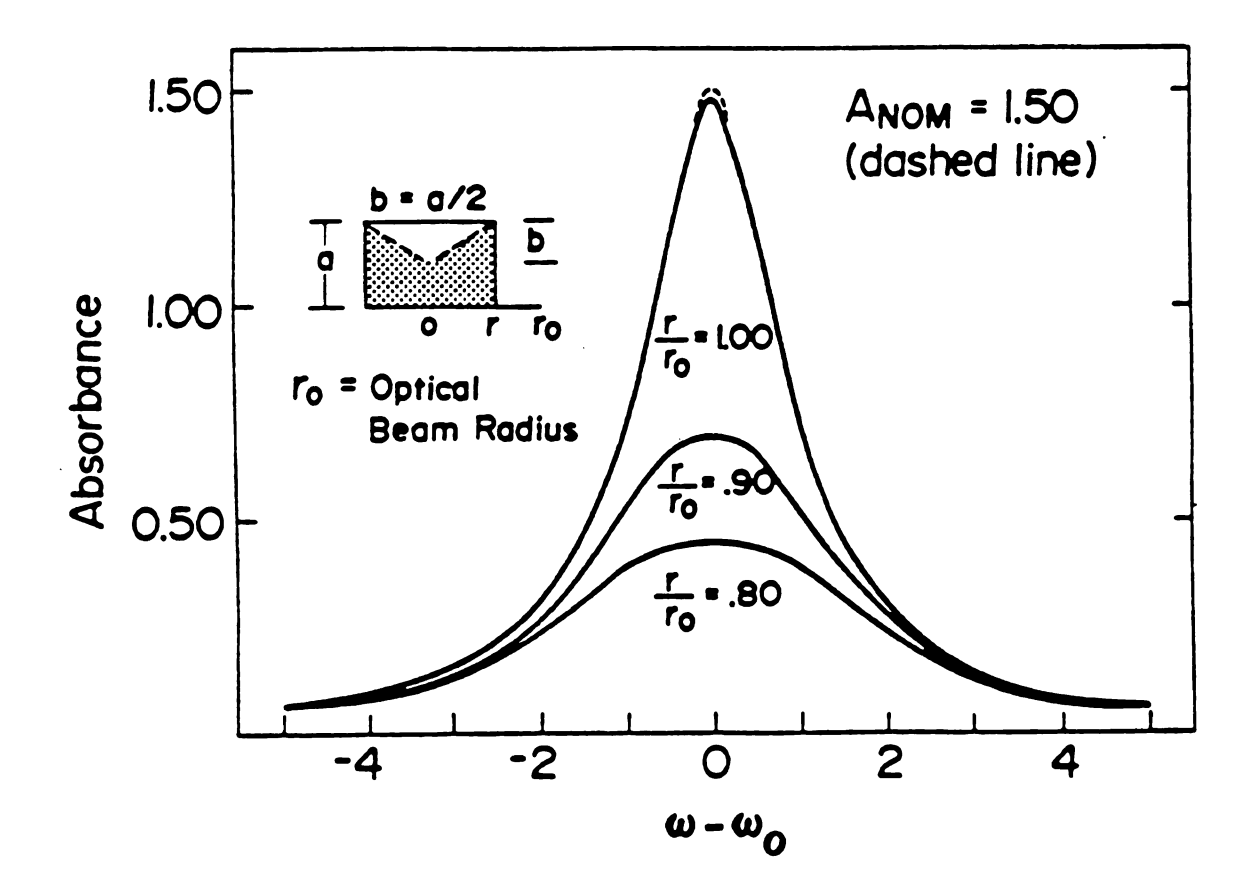


Figure B-3. Effect on a Lorentzian absorption peak with a nominal 1.50 absorbance when the optical film is of non-uniform thickness (shape as indicated) and when it fills various amounts of optical beam.

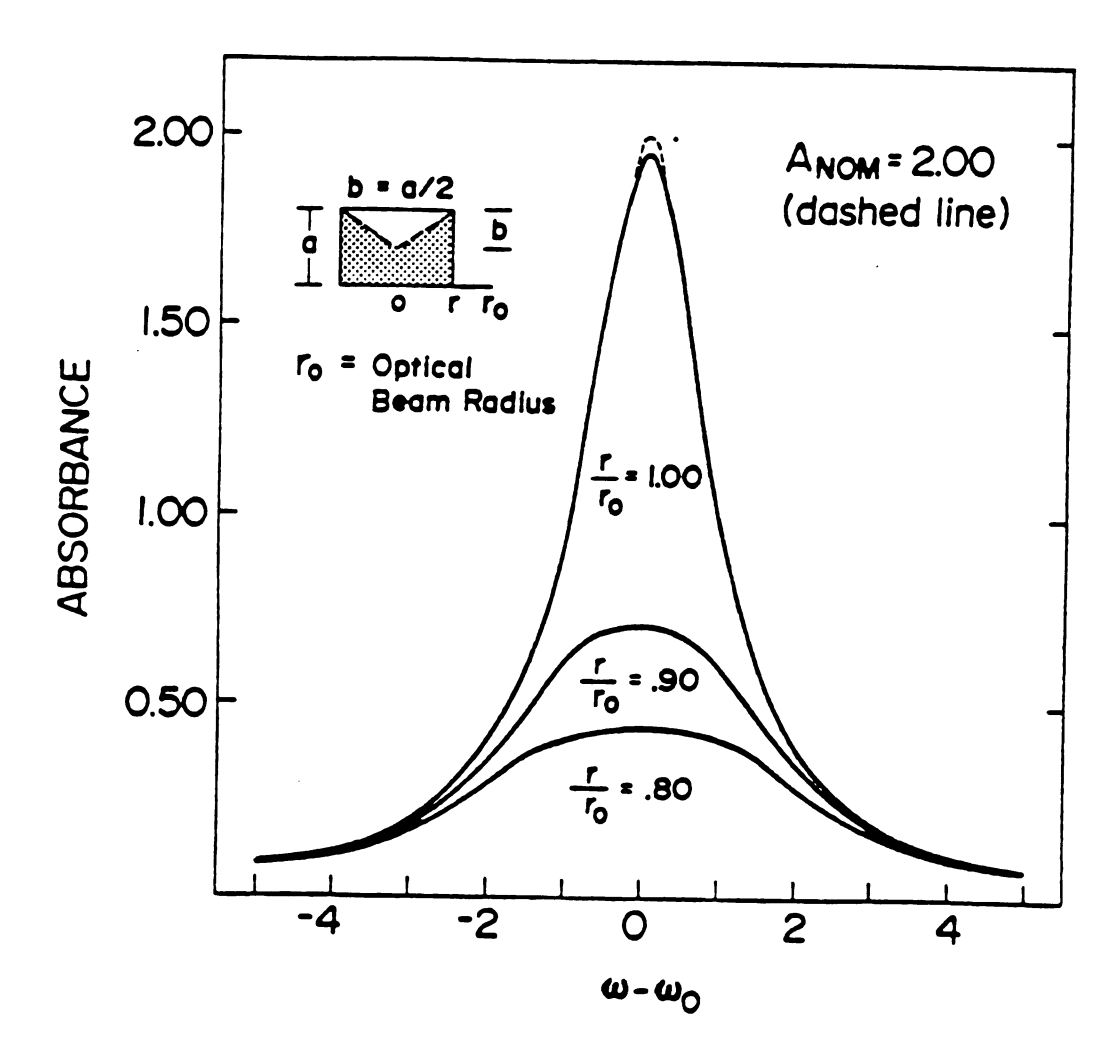
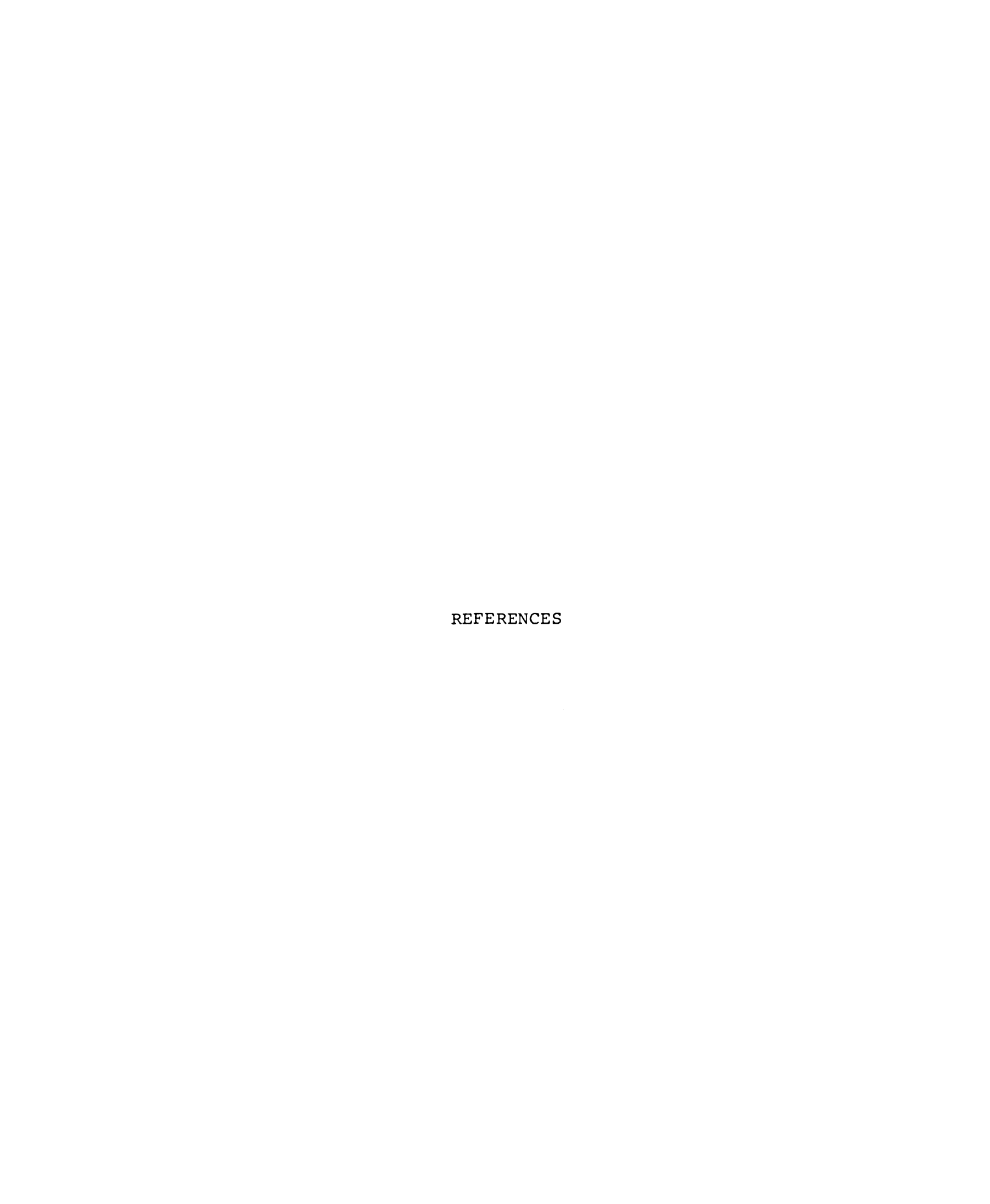


Figure B-4. Effect on a Lorentzian absorption peak with a nominal 2.00 absorbance is of non-uniform thickness (shape as indicated) and when it fills various amounts of the optical beam.

However, most films in this study covered much of the optical cell walls, and with the beam passing through two walls, the probability of only 81% or 64% coverage as depicted in Figures B-3 and B-4 seems remote. It is very difficult to judge the uniformity of film thicknesses, so no one geometry in this study should be considered more likely than any other. It should be noted, however, that as films become very thin (the center of the disk for Table B-3 or the edges for Table B-4), the deviations from nominal absorbance become quite large.



#### REFERENCES

- 1. W. Weyl, Ann. Phys. 197, 601 (1863).
- G. Lepoutre and M. J. Sienko (eds.), "Metal-Ammonia Solutions, Colloque Weyl I", W. A. Benjamin (New York) 1964.
- 3. J. J. Lagowski and M. J. Sienko (eds.), "Metal-Ammonia Solutions", Butterworths (London) 1970.
- 4. J. Jortner and N. R. Kestner (eds.), "Electronics in Fluids", Springer-Verlag (New York) 1973.
- 5. J. Phys. Chem. 79 (26) 1975.
- 6. J. Phys. Chem., in press.
- 7. J. L. Dye, M. G. DeBacker and V. A. Nicely, <u>J. Am.</u> Chem. Soc., 92, 5226 (1970).
- 8. J. L. Dye, M. T. Lok, F. J. Tehan, R. B. Coolen, N. Papadakis, J. M. Ceraso, and M. G. DeBacker, Ber. Bunsenges. Phys. Chem., 75, 659 (1971).
- 9. J. L. Dye in "Electrons in Fluids, Colloque Weyl III", J. Jortner and N. R. Anloniewicz, Phys. Rev. A. 4, 427 (1971).
- J. L. Dye, J. M. Ceraso, M. T. Lok, B. L. Barnett and F. J. Tehan, J. Am. Chem. Soc., 96, 608 (1974).
- 11. G. Lepoutre and J. P. Lelieur, Reference 3, p. 247.
- 12. R. A. Ogg, J. Am. Chem. Soc., 68, 155 (1946).
- 13. J. Jortner, J. Chem. Phys., 30, 829 (1959).
- 14. G. A. Kenney-Wallace, Acc. Chem. Res., 11, 433 (1978).
- 15. J. L. Dye, Reference 3, p. 1.
- M. Gold, W. L. Jolly and K. S. Pitzer, <u>J. Am. Chem.</u> Soc., 84, 2264 (1962).
- 17. J. V. Acrivos and K. S. Pitzer, <u>J. Phys. Chem.</u>, <u>66</u>, 1693 (1962).

- 18. J. P. Lelieur, P. Damay, and G. Lepoutre, Reference 5, p. 2879.
- 19. E. Huster, Ann. Phys. 33, 477 (1938).
- S. Freed and N. Sugarman, <u>J. Chem. Phys.</u>, <u>11</u>, 354 (1943).
- 21. C. A. Hutchison, Jr., and R. C. Pastor, <u>Rev. Mod.</u> Phys. <u>25</u>, 285 (1953); <u>J. Chem. Phys. <u>21</u>, 7959 (1953).</u>
- 22. A. Demortier and G. Lepoutre, <u>C. R. Acad. Sci. Paris</u> 268, 453 (1969).
- 23. A. Demortier, M. DeBacker, and G. Lepoutre, J. Chim. Phys. 69, 380 (1972).
- 24. J. C. Thompson, "Electrons in Liquid Ammonia", Clarendon Press (Oxford) 1976.
- 25. T. A. Beckman and K. S. Pitzer, <u>J. Phys. Chem.</u> <u>65</u>, 1527 (1961).
- 26. R. R. Dewald and J. L. Dye, <u>J. Phys. Chem.</u> <u>68</u>, 128 (1964).
- 27. R. R. Dewald and J. L. Dye, <u>J. Phys. Chem.</u> <u>68</u>, 121 (1964).
- 28. I. Hurley, T. R. Tuttle, Jr., and S. Golden, <u>J. Chem.</u> Phys. 48, 2818 (1968).
- 29. S. Matalon, S. Golden, and M. Ottolenghi, <u>J. Phys.</u> Chem. 73, 3098 (1969).
- G. W. A. Fowles, W. R. McGregor, and M. C. R. Symons,
   J. Chem. Soc., 3329 (1957).
- 31. M. C. R. Symons, <u>J. Chem. Phys.</u> <u>30</u>, 1628 (1959; <u>Quart. Rev.</u> <u>13</u>, 99 (1959).
- 32. L. R. Dalton, J. D. Rynbrandt, E. M. Hansen, and J. L. Dye, J. Chem. Phys. 44, 3969 (1966).
- 33. M. G. DeBacker and J. L. Dye, <u>J. Phys. Chem.</u> <u>75</u>, 3092 (1971).
- 34. J. L. Dye, M. G. DeBacker, J. A. Eyre, and L. M. Dorfman, J. Phys. Chem 76, 839 (1972).
- 35. L. J. Gilling, J. G. Kloosterboer, R. P. H. Retts-chinck, and J. D. W. vanVoorst, Chem. Phys. Lett. 8, 457, 462 (1971).

- 36. G. Gabor and K. H. Bar-Eli, <u>J. Phys. Chem.</u> <u>75</u>, 286 (1971).
- 37. M. Fisher, G. Ramme, S. Claesson, and M. Swarc, Chem. Phys. Lett. 9, 309 (1971).
- 38. A. Gaathon and M. Ottolenghi, Israel <u>J. Chem.</u> <u>8</u>, 165 (1970).
- 39. D. Huppert and K. H. Bar-Eli, <u>J. Phys. Chem.</u> <u>74</u>, 3285 (1970).
- 40. S. H. Glarum and J. H. Marshall, <u>J. Chem. Phys.</u> <u>52</u>, 5555 (1970).
- 41. R. R. Dewald and K. W. Browall, <u>J. Phys. Chem.</u> <u>74</u>, 129 (1970).
- 42. T. R. Tuttle, Jr., Chem. Phys. Lett. 20, 371 (1973).
- 43. K. D. Vos and J. L. Dye, <u>J. Chem. Phys.</u> <u>38</u>, 2033 (1963).
- 44. K. Bar-Eli and T. R. Tuttle, Jr., <u>J. Chem. Phys.</u> <u>40</u>, 2508 (1964).
- 45. V. A. Nicely and J. L. Dye, <u>J. Chem. Phys.</u> <u>53</u>, 119 (1970).
- 46. L. R. Dalton, M. S. Thesis, Michigan State University, 1966.
- 47. B. Bockrath and L. M. Dorfman, <u>J. Phys. Chem.</u> <u>77</u>, 1002 (1973).
- 48. J. W. Fletcher and W. A. Seddon, <u>J. Phys. Chem.</u> 79, 3055 (1975).
- 49. W. A. Seddon, J. W. Fletcher, and R. Catterall, <u>Can.</u> <u>J. Chem.</u> <u>55</u>, 2017 (1977).
- 50. W. A. seddon, J. W. Fletcher, F. C. Sopchyshyn, and R. Catterall, Can. J. Chem. 55, 3356 (1977).
- 51. J. L. Dye, Reference 4, p. 77.
- 52. C. J. Pedersen, J. Am. Chem. Soc. 89, 2495 (1967).
- 53. C. J. Pedersen, <u>J. Am. Chem. Soc.</u> <u>89</u>, 7017 (1967); 90, 3299 (1968).
- 54. B. Dietrich, J.-M. Lehn, and J.-P. Sauvage, <u>Tetra-hedron Lett.</u>, 2885, 2889 (1969).

- 55. J.-M. Lehn and J. P. Sauvage, <u>J. Am. Chem. Soc.</u> <u>97</u>, 6700 (1975).
- 56. E. Kauffmann, J.-M. Lehn, and J.-P. Sauvage, <u>Helv.</u> Chim. Acta 59, 1099 (1976).
- 57. G. W. Gokel and H. D. Durst, Synthesis, 168 (1976).
- 58. A. C. Knipe, J. Chem. Ed. 53, 618 (1976).
- 59. J.-M. Lehn, Pure Appl. Chem. 49, 857 (1977).
- 60. J.-M. Lehn, Acc. Chem. Res. 11, 49 (1978).
- 61. R. M. Izatt and J. J. Christensen (eds.), "Progress in Macrocyclic Chemistry", Vol. 1, Wiley-Interscience (New York) 1979.
- 62. I. M. Kolthoff, Anal. Chem. 51, 1R (1979).
- 63. J. L. Dye, M. G. DeBacker, and V. A. Nicely, <u>J. Am.</u> Chem. Soc. 92, 5226 (1970).
- 64. J. L. Dye, M.-T. Lok, F. J. Tehan, R. B. Coolen, N. Papadakis, J. M. Ceraso and M. G. DeBacker, Ber. Bunsenges. Phys. Chem. 75, 659 (1971).
- 65. J. Lacoste, F. Schué, S. Bywater, and B. Kaempf, J. Polym. Sci. Polym. Lett. Ed. 14, 201 (1976)
- 66. J. M. Ceraso and J. L. Dye, <u>J. Chem. Phys.</u> <u>61</u>, 1585 (1974).
- 67. J. L. Dye, C. W. Andrews, and S. E. Matthews, <u>J.</u> Phys. Chem. 79, 3065 (1975).
- 68. M. S. Greenberg, R. L. Bodner, and A. I. Popov, <u>J. Phys. Chem.</u> 77, 2449 (1973).
- 69. M. Herlem and A. I. Popov, <u>J. Am. Chem. Soc.</u> <u>94</u>, 1431 (1972).
- 70. R. H. Erlich and A. I. Popov, <u>J. Am. Chem. Soc.</u> 93, 5620 (1971).
- 71. R. H. Erlich, E. Roach, and A. I. Popov, <u>J. Am. Chem. Soc.</u> <u>92</u>, 4989 (1970).
- 72. J. M. Ceraso, Ph.D. Dissertation, Michigan State University, 1975.
- 73. J. L. Dye, J. M. Ceraso, M.-T. Lok, B. L. Barnett, and F. J. Tehan, <u>J. Am. Chem. Soc.</u> <u>96</u>, 608 (1974).

- 74. F. J. Tehan, B. L. Barnett, and J. L. Dye, <u>J. Am.</u> Chem. Soc. 96, 7203 (1974).
- 75. The synthetic procedure and other aspects of alkali metal anion salts are patented: U.S. Patent 4,107,180. Inventors are J. L. Dye, J. M. Ceraso, F. J. Tehan, and M.-T. Lok. Patent is assigned to U.S. Government.
- 76. J. L. Dye, C. W. Andrews, and S. E. Matthews, <u>J.</u> Phys. Chem. 79, 3065 (1975).
- 77. M.-T. Lok, Ph.D. Dissertation, Michigan State University, 1973.
- 78. F. J. Tehan, Ph.D. Dissertation, Michigan State University, 1973.
- 79. J. L. Dye, M. R. Yemen, M. G. DaGue, and J.-M. Lehn, J. Chem. Phys. 68, 1665 (1978).
- 80. Sienko private communication (probably Sienko or Stacy, Chem. Phys.).
- 81. 18-Crown-6 is 1,4,7,10,13,16-hexaoxacyclooctadecane and cryptand (2,2,2) is 4,7,13,16,21,42-hexaoxa-1,10-diazabicyclo-(8,8,8)-hexacosane in the IUPAC system.
- 82. W. L. Jolly, "The Synthesis and Characterization of Air-Sensitive Compounds", Prentice Hall (Englewood Cliffs, New Jersey) 1970.
- 83. G. W. Gokel, D. J. Cram, C. L. Liotta, H. P. Harris, and F. L. Cook, J. Org. Chem. 39, 2445 (1974).
- 84. R. N. Green, Tetrahedron Lett., 1793 (1973).
- 85. L. H. Feldman, R. R. Dewald, and J. L. Dye, <u>Adv.</u> Chem. Ser. 50, 163 (1965).
- 86. E. C. Ashby and R. D. Schwartz, <u>J. Chem. Ed.</u> <u>51</u>, 65 (1974).
- 87. D. F. Shriver, "The Manipulation of Air-Sensitive Compounds", McGraw-Hill (New York) 1969, Ch. 8.
- 88. R. C. Douthit, Ph.D. Thesis, Michigan State University, 1959.
- 89. Conductivity Measurements on Solids Ed. by K. Lack-Hororitz and V. A. Johnson, Vol. 6, Solid State Physics Part B Electrical, Magnetic and Optical Properties. 1959. QC 176 L3 1959 V2 C4.

- 90. The following co-workers supplied powder samples:

  Long; (Na<sup>+</sup>C222)Na<sup>-</sup>.

  H. Lewis and Long; (K<sup>+</sup>C222)Na<sup>-</sup> and (Rb<sup>+</sup>C222)Na<sup>-</sup>

  Dheeb Issa; (Cs<sup>+</sup>18C6)Na
- 91. E. Mei, A. I. Popov, and J. L. Dye, <u>J. Am. Chem. Soc.</u> 99, 6532 (1977).
- 92. M. T. Lok, F. J. Tehan, and J. L. Dye, <u>J. Phys. Chem.</u> 76, 2975 (1972).
- 93. M. F. Fox and E. Hayon, <u>J. Chem. Soc. Faraday Trans. 1</u> 72, 1990 (1976).
- 94. R. Payan, Ann. Phys. (Paris) 4, 543 (1969).
- 95. M. H. Cohen, J. Jortner, and J. C. Thompson, <u>J. Chem. Phys.</u> 63, 3741 (1975).
- 96. D. Moras and R. Weiss, Acta Crystallogr. Sect. B 29, 396 (1973).
- 97. H. Aulich, L. Nemac, and P. Delahay, <u>J. Chem. Phys.</u> 61, 4235 (1974).
- 98. T. A. Patterson, H. Hotop. A. Kasdan, D. W. Norcross, and W. C. Lineberger, Phys. Rev. Lett. 32, 189 (1974).
- 99. H. J. Hesse, W. Fuhs, G. Weiser, and L. Von Szentplay, Chem. Phys. Lett. 41, 104 (1976).
- 100. M. G. DeBacker and J. L. Dye, <u>J. Phys. Chem.</u> <u>75</u>, 3092 (1971).
- 101. F. J. Tehan, B. L. Barnett, and J. L. Dye, <u>J. Am.</u> Chem. Soc. <u>96</u>, 7203 (1974).
- 102. T. Shida, S. Iwata, and T. Watanabe, <u>J. Phys. Chem.</u> 76, 3683 (1972).
- 103. J. J. Markham, "F-Centers in Alkali Halides", Academic Press (New York) 1966.
- 104. M. G. DaGue, Ph.D. Thesis, Michigan State University, 1979.
- 105. J. E. Willard, J. Phys. Chem. 79, 2966 (1975).
- 106. J. L. Dye, C. W. Andrews, and J. M. Ceraso, <u>J. Phys.</u> Chem., <u>79</u> 3076 (1975).

- 108. J. W. Fletcher and W. A. Seddon, <u>J. Phys. Chem.</u> 79, 3055 (1975).
- 109. R. Catterall, J. Slater, W. A. Seddon, and J. W. Fletcher, Can. J. Chem. 54, 3110 (1976).
- 110. W. A. Seddon, J. W. Fletcher, F. C. Sopchyshyn, and R. Catterall, Can. J. Chem. 55, 3356 (1977).
- 111. Most of the spectra taken of the Rb/18C6 system were obtained by M. H. DaGue.
- 112. C. J. Pedersen, J. Am. Chem. Soc. 89, 7017 (1967);
  92, 386 (1970); (b) C. J. Pedersen, Fed. Proc. 27,
  1305 (1968); (c) C. J. Pedersen and H. K. Frensdorff,
  Angew. Chem., Int. Ed. Engl. 11, 16 (1972).
- 113. H. K. Frensdorff, <u>J. Am. Chem. Soc.</u> <u>93</u>, 600 (1971).
- 114. E. Mei, A. I. Popov, and J. L. Dye, <u>J. Phys. Chem.</u>, <u>81</u>, 1677 (1977).
- 115. The <sup>23</sup>Na NMR spectra were obtained by P. Smith and J. Ceraso.
- 116. The proton NMR spectra used to determine the ratio of methylamine: 18C6 were obtained by P. Smith.
- 117. C. Kittel, <u>Introduction to Solid State Physics</u>, 5th Edition, John Wiley and Sons, Inc., New York, NY, pp. 207-211.
- 118. N. Kh. Abrekosov, V. F. Bankina, L. V. Porztshaya, L. E. Shelimova and E. V. Saudnova, Semi-Conducting II-VI, IV-VI and V-VI Compounds, Plenum Press, New York, NY. 1969. pp. 26; 32.
- 119. D. Halliday and R. Resnick, Physics Part I and II, John Wiley and Sons, Inc., New York, NY, 1966. p. 770-785.
- 120. Semiconductors, N. B. Hannay, Reinhold Publishing Corp., New York, NY. 1959. p.
- 121. Samples of (K+C222)Na were prepared by Long. D. Le.
- 122. Samples of "(Ba<sup>++</sup>C222)Na<sub>2</sub> were prepared by B. VanEck.
- 123. Samples of (Li<sup>+</sup>C211)e<sup>-</sup> were prepared by J. S. Landers. For a detailed description of (Li<sup>+</sup>C211)e<sup>-</sup> see J. S.

Landers Doctoral Dissertation, Michigan State University, 1980.

- 124. J. L. Dye, Scientific American, p. 92, July 1977.
- 125. B. Dietrich, J.-M. Lehn, J. P. Sauvage, and J. Blanzat, <u>Tetrahedron</u> 29, 1629 (1973).